



University of Kentucky  
UKnowledge

---

Theses and Dissertations--Animal and Food  
Sciences

Animal and Food Sciences

---

2015

## Steroid-dependent regulation of the oviduct: A cross-species transcriptomal analysis

Katheryn L. Cerny

University of Kentucky, [katheryn.cerny@gmail.com](mailto:katheryn.cerny@gmail.com)

[Right click to open a feedback form in a new tab to let us know how this document benefits you.](#)

---

### Recommended Citation

Cerny, Katheryn L., "Steroid-dependent regulation of the oviduct: A cross-species transcriptomal analysis" (2015). *Theses and Dissertations--Animal and Food Sciences*. 49.  
[https://uknowledge.uky.edu/animalsci\\_etds/49](https://uknowledge.uky.edu/animalsci_etds/49)

This Doctoral Dissertation is brought to you for free and open access by the Animal and Food Sciences at UKnowledge. It has been accepted for inclusion in Theses and Dissertations--Animal and Food Sciences by an authorized administrator of UKnowledge. For more information, please contact [UKnowledge@lsv.uky.edu](mailto:UKnowledge@lsv.uky.edu).

## **STUDENT AGREEMENT:**

I represent that my thesis or dissertation and abstract are my original work. Proper attribution has been given to all outside sources. I understand that I am solely responsible for obtaining any needed copyright permissions. I have obtained needed written permission statement(s) from the owner(s) of each third-party copyrighted matter to be included in my work, allowing electronic distribution (if such use is not permitted by the fair use doctrine) which will be submitted to UKnowledge as Additional File.

I hereby grant to The University of Kentucky and its agents the irrevocable, non-exclusive, and royalty-free license to archive and make accessible my work in whole or in part in all forms of media, now or hereafter known. I agree that the document mentioned above may be made available immediately for worldwide access unless an embargo applies.

I retain all other ownership rights to the copyright of my work. I also retain the right to use in future works (such as articles or books) all or part of my work. I understand that I am free to register the copyright to my work.

## **REVIEW, APPROVAL AND ACCEPTANCE**

The document mentioned above has been reviewed and accepted by the student's advisor, on behalf of the advisory committee, and by the Director of Graduate Studies (DGS), on behalf of the program; we verify that this is the final, approved version of the student's thesis including all changes required by the advisory committee. The undersigned agree to abide by the statements above.

Katheryn L. Cerny, Student

Dr. P.J. Bridges, Major Professor

Dr. D.L. Harmon, Director of Graduate Studies

STEROID-DEPENDENT REGULATION OF THE OVIDUCT:  
A CROSS-SPECIES TRANSCRIPTOMAL ANALYSIS

---

DISSERTATION

---

A dissertation submitted in partial fulfillment of the  
Requirements for the degree of Doctor of Philosophy in the  
College of Agriculture at the University of Kentucky

By

Katheryn Leigh Cerny  
Lexington, Kentucky

Director: Dr. Phillip J. Bridges, Ph.D. Assistant Professor  
Lexington, Kentucky

Copyright © Katheryn Leigh Cerny, 2015

## ABSTRACT OF DISSERTATION

### STEROID-DEPENDENT REGULATION OF THE OVIDUCT: A CROSS-SPECIES TRANSCRIPTOMAL ANALYSIS

Reproductive success depends on a functional oviduct for gamete storage, maturation, fertilization, and early-conceptus development. The ovarian-derived sex steroids estradiol and progesterone are known to affect functionality of the oviduct. Advances in microarray and NanoString technology allow for gene expression analysis to increase understanding of processes critical for fertility. Studies were conducted to investigate mechanisms regulating oviductal function in cattle and mice by using the Bovine Gene 1.0 ST array and the Mouse Gene 430-2.0 arrays (Affymetrix Inc., CA), respectively.

For the first study, oviducts were collected from heifers assigned to luteal or follicular phase groups. In the second study oviducts were collected from immature mice with a global deletion of estrogen receptor-1 (ESR1) and their wild-type littermates at 23 days of age or 48 hr after treatment with 5 IU of PMSG. Following microarray hybridization, the resulting datasets were analyzed using Partek Genomics Suite 6.6 (Partek Inc., MO).

The results of the first two studies illustrated a dynamic hormonal regulation of the oviductal epithelium and revealed the identity of novel genes affecting fertility in cattle and gave us insights into the genes regulated by estrogen and ESR1 in mice. Many genes identified as differentially regulated are believed to play an integral role in the regulation of oviductal inflammation. Therefore, the objective of the third study was to test the hypothesis that intraperitoneal administration of *E. Coli*-derived lipopolysaccharide induces the expression of inflammatory mRNAs in the mouse oviduct. Mice were treated with 0, 2  $\mu$ g or 10  $\mu$ g of LPS from *E. Coli*. and killed 24 h later.

Oviducts were collected for determination of inflammatory gene expression by a targeted NanoString approach using the nCounter GX Mouse Inflammation Kit (NanoString Technologies, Wa). Results indicate that systemic treatment with LPS induces inflammation in the oviducts of mice and provides evidence of a repeatable animal model of oviductal inflammation. Overall, data from these studies extends our knowledge of the mechanisms regulating oviductal functions and immune response, as well as identified target molecules and processes to improve production animal and human fertility.

Keywords: Oviduct, Steroid hormones, LPS-induced inflammation, Tubal-factor infertility, immune response

Katheryn L. Cerny  
\_\_\_\_\_  
Student's Signature

7/21/2015  
\_\_\_\_\_  
Date

STEROID-DEPENDENT REGULATION OF THE OVIDUCT: A CROSS-SPECIES  
TRANSCRIPTOMAL ANALYSIS

By

Katheryn Leigh Cerny

Dr. P.J. Bridges

Director of Dissertation

Dr. J.C. Matthews

Co-Chair of Dissertation

Dr. D.L. Harmon

Director of Graduate Studies

7/21/2015

Date

## ACKNOWLEDGEMENTS

Earning a Ph.D. has been a lifelong goal and I am fortunate to have had an inspiring group of advisors along the way. First and foremost I would like to thank Dr. P.J. Bridges, my Ph.D. advisor and chairman of my doctoral committee for guiding me through my graduate career. I first met Dr. Bridges as an equine professional looking to expand my experiences in research to other species. It was my lucky day when Dr. Bridges offered me a position as a graduate research assistant in his lab where I could learn valuable lab techniques applicable to reproductive physiology and work with cattle and mice for my Ph.D. Through all the twists and turns of graduate school I could always count on Dr. Bridges to help guide my direction. I would also like to express my appreciation and thanks to my doctoral committee members: Co-chair Dr. J.C. Matthews, Dr. L. Anderson, Dr. K. McDowell, and Dr. B.A. Ball for their advice and support during my Ph.D. projects and allowing me to grow as a research scientist.

I would especially like to acknowledge my parents, Bridget and Max Cerny for their continuous encouragement and support in achieving my goals. I am extremely grateful for the sacrifices they have made throughout my life and I consider myself an exceptionally fortunate person.

## TABLE OF CONTENTS

ACKNOWLEDGEMENTS .....	iii
LIST OF TABLES .....	vi
LIST OF FIGURES .....	vii
FREQUENTLY USED ABBREVIATIONS.....	viii
CHAPTER 1. INTRODUCTION.....	1
CHAPTER 2. A REVIEW OF THE LITERATURE.....	3
Structure of the Oviduct .....	3
Steroidal Regulation of the Oviduct.....	4
Gamete Storage and Maturation .....	7
Fertilization and Conceptus Development.....	10
Oviduct Epithelial Cell Secretions .....	11
Inflammatory Response in the Oviduct.....	13
CHAPTER 3. STATEMENT OF THE PROBLEM.....	16
CHAPTER 4. A TRANSCRIPTOMAL ANALYSIS OF OVIDUCTAL EPITHELIAL CELLS COLLECTED DURING THE FOLLICULAR VERSUS LUTEAL PHASE IN CATTLE .....	19
Abstract.....	19
Introduction .....	21
Methods .....	23
Results and Discussion .....	29
Conclusions .....	47
CHAPTER 5. REGULATION OF OVIDUCTAL FUNCTION THROUGH ESTROGEN- RECEPTOR ALPHA (ESR1): A TRANSCRIPTOMAL ANALYSIS USING TRANSGENIC MICE.....	48
Abstract.....	48
Introduction .....	50
Methods .....	52

TABLE OF CONTENTS (CONTINUED)

Results.....59

Discussion and Conclusions.....68

CHAPTER 6. INTRAPERITONEAL ADMINISTRATION OF LIPOPOLYSACCHARIDE INDUCES DIFFERENTIAL EXPRESSION OF mRNA ENCODING INFLAMMATORY MEDIATORS IN THE OVIDUCTS OF MICE .....73

    Abstract.....73

    Introduction.....75

    Methods .....76

    Results.....81

    Discussion and Conclusions.....88

CHAPTER7. CONCLUSIONS AND IMPLICATIONS .....90

APPENDIX 1. DIFFERENTIAL EXPRESSION OF mRNA ENCODING CYTOKINES AND CHEMOKINES IN THE REPRODUCTIVE TRACT AFTER INFECTION OF MICE WITH *CHLAMYDIA TRACHOMATIS*.....94

    Abstract.....94

    Introduction.....96

    Methods .....98

    Results.....101

    Discussion and Conclusions.....108

APPENDIX 2. SUPPLEMENTARY TABLES AND FIGURES.....114

LITERATURE CITED .....157

VITA .....170

## LIST OF TABLES

Table 4.1. Comparison of gene expression for selected mRNA by microarray and real-time RT-PCR .....	30
Table 4.2. Number of differentially expressed genes (DEGs) in epithelial cells of the ampulla and isthmus between follicular and luteal phase groups .....	33
Table 4.3. Most highly up- and down-regulated DEGs within epithelial cells of the ampulla in follicular versus luteal phase groups .....	35
Table 4.4. Most highly up- and down-regulated DEGs within epithelial cells of the isthmus in follicular phase versus luteal phase groups .....	43
Table 5.1. Comparison of gene expression for selected mRNA by Microarray and Real-time RT-PCR in oviducts collected from PMSG-treated ESR1KO versus PMSG-treated WT mice .....	59
Table 5.2. Number of genes differentially regulated in whole oviducts from ESR1KO and WT mice .....	61
Table 5.3. Most highly up- and down-regulated genes from PMSG-treated ESR1KO versus PMSG-treated WT mouse oviducts .....	62
Table 6.1. Comparison of gene expression for selected mRNA by NanoString and Real-time RT-PCR .....	82
Table 6.2. Differentially expressed transcripts between low dose (2 ug LPS) and control (PBS only) oviducts collected from CD1 mice .....	84
Table 6.3. Differentially expressed transcripts between high dose (10 ug LPS) and control (PBS only) oviducts collected from CD1 mice .....	85
Table 6.4. Differentially expressed transcripts between high dose (10 ug LPS) and low dose (2 ug LPS) oviducts collected from CD1 mice .....	87
Table A1.1. Effect of treatment on the expression of mRNAs in the vagina at 28 and 35 days post-infection .....	102
Table A1.2. Effect of treatment on the expression of mRNAs in the uterus at 28 days post-infection .....	104
Table A1.3. Effect of treatment on the expression of mRNAs in the oviduct at 28 and 35 days post-infection .....	105
Table A1.4. Effect of treatment on the expression of mRNAs in the uterus at 35 days post-infection .....	107
Supplementary Table 1. Differentially expressed genes from PMSG-treated ESR1KO versus PMSG-treated WT mouse oviducts .....	118

## LIST OF FIGURES

Figure 4.1. Principal component analysis of microarray transcriptome results of epithelial cells from the ampulla and isthmus taken from heifers killed in the follicular phase (FP) and luteal phase (LP) of the estrous cycle .....	32
Figure 4.2. Venn diagram depicting the number of differentially expressed genes in follicular phase versus luteal phase epithelial cells from the ampulla and isthmus ..	34
Figure 4.3. Representative images of the ampulla (A,B) of the bovine oviduct .....	37
Figure 4.4. Representative images of the isthmus (A,B) of the bovine oviduct.....	42
Figure 5.1. Box plot of the log <sub>2</sub> expression signal for each sample (microarray chip) .....	54
Figure 5.2. Principal component analysis of microarray transcriptome results of oviducts collected from ESR1KO and WT littermates with or without PMSG treatment .....	55
Figure 5.3. Gene ontology analysis from PMSG-treated ESR1KO versus PMSG-treated WT mice.....	65
Figure 5.4. The six most significant pathways identified by Ingenuity Pathway Analysis software from the 1185 DEGs identified in PMSG-treated ESR1KO versus PMSG-treated WT mice .....	67
Figure 6.1. Venn diagram depicting the number of differentially genes between high dose (10 ug LPS), low dose (2 ug LPS) and control oviducts collected from CD1 mice .....	83
Supplementary Figure 1. Box plot of the log <sub>2</sub> expression signal for each sample (microarray chip) .....	114
Supplementary Figure 2. Overlapping sample signal intensity histogram indicating the frequency of transcripts at specific signal intensity values.....	115
Supplementary Figure 3. Top 6 Canonical pathways from up- and down-regulated differentially expressed genes within epithelial cells of the ampulla in the follicular versus luteal phase.....	116
Supplementary Figure 4. Top 6 Canonical pathways from up- and down-regulated differentially expressed genes within epithelial cells of the isthmus in the follicular versus luteal phase.....	117

## FREQUENTLY USED ABBREVIATIONS

ANOVA: Analysis of Variance

FDR: False discovery rate

PCA: Principal Component Analysis

DEGs: Differentially expressed genes

mRNA: messenger RNA

miRNA: micro RNA

FP: Follicular phase

LP: Luteal phase

ESR1: Estrogen receptor alpha

ESR1KO: Estrogen receptor knockout

WT: Wildtype

PMSG: Pregnant mare serum gonadotropin

LPS: Lipopolysaccharide

IP: Intraperitoneal

## **CHAPTER 1.**

### **INTRODUCTION**

The female reproductive organs consist of the external genitalia, cervix, uterus, oviducts (uterine tubes or fallopian tubes in women), and ovaries. A normally functioning female reproductive tract is essential for gamete production and transport, fertilization, conceptus development and fetal development leading to the birth of live offspring.

The oviduct in particular can be considered an understudied organ as less intense investigation has been directed toward the oviduct compared to the uterus and ovaries, specifically at the transcriptional level. In more recent decades, a paradigm shift has occurred and the oviduct is being increasingly recognized as a biologically active organ that undergoes significant physiological and morphological changes throughout the estrous cycle to facilitate early events in reproduction, rather than just a tube involved in gamete transport.

Analysis of the causes for women to seek assisted reproductive technologies (ART) to establish a pregnancy highlights the importance of further understanding the function of the oviduct in fertility. In women under 35 years of age, oviductal factors exceed both ovulatory dysfunction and endometriosis as the causal factors of these women to seek ART [1-3]. Observations using oviduct epithelial cell cultures have provided evidence of the complex interaction between gametes, conceptus, and the oviduct. Co-culture of a conceptus with oviductal epithelial cells improves developmental potential when compared with culture in conventional media and

the incidence of persistent or recurrent inflammation, fibrosis, scarring in the oviduct as well as pelvic inflammatory disease (PID) and ectopic pregnancy are known to impact female fertility [1-4]. Targeted investigations of the oviduct have been completed; however, less extensive investigations have been done regarding the molecular mechanisms involved in oviduct function in humans.

In cattle, the impact of tubal dysfunction is less clear. First service conception rates range from 50 to 70% in beef cattle and as low as 30% in dairy cattle [5]. It is difficult to determine the role of the oviduct in the failure of cattle to establish successful pregnancies. Since early embryonic death occurs within one estrous cycle, often producers are unaware that an embryo existed. In addition, confounding factors such as oocyte viability, spermatozoa quality, and management practices influence conception and pregnancy rates. Low conception and subsequent pregnancy rates represent lost economic opportunity for dairy and beef cattle producers warranting further investigation of oviduct function.

The following review of literature will discuss the key findings related to oviduct structure and function as it pertains to the establishment of pregnancy.

## CHAPTER 2.

### A REVIEW OF THE LITERATURE

#### Structure of the Oviduct

The mammalian oviduct contains an epithelial mucosa called the endosalpinx comprised of ciliated and secretory simple columnar epithelial cells surrounded by a smooth muscle layer called the myosalpinx and the perisalpinx which contains connective tissue and blood vessels. The oviduct is comprised of four distinct regions. The infundibulum is located near the surface of the ovary and includes the fimbriae which are finger-like projections that aid in the capture of the cumulus-oocyte complex and the majority of cells in this segment are ciliated [6]. The ampulla is located below the infundibulum and has a large diameter compared to the other regions of the oviduct. Through ciliary beats and myosalpingeal contraction towards the uterus, the oocyte is transported to the ampulla where fertilization occurs. The epithelial mucosa of the ampulla is elaborately folded and adjacent to a thin layer of smooth muscle. Electron microscopy and histological evaluations have revealed that ciliated and secretory cells are equally abundant in the ampulla with ovarian steroid hormones influencing morphological changes in ciliated cells and hypertrophy of secretory cells [6-8].

The isthmus spans the interval from the ampulla to the utero-tubal junction and is adjacent to a prominent musculature. The epithelial mucosa of the isthmus is well defined; however, less elaborate relative to the ampulla. The isthmus in particular serves as a reservoir and functional filter for spermatozoa and entrance

of the conceptus into the uterus [9]. Similar to the isthmus, the muscle layer of the utero-tubal junction is well defined and is the segment of the oviduct that transitions the isthmus region to the uterus [6-8, 10].

### **Steroid Regulation of the Oviduct**

Steroid environment affects morphological and functional changes in the mammalian oviduct. Ovarian steroids estradiol and progesterone are known regulators of oviductal function as receptors are abundant in the mucosal epithelium. Prostaglandins are also major physiological regulators of oviductal function. A counter-current vascular route between the ovarian vein and artery exists where steroids and prostaglandins can reach the oviduct via the utero-tubal artery. For example, estradiol produced by a preovulatory follicle is transported through arterioles and can affect ipsilateral oviduct epithelial cell function in preparation for male gametes and ovulation. In pigs, estradiol and progesterone concentrations are 10 fold higher in arteriolar samples compared to systemic circulation demonstrating the local delivery of ovarian steroids [11]. Peritoneal fluid is another source of concentrated ovarian steroids and other hormones. Cincinella et al, 2009, evaluated progesterone levels in peritoneal fluid near the corpus luteum and ipsilateral oviduct of women and found concentrations were higher compared to systemic blood samples [12]. Furthermore, Paracrine delivery also exists, for example the cumulus-oocyte complex and follicular fluid can deliver paracrine factors affecting oviduct function after ovulation.

The physiological changes that occur within the oviducts' mucosal epithelia can in part be attributed to estradiol and progesterone. A number of authors have reported a difference in ratio of ciliated to secretory cells throughout the estrous cycle in primates [13], sheep [14], cattle [8, 15], and rodents [16]. In the bovine, a decrease in ciliated cells and increase in secretory cells is observed in the infundibulum and ampulla during the luteal phase (progestogenic environment), but not the other regions of the oviduct [8, 17]. Similar findings have been observed in primates with the number of ciliated cells increasing in the ampulla during the follicular phase (estrogen environment) [13]. Cyclic changes in the epithelial mucosa are related to function such as gamete transport through the oviduct as well as gene expression changes such as an increase in immune related genes during the luteal phase [18].

Estradiol exerts its effects through two receptor subtypes, estrogen receptor alpha (ESR1) and estrogen receptor beta (ESR2). Ulbrich et al, 2003, described the region-specific and cycle-phase dependent changes in hormone receptors where ESR1 mRNA increased in the bovine isthmus during the follicular phase compared to the luteal phase, but remained unchanged in the ampulla [19]. Gamete storage and maturation as discussed below occur during an estrogen dominant environment and many molecules have been shown to be regulated in an estrogen dependent manner. For example, interleukin-6 (IL-6), a proinflammatory cytokine has been reported to be regulated by estrogens in the oviduct and increases in women with tubal ectopic pregnancy [20-22]. Furthermore, ESR1 mutant mice lack

the expression of hematopoietic form of prostaglandin D synthase (HPGDS), a proposed regulator of oviductal inflammation [23].

Progesterone produced by luteal cells from the corpus luteum is also a known regulator of oviductal function. Progesterone exerts its effects through progesterone receptor-A (PR-A) and progesterone receptor-B (PR-B) [24]. Okado et al., 2003, described the mRNA expression and protein localization of progesterone receptors in the rat oviduct during different stages of the estrous cycle and suggested effects of progesterone on ciliogenesis [25]. Expression profiles of mRNA have also been described in bovine oviductal epithelial cells during the luteal phase (progestogenic environment) with significant gene ontology classifications related to cell proliferation and transcriptional regulation supporting the phenotype of secretory cell differentiation during the progesterone dominant phase [4, 8, 17].

Estradiol and progesterone are also thought to act synergistically with prostaglandins to control reproductive functions in females [26]. Prostaglandins are synthesized through the liberation of arachidonic acid (AA) from phospholipids by phospholipase A<sub>2</sub> (PLA<sub>2</sub>) and phospholipase C (PLC) whereby cyclooxygenases COX-1 or COX-2 convert AA to an intermediary form, prostaglandin H<sub>2</sub>. Cell specific synthases convert the intermediate prostaglandin into distinct forms with differing functions [27, 28]. Certainly the role of prostaglandin F<sub>2</sub>alpha in luteolysis and smooth muscle contraction in the uterus is well known, however, prostaglandins are also implicated in the function of the oviduct as bovine oviductal epithelial cells secrete prostaglandins [29, 30]. For example, prostaglandin E<sub>2</sub> (PGE<sub>2</sub>) concentrations in the bovine oviduct increase during the peri-ovulatory period and

luteinizing hormone (LH) has a stimulatory effect on PGE<sub>2</sub> production which is thought to act as an immunosuppressive factor by down-regulating phagocytosis of sperm [31]. Other than immune-regulatory functions, prostaglandins also aid in oviduct contractility which facilitates gamete transport, fertilization, and zygote transport to the uterus [32, 33].

### **Gamete Storage and Maturation**

Gamete and oviduct interactions are well documented in the literature. In order for fertilization to occur motile spermatozoa must first enter the oviduct through the utero-tubal junction. Properties of the sperm membrane have been shown to influence the passage of spermatozoa through the utero-tubal junction. For example, there are several male mutant mouse models that appear to have normal sperm morphology but are infertile because they lack the necessary proteins or enzymes involved in sperm passage through the utero-tubal junction [34-36]. After passage through the utero-tubal junction sperm enter the isthmus where a storage and maturation reservoir is formed. As reviewed by Holt (2011), the formation of the sperm reservoir is essential for fertilization as it allows for sperm to survive until ovulation. The sperm reservoir may also act to decrease the incidence of polyspermy by releasing sperm in intervals and impact sperm maturation processes [37, 38]. In the bovine, binding of sperm to epithelial cells in the isthmus is facilitated, in part, by seminal plasma proteins on the sperm membrane [9, 39]. Binder of sperm proteins (BSP 1, 3, and 5) are secreted by seminal vesicles and coat the sperm membrane. Once in the isthmus, sperm can

then bind fucosylated molecules located on the epithelium of the oviduct [40, 41]. Oviduct epithelial cell secretions and membrane proteins are also known to affect the sperm reservoir with heat shock proteins and glycoprotein secretion playing a role in prolonging sperm viability [42].

Near to or immediately after ovulation various factors influenced by the contact of sperm with oviductal epithelial cells and steroid hormones enable capacitation, acrosome reaction, and hyperactivation. Capacitation is a biochemical event in which sperm acquire the ability to fertilize the oocyte. The acrosome reaction is the fusion of the acrosome with the plasma membrane of the sperm in order to release enzymes needed for sperm to penetrate the zona pellucida. Hyperactivation is an increase in sperm motility required for sperm penetration of the zona pellucida. Calcium concentration in the lumen of the oviduct is one of the most well-known and studied factors affecting sperm motility and fertilization ability with increasing concentrations associated with the acrosome reaction [43]. More recently, neurotensin has been localized in both the isthmus and ampulla epithelium of mice with receptors expressed on spermatozoa. Hird et al., 2014, demonstrated that neurotensin induced tyrosine phosphorylation in sperm which is known to occur during sperm capacitation. Furthermore, neurotensin was found to facilitate the acrosome reaction in vitro in a dose dependent manner [44]. As far as gamete storage and maturation is concerned the literature is well established with numerous targeted investigations illustrating evidence in support of a sperm reservoir and factors influencing sperm maturation. Sperm maturation events have been linked to the release of sperm from the reservoir. For example, the presence of

binder of sperm protein 1, 3, and 5 on the sperm membrane decrease after capacitation which may lead to the release of sperm from the reservoir [45].

Although the presence of proteins such as BSP 1, 3, and 5 have been extensively investigated, less is understood about the role of thermotaxis and chemotaxis. These two processes involve chemoattractants and thermal gradients which are thought to affect sperm motility and direct them toward the ampulla for fertilization. In regards to thermotaxis, a temperature gradient has been observed in the mammalian oviduct since the 1970's. There is evidence that the sperm reservoir in the isthmus region is cooler in temperature than the ampulla and the described temperature difference between the isthmus and ampulla is a proposed mechanism for sperm release from the reservoir to the site of fertilization [46-48]. As far as chemotaxis is concerned, Kaupp et al., 2008 and 2012 conclude that the oocyte cumulus complex releases chemical factors that attract sperm [49, 50]. The role of other factors such as steroid hormones and epithelial cell secretions in chemotaxis have yet to be clearly defined; increasing the importance of investigating gene expression changes during these critical events.

## **Fertilization and Conceptus Development**

After ovulation the cumulus oocyte complex (COC) is captured in the fimbriae and transported through the infundibulum to the ampulla. Contact with epithelial cells aids in the movement of the COC so that the oocyte may come in contact with sperm. A number of studies have attributed oocyte transport through the oviduct to ciliated epithelial cells beating in the direction of the uterus as well as smooth muscle contraction. The fertilization cascade initiated by oocyte-sperm contact will not be discussed here; however, the role of oviduct epithelial cells in facilitating fertilization will be included.

Recently in cattle, epithelial cadherin (E-cadherin) was localized to ampulla and isthmus epithelial cells in the follicular and luteal phases of the estrous cycle. Furthermore, E-cadherin and  $\beta$ -catenin expression was found in the cumulus oocyte complex, mature oocytes and spermatozoa. When monoclonal anti-E-cadherin antibody was used, sperm interaction with oviduct epithelial cells and cumulus oocyte complex was impaired in vitro suggesting that oviduct epithelial expression of E-cadherin is involved in sperm-oocyte adhesion events [51]. Presence of glycosidases and glycoproteins such as oviductal glycoprotein 1 (OVG1) have also been implicated in aiding gamete transport and sperm-oocyte interaction therefore analyses of the oviduct epithelium transcriptome will assist in identifying specific molecules participating the fertilization process [52, 53].

Upon successful fertilization, several rounds of embryonic cleavage occur, a morula develops and travels the remaining length of the oviduct before reaching the uterus as a late morula or differentiated blastocyst at around day 5.5 (in cattle) after

ovulation. A normally functioning oviduct is critical for conceptus growth and differentiation and movement towards the uterus. Ciliary beats and smooth muscle contraction are involved in transport and epithelial cell secretions provide an optimal environment for conceptus survival. Similar to gamete storage and maturation, many bioactive compounds are involved in conceptus development such as glutamate, bicarbonate, potassium, arginine, alanine, and glycoprotein specific to the oviduct. Steroid environment as discussed above is also vital to successful development and transport of the conceptus.

### **Oviduct Epithelial Cell Secretions**

As mentioned above, factors such as calcium concentration, thermal gradient, chemoattractants from the cumulus oocyte complex, and oviduct epithelial cell secretions influence the ability of spermatozoa to travel through the utero-tubal junction and isthmus before reaching the ampulla, the site of fertilization. Although *in vivo* fertilization and early cleavage events in the oviduct are not completely understood, the oviduct epithelial cell layer is clearly an active site of biosynthesis and secretion.

Reports on the structural characteristics of secretory cells within the oviduct identify differences in the size and amount of secretory granules between the phases of the estrous cycle and spatial location [54, 55]. During the follicular phase biosynthetic activity of the oviductal mucosa increases in an estrogen dependent manner in multiple species, as reviewed by Buhi et al., 2000 [56]. Epithelial cells within the infundibulum and ampulla also appear to have a greater biosynthetic

activity than the isthmus and utero-tubal junction [53, 56, 57]. Studies involving both in vitro [58] and in vivo [59, 60] systems distinguish the composition of oviductal fluid as clearly different from that of serum or uterine fluid, further supporting the importance of oviductal function on early reproductive events. Evaluations of oviductal fluid describe components such as amino acids and proteins, carbohydrates, ions, lipids, and metabolic substrates [51, 53, 59-62]. Of note is the identification of estrogen-dependent, oviduct-specific glycoproteins which have been described in many studies. Oviduct-specific glycoproteins are thought to act by binding gametes and the developing conceptus and have been found to increase capacitation and fertilization capabilities in bovine sperm [63] and increase blastocyst cleavage rates pigs in vitro [64]. However reports on in vivo function are conflicting based on species.

Although significant changes in the composition of oviductal fluid exist between the phases of the estrous cycle with ovarian steroids being a major regulator, the presence of gametes and the conceptus also affects cell secretions. Spermatozoa have been shown to modulate gene expression and protein synthesis. Ellington et al., 1993, described the de novo synthesis of proteins in bovine oviductal epithelial cells from the isthmus when co-cultured with bull spermatozoa [62]. In turn, oviduct secretions regulate sperm function and the process of fertilization [44, 51]. Reports on the presence and interaction of a conceptus with the oviduct describe changes in oviduct gene expression and cell secretions [57, 65, 66]. For example, oviduct derived embryotrophic factors such as complement protein component-3 has been described to be synthesized and secreted in the

oviducts of mice when a conceptus is present compared to pseudo-pregnant females [67]. Together these studies indicate the important balance in oviduct biosynthesis and secretion regulating the microenvironment required for gamete and conceptus health.

### **Inflammatory Response in the Oviduct**

A key aspect of function is understanding both normal, cyclic and pathogen-induced inflammatory responses within the oviduct. Existing research recognizes the critical role played by the immune system in female reproduction with estradiol and progesterone being important regulators. The inflammatory response within the oviduct can be considered a normal and necessary physiological occurrence in response to ovulation, post-ovulatory follicular debris, and presence of sperm; however, salpingitis or aberrant inflammation can lead to tubal dysfunction. In women, inflammatory insults can be caused by retrograde flow of endometrial fluid or exposure to pathogens resulting in oviduct epithelial cell secretion of proinflammatory cytokines and chemokines that recruit leukocytes and induce a cellular immune response [68]. Although innate and adaptive immune responses are critical, persistent or recurrent inflammation can lead to oviduct scarring, fibrosis, pelvic inflammatory disease, infertility, and potentially the formation of serous ovarian cancer [2, 69].

Currently, methods to investigate tubal inflammation in women involve in vitro cell culture systems or in vivo mouse models; however, obstacles exist with these models as repeatability and variability are difficult to overcome. A common

approach to investigating the immune response in the oviduct is through the use of *chlamydia trachomatis* induced inflammation using mice as a model for women. *C. trachomatis* is the most frequently reported sexually transmitted bacterium in the United States [70] and recurrent or untreated infection can lead to tubal factor infertility [71]. Overall, the evidence suggests that once *C. trachomatis* has established infection within epithelial cells, the innate immune response allows for the production of pro-inflammatory cytokines such as interleukins 1, 6, 8, (Il-1, Il-6, Il-8) tumor necrosis factor- $\alpha$  (Tnf- $\alpha$ ), and colony stimulating factor 2 (Csf2) [72]. Regulation by cytokines, chemokines, and other inflammatory mediators is involved in the recruitment of immune cells such as natural killer cells and phagocytes [73, 74]. The T-cell mediated immune response is another critical element and has been found to contribute to pathology following infection where Th1 cells limit replication of *C. trachomatis*, but Th2 cells inhibit Th1 responses leading to continued production of pro-inflammatory molecules which can lead to fibrosis [75]. Although these findings help us understand the inflammatory response by oviductal epithelial cells, there are large discrepancies in disease outcomes following infection due in part by host genetic factors, pathogenic strain, and experimental methods used.

Recently, Kowsar et al., 2014, investigated factors involved in the regulation of immune function in the bovine oviduct. In this study an in vitro model of cultured bovine oviductal epithelial cells was used to determine the expression and secretion of alpha 1-acid glycoprotein (AGP), an acute phase protein regulated by ovarian steroids and potentially involved in regulating the inflammatory response in the

oviduct. Interestingly, when bovine oviductal epithelial cells were stimulated with AGP and LPS in vitro, a decrease in TNF- $\alpha$  and TLR-2 gene expression was observed suggesting a role of AGP in modulating the immune response [76]. Local immune responses were further investigated in bovine oviductal epithelial cells in response to LPS stimulation and the interaction of ovarian steroids on LPS induced inflammatory mediators [77]. The results provided key information on the upregulation of pro-inflammatory molecules such as TLR-4, Interleukin 1 $\beta$ , and tumor necrosis factor  $\alpha$  and provided evidence that ovarian steroids may play a role in controlling pro-inflammatory responses after oviductal epithelial cells are exposed to pathological agents [77].

## **CHAPTER 3.**

### **STATEMENT OF THE PROBLEM**

Existing literature recognizes the significance of the oviduct in gamete storage, maturation and transport, fertilization and subsequent zygote development. The early reproductive events that occur within the oviduct are therefore critical for the successful establishment of pregnancy; however, the mechanisms regulating function of this organ are not well understood.

Of the factors found to be influencing fertility in humans, 37% are reported to be due to female factor infertility [78] with the prevalence of oviductal dysfunction comparable or greater than endometriosis or ovulatory defects [3]. In cattle, up to 43% of reproductive failure can be attributed to loss of the conceptus prior to day 16 after ovulation; however, the role of the oviduct in these losses has yet to be elucidated [79].

Using microarray and NanoString based transcriptional profiling, the objectives of this dissertation were (1) to delineate steroid-driven mechanisms regulating oviductal function as a whole (Chapter 4 and 5), and (2) to specifically examine the inflammatory response within this reproductive organ (Chapter 6 and Appendix 1). Delineating the inflammatory response within the oviduct is of particular interest as aberrant inflammation is reported as one of the most common forms of pelvic inflammatory disease which can lead to fibrosis, tubal infertility and/or ectopic pregnancy in women [2].

Below is a detailed description of the hypothesis and objectives of each study included in this dissertation.

#### **Chapter 4:**

**Title:** A transcriptomal analysis of oviductal epithelial cells collected during the follicular versus luteal phase in cattle

**Hypothesis:** Gene expression profiles of bovine oviductal epithelial cells will differ between the follicular phase (estrogenic environment) versus the luteal phase (progestogenic environment) within the ampulla and isthmus.

**Objectives:** Using microarray based transcriptional profiling, identify spatial and steroid-dependent changes in mRNA and miRNA expression in epithelial cells isolated from the ampulla and isthmus of heifers.

#### **Chapter 5:**

**Title:** Regulation of oviductal function through estrogen-receptor alpha (ESR1): a transcriptomal analysis using transgenic mice

**Hypothesis:** Gene expression profiles of the mouse oviduct will differ between ESR1KO and WT littermates after administration of PMSG at 23 days of age.

**Objectives:** Using an ESR1 knockout mouse model, perform microarray based analysis to identify genes induced by estradiol production and regulated by ESR1.

#### **Chapter 6:**

**Title:** Intraperitoneal administration of lipopolysaccharide induces differential expression of mRNA encoding inflammatory mediators in the oviducts of mice

**Hypothesis:** Intraperitoneal (IP) administration of *E. Coli* -derived lipopolysaccharide (LPS) induces the expression of inflammatory mRNAs in the mouse oviduct.

**Objectives:** With LPS as a systemic inflammatory insult, determine expression changes of inflammatory mRNAs in the oviducts of mice following IP injection with LPS from *E. Coli* using a targeting Nanostring assay to provide evidence of a reliable and repeatable model for the study of oviductal inflammation.

**Appendix 1:**

**Title:** Differential expression of mRNA encoding cytokines and chemokines in the reproductive tract after infection of mice with *chlamydia trachomatis*

**Hypothesis:** mRNA encoding pro-inflammatory cytokines and chemokines will be differentially expressed in the female reproductive tract of mice infected with *C. trachomatis* at both 28 and 35 days post-infection compared to controls.

**Objectives:** Using target superarray gene expression analysis, determine within the reproductive tract the concurrent level of expression of mRNA encoding inflammatory mediators during the later phases of infection using a relatively low infectious load of *C. trachomatis* biovar, serovar D, one of the most prevalent serovars involved in urogenital infections of humans.

## CHAPTER 4.

### A TRANSCRIPTOMAL ANALYSIS OF OVIDUCTAL EPITHELIAL CELLS COLLECTED DURING THE FOLLICULAR VERSUS LUTEAL PHASE IN CATTLE

#### Abstract

Reproductive success depends on a functional oviduct for gamete storage, maturation, fertilization, and early conceptus development. The ovarian-derived steroids estradiol and progesterone are key regulators of oviductal function. The objective of this study was to investigate luteal and follicular phase-specific oviductal epithelial cell function by using microarray-based transcriptional profiling, to increase our understanding of mRNA regulating epithelial cell processes, and to identify novel genes and biochemical pathways that may be found to affect fertility in the future. Six normally cycling Angus heifers were assigned to either luteal phase (LP, high progesterone, n=3) or follicular phase (FP, high estradiol, n=3) treatment groups. Heifers in the LP group were killed between day 11 and 12 after ovulation. Heifers in the FP group were treated with 25 mg PGF<sub>2α</sub> (Lutalyse, Pfizer, NY) at 8 pm on day 6 after ovulation and killed 36 h later. Transcriptional profiling by microarray analysis was performed using total RNA from epithelial cells isolated from sections of the ampulla and isthmus collected from LP and FP treatment groups. Differentially expressed genes were subjected to gene ontology classification and bioinformatic pathway analyses. Statistical one-way ANOVA using Benjamini-Hochberg multiple testing correction for false discovery rate (FDR) and pairwise comparison of epithelial cells in the ampulla of

FP versus LP groups revealed 972 and 597 transcripts up- and down-regulated, respectively ( $P < 0.05$ ). Within epithelial cells of the isthmus in FP versus LP groups, 946 and 817 transcripts were up- and down-regulated, respectively ( $P < 0.05$ ). Up-regulated genes from both ampulla and isthmus were found to be largely involved in cholesterol biosynthesis and cell cycle pathways, while down-regulated genes were found in numerous inflammatory response pathways. Microarray-based transcriptional profiling revealed steroid-dependent changes in the expression of mRNA and miRNA within the epithelium of the oviducts' ampulla and isthmus.

## Introduction

Reproductive success depends on a functional oviduct for gamete storage and maturation, fertilization, and early conceptus development. Ovarian-derived steroids are well known regulators of oviductal function, both estrogen and the progesterone receptors are abundant in the bovine oviducts' mucosal epithelium [80-85], yet our understanding of how the steroidal environment affects the ability of the oviduct to function remains only partially understood. Maturation of gametes and breeding will occur in an estrogen dominant environment, fertilization and early cleavage after the steroidogenic shift and later stages of cleavage and formation of the morula occur within an oviduct exposed to increasing concentrations of circulating progesterone. Increasing our understanding of the steroidal control of oviductal function is critical to the design and implementation of interventions used to manage breeding and the establishment of a pregnancy.

Functionally, the oviduct is divided into two distinct segments: the upper ampulla situated immediately below the ovarian bursa and infundibulum, and the lower isthmus which spans the interval from the ampulla to the uterus. The epithelial mucosa within these two sections consists of ciliated and secretory simple columnar epithelial cells [17], the ratio of which is regulated by steroid hormones [86, 87]. Steroidal regulation of processes that facilitate sperm binding [88], sperm release [89], capacitation [90] and hyperactivation [91] are all established in the literature. Epithelial cells are also an active site of biosynthesis and secretion. A 3- to 5-fold increase in the rate of oviductal secretions can be expected around the time

of estrus [92] and amino acids including glycine, glutamate, aspartate, alanine and lysine are all found in higher concentrations in oviductal fluid than in peripheral plasma [93]. Overall, steroid-regulated epithelial cell secretions can be considered an important mediator of the microenvironment that facilitates gamete and zygote health and early development.

While major efforts have been directed at investigating the ovary and uterus at the transcriptional level [94-96], less extensive investigation has been directed towards the oviduct. Suppressive subtractive hybridization was used in the detailed study of Bauersachs et al., 2004 [18], in which changes in gene expression within the oviductal epithelium were determined in heifers killed on the morning of estrus or 12 days thereafter; our report expanding on their analysis with the use of more current transcriptomal profiling technologies and the determination of spatial differences between the ampulla and the isthmus.

The objective of this descriptive study was therefore to determine global oviductal epithelial cell gene expression profiles during the follicular and luteal phases of the estrous cycle. Specifically, microarray-based transcriptional profiling was used to identify spatial and phase of the cycle-dependent changes in mRNA expression in epithelial cells isolated from the ampulla and isthmus, with the overall goals of increasing our understanding of epithelial processes and identifying novel genes that may be identified as key regulators of fertility in the future. Our results must be interpreted, however, with the knowledge that this analysis does not extract potential spatial (isthmus to ampulla and *visa versa*) signaling mechanisms that could affect oviductal epithelial cell gene expression profiles independent to

phase of the estrous cycle. Given the size of the dataset generated by this analysis, our approach to this descriptive study is not to provide a detailed discussion of genes or processes affected by phase of the estrous cycle, but to summarize the results generated, provide our bioinformatic analyses (as Tables and Supplemental Tables) and make available our data for further analysis by others. The microarray raw data (\*.cel files) collected with the GCOS software, plus the RMA-normalized and log<sub>2</sub> transformed transcript data (Park Genomics Suite [97]), have been deposited into the Gene Expression Omnibus (National Center for Biotechnology Information, <http://www.ncbi.nlm.nih.gov/geo>) as accession number GSE63969.

## **Methods**

### *Animals and Tissue Collection*

Animal procedures involved in this study were approved by the University of Kentucky Animal Care and Use Committee. Six normally cycling Angus heifers were used and at least one spontaneous ovulation was observed in each animal prior to being included in the study. All animals were monitored for behavioral estrus and examined a minimum of every other day by trans-rectal ultrasonography throughout the study period, as described before [98, 99]. After ovulation was confirmed, heifers were assigned to either luteal phase (LP) or follicular phase (FP) treatment groups. Heifers in the LP group (n=3) were killed between day 11 and 12 after ovulation. The rationale for collection of LP oviducts on Day 11 or 12 post-

ovulation was to collect samples under a stable, high progestogenic environment, at a time when the oviduct is undergoing progesterone-dependent remodeling and repair. Heifers in the FP group (n=3) were treated with 25 mg PGF<sub>2α</sub> (Lutalyse, Pfizer, New York, NY) at 8 pm on day 6 after ovulation and killed 36 h later. This is an established protocol in which the dominant follicle of the first follicular wave of the estrous cycle is induced to differentiate into a preovulatory follicle [98-101]. The diameter of the preovulatory follicle (FP group) and the corpus luteum (LP group) prior to retrieval of the tissues was 14.6 +/- 1.0 mm and 21.5 +/- 0.8 mm, respectively. Stage of the cycle was confirmed by visual appearance of the ovaries collected at slaughter.

Heifers were killed by stunning with a captive-bolt pistol and exsanguinated in the Department of Animal and Food Sciences' USDA approved Meat Science Lab. Immediately after exsanguination, the oviduct ipsilateral to the corpus luteum (LP group) or preovulatory follicle (FP group) was dissected free from surrounding connective tissue. Epithelial cells were isolated from small sections of the ampulla and isthmus by using a well-established technique for the collection of bovine oviductal epithelial cells [32, 102, 103]. Briefly, sections of ampulla and isthmus were gently squeezed with fine forceps under a dissecting microscope to separate epithelial cells from residual stroma. Epithelial cells were briefly centrifuged to form a pellet and then snap-frozen in liquid N<sub>2</sub> for later extraction of RNA. Small sections of the ampulla and isthmus were also fixed for 24 h in Bouin's fixative (Sigma-Aldrich, St. Louis, MO) then processed, sectioned and stained by the University of Kentucky Imaging Facility. Tissues were processed through an

ascending series of graded ethyl alcohols, xylene and paraffin then embedded in paraffin. Embedded tissues were sectioned on a microtome at 5  $\mu\text{m}$ , floated on to SuperFrost Plus slides then heat-fixed for a minimum of 2 hours at 48°C on a slide warmer. Hematoxylin and Eosin staining was performed using a ThermoShandon GLX Slide Stainer with Hematoxylin (EKI hematoxylin solution Gills III) and Eosin Y.

### *RNA Extraction and Analysis*

Epithelial cells were isolated from the ampulla and isthmus of the oviduct ipsilateral to the ovary bearing the preovulatory follicle (FP group) or the corpus luteum (LP group). Total RNA was extracted from each sample of epithelial cells using TRIzol reagent (Invitrogen Corporation, Carlsbad, CA, USA) and purified with RNeasy columns (QIAGEN, Valencia, CA) according to the manufacturer's instructions. RNA quality was analyzed by determining the RNA integrity number (RIN) using an Agilent 2100 Bioanalyzer (Agilent Technologies, Palo Alto, CA) at the University of Kentucky Microarray Core Facility. RNA integrity numbers were greater than 9.2 and 28S/18S rRNA absorbance ratios greater than 1.5 for all samples. RNA concentration was then determined via spectrophotometry using a NanoDrop 2000 (Thermo Fischer Scientific-NanoDrop products, Wilmington, DE, USA). Spectrophotometry results revealed 260/280 absorbance ratios greater than 1.95 and 260/230 absorbance ratios greater than 1.5 for all samples.

## *Microarray Analysis*

The Bovine gene 1.0 ST array (GeneChip, Affymetrix, Inc., Santa Clara, CA) was used. Microarray analysis was conducted according to the manufacturer's instructions at the University of Kentucky Microarray Core Facility, as described before [23, 104]. Briefly, RNA (3  $\mu\text{g}/\text{sample}$ ) was reverse transcribed to cDNA using primers containing T7 RNA polymerase, so that the resulting cDNA contained the T7 sequence. In-vitro transcription was then used for the preparation and labeling of cRNA. The biotinylated cRNA were further fragmented and used as probes to hybridize the GeneChips in the GeneChip Hybridization Oven 640, using 1 chip per RNA sample. The raw expression intensity values generated by microarray hybridization were imported into Partek Genomics Suite 6.6 (Partek Inc., St. Louis, MO). Robust Multiarray Analysis algorithm, quantile normalization, and Median Polish were applied for GeneChip background correction, log base<sub>2</sub> transformation, conversion of expression values and probeset summarization [105, 106]. Transcripts were annotated using NetAffx annotation database for the Bovine gene 1.0 ST array and last updated in June 2014.

After data were processed for background adjustment, normalization and log<sub>2</sub> transformed, quality of data was assessed using light intensity expression values on a per chip and per gene basis. For statistical analysis, Partek Genomics Suite 6.6 (Partek Inc.) was used to complete an *F*-test on least-square means to determine significance of each transcript in each comparison. Benjamini-Hochberg multiple testing correction for false discovery rate (FDR) was applied and

significance set to FDR adjusted P-value < 0.05. A post-hoc pairwise comparison of FP compared to LP epithelial cells from the ampulla and isthmus was completed using Fisher's Least Significant Difference (LSD) to determine which means differed [107, 108]. Only transcripts with a fold-change value in expression of at least 1.5 were included in the results. The raw data (\*.cel files), plus the RMA-normalized and log<sub>2</sub> transformed transcript data (Park Genomics Suite [106], have been deposited into the Gene Expression Omnibus (National Center for Biotechnology Information [109]) as accession number GSE63969 (<http://www.ncbi.nlm.nih.gov/geo/query/acc.cgi?acc=GSE63969>).

#### *Real-time RT-PCR Analysis*

Real-time RT-PCR was performed using RNA samples from each tissue and phase of the estrous cycle to determine the expression of mRNA for neurotensin (NTS), binder of sperm 3 (BSP3), lactate dehydrogenase A (LDHA), cyclin D2 (CCND2), early growth response 1 (EGR1) and hydroxysteroid (17 $\beta$ ) dehydrogenase 7 (HSD17B7) using an Eppendorf Mastercycler ep *realplex*<sup>2</sup> system (Eppendorf, Hamburg, Germany) with iQ SYBR Green Supermix (Bio-RAD, Hercules, CA), as described before [23]. Additional validation of the Bovine gene 1.0 ST array has been reported by our laboratory [110]. The following oligonucleotide primer pairs (5' to 3') were used: NTS, F: GTG TGG AAA TGT GAC AGA GCA C and R: GGT AGG CTA GAC TTT GCG GT; BSP3, F: ATT CCT GTG GTG TTC CCT CG and R: GCT CAG AGC ATC ACC TTT GC; LDHA, F: CCA ACA TGG CAG CCT TTT CC and R: ACC GCT TTC CAC

TGT TCC TT; CCND2, F: CCG ACA ACT CCA TCA AGC CT and R: TGA AGT AGT GGC GCA CAG AG; EGR1, F: AGA AAG TTT GCC AGG AGC GA and R: GGA GGG ACG GAG GAG TAT GT; HSD17B7, F: ACA GCT GAA GGA CTG CTG AC and R: CCA GAC AGT GCT TCT GTT CCA; and 18S, F: CGG GGA GGT AGT GAC GAA A and R: CCG CTC CCA AGA TCC AAC TA.

Briefly, cDNA was synthesized using the SuperScript III 1<sup>st</sup> Strand Synthesis System (Invitrogen), with 0.5 µg of RNA used for each reverse transcription reaction. Real-time RT-PCR was performed with a total volume of 25 µL per reaction, with each reaction containing 5 µL of cDNA, 1 µL of a 10 µM stock of each primer (forward and reverse), 12.5 µL of 2× SYBR Green PCR Master Mix, and 5.5 µL of nuclease-free water. The typical dissociation curves of these cDNA, plus 18S as the housekeeping gene was confirmed. RT-PCR reactions were run in triplicate and gene expression was analyzed by the  $2^{\Delta\Delta CT}$  method [111].

#### *Gene Ontology and Pathway Analysis*

Differentially expressed transcripts were interrogated for their gene ontology classes using Partek Genomics Suite 6.6 (Partek Inc.). Partek derives biological processes, molecular functions and cellular components from geneontology.org and/or the affymetrix database. GO hierarchies leads to division of the gene list into significant classifications using Fischer's exact test, right-tailed. When the observed number of genes in a GO category is greater than expected, the GO category is enriched. Pathway analysis was completed by importing

differentially expressed transcripts into QIAGEN'S Ingenuity Pathway Analysis (IPA, QIAGEN, Redwood City, CA, USA, [www.qiagen.com/ingenuity](http://www.qiagen.com/ingenuity)). Ingenuity Pathway Analysis uses data from multiple databases to extrapolate significant pathways and Fischer's exact test was used to determine significant pathways. Significance was set to P-value < 0.05.

## **Results and Discussion**

### *Real-time RT- PCR Analysis of Selected Transcripts*

The effect of stage of the estrous cycle and tissue on the expression of mRNA for NTS, BSP3, LDHA, CCND2, EGR1 and HSD17B7 was performed by real-time RT-PCR. A comparison of the results obtained by RT-PCR and microarray analysis is described in Table 4.1 as a validation of the microarray platform. Additional validation of this Bovine gene 1.0 ST array by real-time RT-PCR performed within our laboratory has been reported [112]. Overall, RT-PCR revealed the same directional trends in gene expression as microarray analysis, with the magnitude of these changes typically lower after analysis using the microarray platform (ratio compression phenomena), as described by others [113]. For example, the expression of mRNA for NTS was found to increase by 32.4- and 150-fold within epithelial cells of the ampulla, and 21.6- and 88-fold within the epithelial cells of the isthmus, in the FP versus the LP groups by microarray analysis and real-time RT-PCR, respectively.

**Table 4.1.** Comparison of gene expression for selected mRNA by microarray and real-time RT-PCR.

<b>Ampulla</b>		<b>Microarray</b>			<b>Real-time RT-PCR</b>			
<b>Gene Symbol</b>	<b>FP vs. LP Fold-Change</b>	<b>FP vs. LP P-value</b>	<b>FP Mean</b>	<b>SEM</b>	<b>LP Mean</b>	<b>SEM</b>	<b>FP vs. LP Fold-Change</b>	<b>FP vs. LP P-value</b>
<b>NTS</b>	32.44	<0.001	1.05	0.12	0.007	0.001	150	<0.001
<b>BSP3</b>	-1.09	0.79	ND					
<b>LDHA</b>	2.22	<0.001	1.13	0.2	0.43	0.1	2.63	0.002
<b>CCND2</b>	1.23	0.35	1.19	0.21	0.91	0.12	1.31	0.27
<b>EGR1</b>	-9.13	0.005	1.19	0.23	111.9	34.2	-94	<0.001
<b>HSD17B7</b>	1.03	0.76	1.07	0.21	0.86	0.12	1.24	0.36
<b>Isthmus</b>		<b>Microarray</b>			<b>Real-time RT-PCR</b>			
<b>Gene Symbol</b>	<b>FP vs. LP Fold-Change</b>	<b>FP vs. LP P-value</b>	<b>FP Mean</b>	<b>SEM</b>	<b>LP Mean</b>	<b>SEM</b>	<b>FP vs. LP Fold-Change</b>	<b>FP vs. LP P-value</b>
<b>NTS</b>	21.57	<0.001	1.51	0.47	0.02	0.008	88	<0.001
<b>BSP3</b>	-7.58	<0.001	1.91	0.74	30.47	11.39	-16	0.01
<b>LDHA</b>	2.34	<0.001	1.05	0.12	0.29	0.08	3.64	<0.001
<b>CCND2</b>	2.36	0.003	1.09	0.18	0.8	0.17	1.38	0.24
<b>EGR1</b>	-5.35	0.019	1.07	0.13	108.4	35.2	-101	<0.001
<b>HSD17B7</b>	-1.13	0.27	1.05	0.12	1.76	0.36	-1.67	0.25

For statistical analysis of the microarray dataset, an F-test on least-square means was used to determine significance of each transcript in each comparison. Benjamini-Hochberg multiple testing correction for false discovery rate (FDR) was applied and significance set to FDR adjusted P-value < 0.05. A post-hoc pairwise comparison of FP compared to LP epithelial cells was completed using Fisher's Least Significant Difference (LSD) to determine which means differed. For the analysis of gene expression by real-time RT-PCR, mean level of expression and SEM are indicated for FP and LP epithelial cells of the ampulla and isthmus, as well as fold change in relative expression (FP vs. LP). For statistical analysis of relative gene expression by real-time RT-PCR, P-values to determine the significance of each transcript were determined using the Student's t-test. ND: Not detectable by real-time RT-PCR.

## *Microarray Quality Control and Principal Component Analysis*

Box plots revealed mean intensity values were similar across all chips and overlapping histograms indicated the frequency of transcripts at specific intensity values for each chip were similar (Supplementary Figure 1 and 2). Quantification of signal intensity to noise revealed that spatial location and phase of the cycle, not error, accounted for the variation within the data set (mean F Ratio for attribute = 30.78, versus mean F value for error = 1.0). Consistent with this, principal component analysis (PCA), which allows for the visualization of patterns through the distribution of samples to highlight similarities and differences [106], revealed clear differences between LP and FP groups, as well as tissue-specific differences within the same phase of the estrous cycle (Figure 4.1). Total variance was 55.5% is the cumulative percent of variance accounted for in our datasets based upon eigenvector multivariate analysis. PC#1 (x-axis, 28%) indicates that the largest proportion of variability is due to phase of the estrous cycle. PC#2 (y-axis, 17.8%) indicates variability between the ampulla and isthmus. PC#3 (z-axis, 9.7%) indicates the variability between phase of the estrous cycle and tissues.

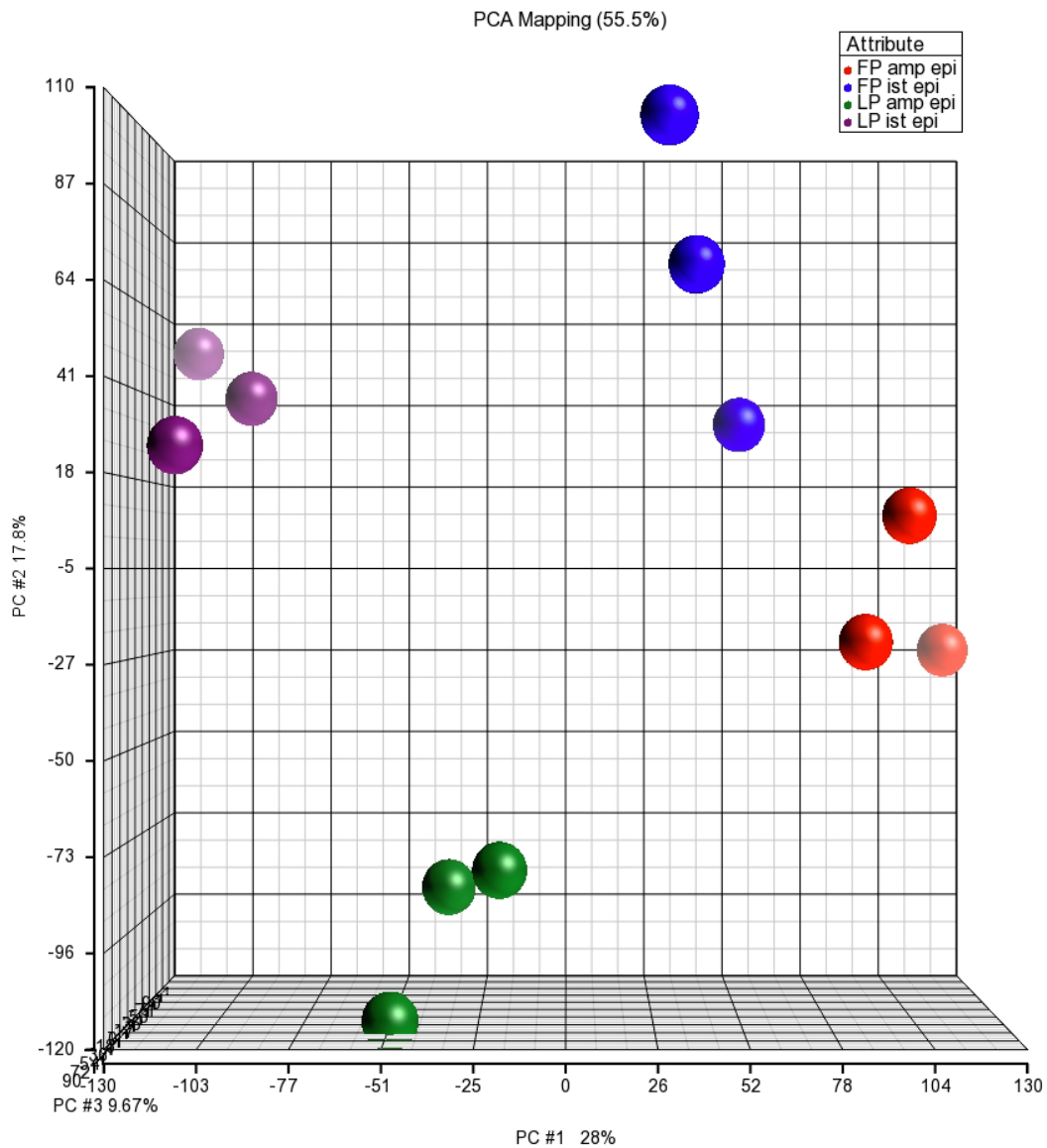


**Figure 4.1.** Principal component analysis of microarray transcriptome results of epithelial cells from the ampulla and isthmus taken from heifers killed in the follicular phase (FP) and luteal phase (LP) of the estrous cycle. Red: FP ampulla, Blue: FP isthmus, Green: LP ampulla, Purple: LP isthmus. Each Bovine 1.0 ST array includes 26,775 probesets.

## Pairwise Comparisons

It is well known that function of the mammalian oviduct is influenced by estradiol and progesterone, with previous studies confirming the presence of mRNA and protein for estrogen receptor alpha (ER $\alpha$ ) and beta (ER $\beta$ ) as well as the nuclear and membrane progesterone receptors (PR, PGRMC1, PGRMC2) within this organ [19, 85]. After chip normalization, a statistical one-way ANOVA and pairwise comparison (LSD test) of gene expression in epithelial cells of the ampulla and isthmus in the FP and LP groups was performed to generate a list of 2374 differentially expressed genes (DEGs). Table 4.2 indicates the number of DEGs in each pairwise comparison. As expected, there were a large number of DEGs identified by FP (1563 DEGs) and LP (1758 DEGs) pairwise comparisons. Among these DEGs, 947 DEGs overlapped between contrasts (Figure 4.2). By pairwise comparison, 616 DEGs were exclusive to the ampulla and 811 DEGs were exclusive to the isthmus.

**Table 4.2.** Number of differentially expressed genes (DEGs) in epithelial cells of the ampulla and isthmus between follicular and luteal phase groups (FDR adjusted  $P < 0.05$ ).

Parameter	DEGs	Up-regulated	Down-regulated
FP vs. LP (Ampulla)	1563	968 (62%)	595 (38%)
FP vs. LP (Isthmus)	1758	943 (54%)	815 (46%)

Heifers in the follicular phase group (n=3) were treated with 25 mg PGF $_{2\alpha}$  at 8 pm on Day 6 of the estrous cycle and killed 36 h later. Heifers in the luteal phase group (n=3) were killed on Day 11 or 12 of the estrous cycle. For statistical analysis, an *F*-test on least-square means was used to determine significance of each transcript in each comparison. Benjamini-Hochberg multiple testing correction for false discovery rate (FDR) was applied and significance set to FDR adjusted  $P$ -value  $< 0.05$ .

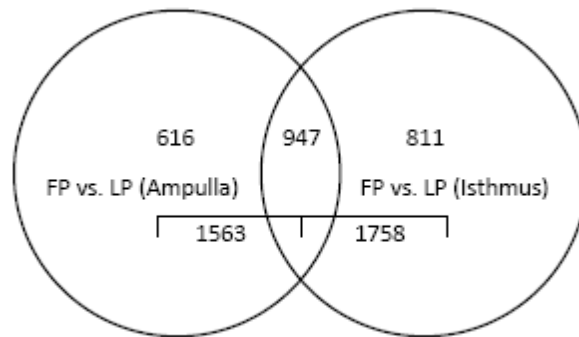


**Figure 4.2.** Venn diagram depicting the number of differentially expressed genes in follicular phase versus luteal phase epithelial cells from the ampulla and isthmus (FDR adjusted  $P < 0.05$ ).

#### *DEGs in Epithelial Cells of the Ampulla*

The ampulla is situated immediately below the ovarian bursa and infundibulum and is the site of fertilization. Histological evaluations have shown the ampulla to have an elaborate, extensively folded epithelial layer adjacent to a thin layer of smooth muscle (Figure 4.3A). Evaluation of the oviducts of cattle [28, 77, 92] confirm that this is a dynamic tissue with multiple, ongoing biological processes that include cell proliferation [17] and tissue remodeling [114]. The most highly up- and down-regulated DEGs within epithelial cells of the ampulla in FP versus LP groups are provided as Table 4.3.

**Table 4.3.** Most highly up- and down-regulated DEGs within epithelial cells of the ampulla in follicular versus luteal phase groups (FDR adjusted P < 0.05).

<b>Gene Symbol</b>	<b>Gene Description</b>	<b>P-value</b>	<b>Fold-Change</b>
NTS	Neurotensin	< 0.001	32.44
PRND	prion protein 2 (dublet)	< 0.001	18.30
CDC20B	cell division cycle 20 homolog B (S. cerevisiae)	< 0.001	17.49
bTrappin-5	trappin 5	< 0.001	11.14
TMEM45A	transmembrane protein 45A	0.004	10.69
CRELD2	cysteine-rich with EGF-like domains 2	< 0.001	9.98
SLC2A10	solute carrier family 2 (facilitated glucose transporter), member 10	< 0.001	9.54
SDF2L1	stromal cell-derived factor 2-like 1	< 0.001	9.29
MIR449C	microRNA mir-449c	< 0.001	9.20
KRT23	keratin 23 (histone deacetylase inducible)	0.004	8.40
DNAJB11	DnaJ (Hsp40) homolog, subfamily B, member 11	< 0.001	6.92
MANF	mesencephalic astrocyte-derived neurotrophic factor	< 0.001	6.90
MFSD2A	major facilitator superfamily domain containing 2A	< 0.001	6.70
CLPH	calcium-binding protein, spermatid-specific 1 (CABS1)	< 0.001	6.61
PLA2G4D	phospholipase A2, group IVD (cytosolic)	< 0.001	6.61
CBLN4	cerebellin 4 precursor	< 0.001	6.57
SERPINE3	serpin peptidase inhibitor, clade E (nexin, plasminogen activator inhibitor type 1), member 3	< 0.001	6.54
RRM2	ribonucleotide reductase M2	< 0.001	6.52
H4	histone H4	< 0.001	6.30
INSIG1	insulin induced gene 1	< 0.001	6.21
<b>Gene Symbol</b>	<b>Gene Description</b>	<b>P-value</b>	<b>Fold-Change</b>
EGR1	early growth response 1	0.005	-9.13
FOS	FBJ murine osteosarcoma viral oncogene homolog	0.002	-8.55
VCAM1	vascular cell adhesion molecule1	< 0.001	-7.11
GABRP	gamma-aminobutyric acid (GABA) A receptor, pi	< 0.001	-6.76
GPR174	G protein-coupled receptor 174	0.003	-5.15
ZBTB16	zinc finger and BTB domain containing 16	0.001	-4.62

**Table 4.3.** (Continued)

BMP4	bone morphogenetic protein 4	0.001	-4.44
LOC777601	uncharacterized LOC777601	< 0.001	-4.37
FIGF	c-fos induced growth factor (vascular endothelial growth factor D)	< 0.001	-4.12
KLRK1	killer cell lectin-like receptor subfamily K, member 1	0.003	-4.09
PDK4	pyruvate dehydrogenase kinase, isozyme 4	0.001	-3.93
LOC100297676	C-type lectin domain family 2 member G-like	0.003	-3.78
LOC100337183	contactin associated protein-like 3-like	0.008	-3.71
LOC768255	GTPase, IMAP family member 4-like	0.001	-3.64
TRAT1	T cell receptor associated transmembrane adaptor 1	0.007	-3.48
CAPN6	calpain 6	0.007	-3.48
CAV1	caveolin 1, caveolae protein, 22kDa	0.005	-3.44
LOC541007	Similar to protein jade-2(PHD finger protein 15) (BT24231-RA)	< 0.001	-3.34
CHRD1	chordin-like 1	0.002	-3.31
MIR29C	microRNA mir-29c	0.001	-3.29

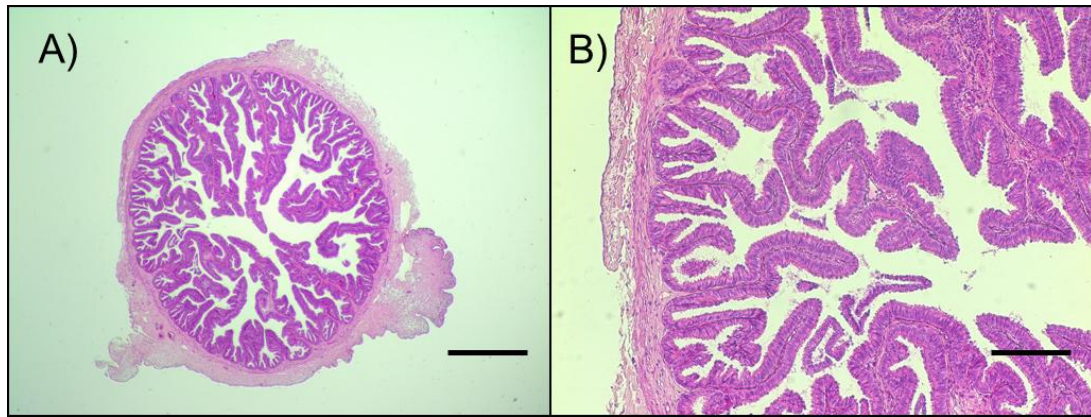


**Figure 4.3.** Representative images of the ampulla (A,B) of the bovine oviduct. Scale bar: A= 1000  $\mu$ M; B= 250  $\mu$ M. Images are from one heifer collected during the follicular phase of the estrous cycle. Sections were stained with hematoxylin and eosin.

As indicated above, a detailed discussion of the role for individual genes identified by this analysis is not our objective, however examples of consistency among our profiling results and more targeted analyses performed by others is warranted. Of the up-regulated genes, the expression of mRNA for neurotensin (NTS) was found to increase by 32.4-fold within epithelial cells of the ampulla in the FP versus the LP groups. Neurotensin has multiple functions and evidence suggests that NTS plays a role in gamete and conceptus transport within the oviduct [115]. Receptors for NTS are expressed on spermatozoa, and increasing NTS administration facilitates sperm protein tyrosine phosphorylation, which is a measure of sperm capacitation [44]. Furthermore, the acrosome reaction is promoted in capacitated spermatozoa in the presence of increasing concentrations of NTS [44], consistent with the increased expression of NTS observed in the

follicular phase, herein. In contrast to this established role of NTS, and consistent with our objective to identify novel genes that may be revealed as critical mediators of function in the future, the transcription factor early growth response 1 (EGR1) was observed to display the highest fold-change (9.1-fold) among down-regulated genes within epithelial cells of the ampulla in the FP versus the LP groups. A gonadotropin-dependent induction of EGR1 has been reported prior to ovulation in bovine follicles [116], however no reports to date are apparent on the function, or importance, of this transcription factor in the epithelium of the oviducts' ampulla.

Up- and down-regulated DEGs were analyzed for enriched gene ontology classifications. Gene ontology analysis of up-regulated DEGs within epithelial cells of the ampulla in the FP versus the LP groups resulted in 117 significant biological processes, 65 significant cellular components, and 46 significant molecular functions ( $P < 0.05$ ). Cell cycle, cholesterol biosynthetic process, cell division, mitosis and protein folding were the top biological processes identified, which is not surprising considering the cell proliferation and secretory activity required to prepare the ampulla for the arrival of the gametes. With respect to cholesterol biosynthesis, steroid-dependent effects on the oviduct are documented in the literature. Cholesterol will affect the ability of spermatozoa to fertilize an oocyte [117], with the process of capacitation well established to require efflux of cholesterol from the plasma membrane of spermatozoa (reviewed in [118]). High density lipoproteins are elevated in bovine oviductal fluid during the follicular phase of the estrous cycle [119]; however, the synthesis and release of cholesterol by oviductal epithelial cells appears to be greater under a progesterone dominant

environment. Esterified-cholesterol containing lipid droplets from oviductal epithelial cells were observed in greater numbers when collected from luteal-phase cows [120] and the concentration of cholesterol was increased in isthmic but not ampullary oviductal fluid collected from the luteal phase versus non-luteal phase animals [121]. Further analysis of the biochemical relationship among the DEGs expressed within these top cholesterol-associated pathways may increase our understanding of the role of cholesterol during the processes of capacitation and fertilization, critical events that occur within the oviduct. Top cellular components of up-regulated DEGs within epithelial cells of the ampulla in the FP versus the LP groups included endoplasmic reticulum lumen and membrane, cytoplasm, and mitochondrion. Top molecular functions involved protein disulfide isomerase activity, FK506 binding, peptidyl-prolyl cis-trans isomerase activity, oxidoreductase activity, and dolichyl-diphosphooligosaccharide-protein glycotransferase activity.

Analysis of down-regulated DEGs within epithelial cells of the ampulla in the FP versus the LP revealed 118 significant biological processes, 18 significant cellular components, and 49 significant molecular functions ( $P < 0.05$ ). The top biological processes were the innate immune response, response to nicotine, myoblast proliferation, negative regulation of MAP kinase activity, and bone morphogenetic protein (BMP) signaling pathway. With respect to immune responses, it can be postulated that increases in estradiol during the follicular phase decrease the induction of pro-inflammatory factors, with the results of our study consistent with an investigation on the effect of ovarian steroids on lipopolysaccharide (LPS)-induced responses in bovine oviductal epithelial cells *in vitro* [77]. In their report,

estradiol reversed the effect of LPS on pro-inflammatory gene expression and we have previously demonstrated ESR1-dependent as well as cyclic changes in the expression of the hematopoietic form of prostaglandin D synthase, a putative regulator of inflammation, in the mouse oviduct [23]. Given that the oviductal epithelium must continually repair itself from any damage caused by exposure to gametes, seminal fluids and post-ovulatory follicular debris, steroid-dependent changes in inflammatory response mechanisms can be considered physiologically important biological processes. Lastly, top cellular components associated with the down-regulated DEGs were plasma membrane, cytoplasm, extracellular region, cytosol, and tight junction and top molecular functions were pancreatic ribonuclease activity, transmembrane signaling receptor activity, protein-L-isoaspartate (D-aspartate) O-methyltransferase activity, serine hydrolase activity, and phosphatidylinositol-3,4-bisphosphate binding.

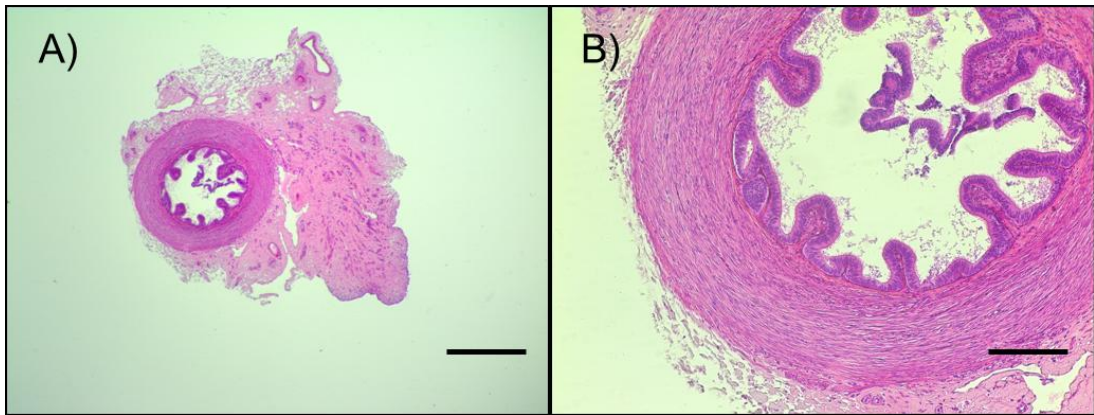
Canonical pathway analysis of DEGs within epithelial cells of the ampulla in the FP versus the LP was then determined using QIAGEN'S Ingenuity Pathway Analysis (IPA, QIAGEN, Redwood City, [www.qiagen.com/ingenuity](http://www.qiagen.com/ingenuity)). Top pathways up-regulated in the follicular phase largely reflected cholesterol biosynthesis (Superpathway of Cholesterol Biosynthesis, Cholesterol Biosynthesis I, Cholesterol Biosynthesis II (via 24,25-dihydrolanosterol), Cholesterol Biosynthesis III (via Desmosterol)), and Oxidative Phosphorylation ( $P < 0.05$ , Supplementary Figure 3A), which was consistent with the results of the gene ontology analysis discussed above. The top pathways for down-regulated genes included Hepatic Fibrosis / Hepatic Stellate Cell Activation, Role of Pattern Recognition Receptors in Recognition of

Bacteria and Viruses, Colorectal Cancer Metastasis Signaling, Ovarian Cancer Signaling, and Role of Macrophages, Fibroblasts and Endothelial Cells in Rheumatoid Arthritis ( $P < 0.05$ , Supplementary Figure 3B). Again, this canonical pathway analysis is consistent with steroid-dependent regulation of inflammation and immune responses extracted by the gene ontology analysis. Worthy to note, given the increasing interest in oviductal epithelial cells as progenitors for ovarian cancer [122-124], down-regulation of the DEGs in the ovarian cancer signaling canonical pathway (MMP7, ARRB1, FZD4, FGF9, SMO, FIGF, CCND1, PDGFC, FZD7, EGFR and BCL2) could provide useful clues that can advance that important field of study. In addition, potential effects of the presence of the conceptus to the oviductal epithelium should not be overlooked. We observed down-regulation of 7 DEGs, including that of insulin-like growth factor binding protein 3 (IGFBP3) in epithelial cells of the ampulla in FP versus LP groups, whose expression in primary bovine oviductal epithelial cells in vitro is increased by the addition of a conceptus to their culture [125].

#### *DEGs in Epithelial Cells of the Isthmus*

Similar to the ampulla, the mucosa of the isthmus appears well defined in histological evaluations (Figure 4.4A and B). However, in contrast to the ampulla, the mucosa of the isthmus is located adjacent to a prominent musculature with this smooth musculature playing a key role in the movement of gametes to the site of fertilization and passage of the early conceptus to the uterus [126-128]. Several of

the DEGs within epithelial cells of the isthmus in the FP versus the LP were similar to those identified within the ampulla; however, there were also many DEGs unique to this spatial location. Among the up-regulated DEGs in the epithelium of the isthmus (Table 4.4), the increased expression of mRNA encoding phospholipase A2, group IVD (cytosolic) (PLA2G4D) and phospholipase A2, group IVF (PLA2G4F) is interesting, especially when considering the key role for prostaglandins within the oviduct [33, 127, 129] and the noted regulations of prostaglandin synthesis by



ovarian steroids as reported by us [23] and others [58, 130].

**Figure 4.4.** Representative images of the isthmus (A,B) of the bovine oviduct. Scale bar: A = 1000  $\mu$ M; B= 250  $\mu$ M. Images are from one heifer collected during the follicular phase of the estrous cycle. Sections were stained with hematoxylin and eosin.

**Table 4.4.** Most highly up- and down-regulated DEGs within epithelial cells of the isthmus in follicular phase versus luteal phase groups (FDR adjusted P < 0.05).

<b>Gene Symbol</b>	<b>Gene Description</b>	<b>P-value</b>	<b>Fold-Change</b>
KRT23	keratin 23 (histone deacetylase inducible)	< 0.001	22.57
NTS	Neurotensin	< 0.001	21.57
PRND	prion protein 2 (dublet)	< 0.001	12.36
STRA6	stimulated by retinoic acid gene 6 homolog (mouse)	< 0.001	11.22
TMEM45A	transmembrane protein 45A	0.004	10.56
PKHD1L1	polycystic kidney and hepatic disease 1 (autosomal recessive)-like 1	0.004	9.86
LPL	lipoprotein lipase	< 0.001	9.40
SLC7A11	solute carrier family 7 (anionic amino acid transporter light chain, xc- system), member 11	< 0.001	8.92
CLEC3A	C-type lectin domain family 3, member A	< 0.001	8.69
GFAP	glial fibrillary acidic protein	< 0.001	8.09
CRELD2	cysteine-rich with EGF-like domains 2	< 0.001	7.69
CA2	carbonic anhydrase II	< 0.001	7.68
PLA2G4D	phospholipase A2, group IVD (cytosolic)	< 0.001	7.64
CHI3L1	chitinase 3-like 1 (cartilage glycoprotein-39)	0.001	7.34
SDF2L1	stromal cell-derived factor 2-like 1	< 0.001	7.31
PPP2R2C	protein phosphatase 2, regulatory subunit B, gamma	0.000	7.30
P2RX2	purinergic receptor P2X, ligand-gated ion channel, 2	0.002	6.86
PLA2G4F	phospholipase A2, group IVF	< 0.001	6.85
SLC2A10	solute carrier family 2 (facilitated glucose transporter), member 10	< 0.001	6.69
CDC20B	cell division cycle 20 homolog B ( <i>S. cerevisiae</i> )	0.001	6.35
<b>Gene Symbol</b>	<b>Gene Description</b>	<b>P-value</b>	<b>Fold-Change</b>
KLF17	Kruppel-like factor 17	< 0.001	-14.70
KSR2	kinase suppressor of ras 2	< 0.001	-8.94
LOC100337391	predicted protein-like	< 0.001	-7.77
BSP3	binder of sperm 3	< 0.001	-7.58
OR9Q2	olfactory receptor, family 9, subfamily Q, member 2	0.001	-6.87
ZBTB16	zinc finger and BTB domain containing 16	< 0.001	-5.91
EGR1	early growth response 1	0.019	-5.35
LOC522479	ovalbumin-like	< 0.001	-5.34
CWH43	cell wall biogenesis 43 C-terminal homolog ( <i>S. cerevisiae</i> )	0.001	-5.09
TFF3	trefoil factor 3 (intestinal)	< 0.001	-4.98

**Table 4.4.** (Continued)

LOC100335 668	mitochondrial import inner membrane translocase subunit Tim9 pseudogene	0.001	-4.94
LOC617981	family with sequence similarity 55, member C- like	< 0.001	-4.92
MEGF10	multiple EGF-like-domains 10	< 0.001	-4.81
LOC100337 183	contactin associated protein-like 3-like	0.003	-4.75
AK5	adenylate kinase 5	< 0.001	-4.74
FOS	FBJ murine osteosarcoma viral oncogene homolog	0.012	-4.54
CA10	carbonic anhydrase X	0.001	-4.40
NDP	Norrie disease (pseudoglioma)	< 0.001	-4.34
SEMA5A	sema domain, seven thrombospondin repeats (type 1 and type 1-like), transmembrane domain (TM) and short cytoplasmic domain, (semaphorin) 5A	< 0.001	-4.26
CAV1	caveolin 1, caveolae protein, 22kDa	0.003	-4.14

Both PLA2G4D and PLA2G4F belong to the phospholipase A2 (PLA2) family, group 4. The PLA2 family of enzymes catalyzes the hydrolysis of phospholipids to liberate free fatty acids, among other molecules. Of these free fatty acids, arachidonic acid released by PLA2 enzymes acts as the precursor for the synthesis of prostaglandins [131, 132]. Consistent with our results, in ovariectomized rabbits, PLA2 activity in epithelial cells of the ampulla is reported to be increased after treatment of rabbits with estradiol [133]. Given that PLA2G4D and PLA2G4F do not appear to be described within the oviduct, our results can be considered as new information on the local regulation of phospholipases and potentially prostaglandin secretion within this organ. Of the down-regulated DEGs expressed by epithelial cells of the isthmus, the expression of binder of sperm 3 (BSP3) is also identified as a novel transcript. BSP3 is reported to be secreted by seminal vesicles and binds to sperm [134], and identified within the epithelial cells of the isthmus herein. Again,

the potential to modify the epithelial cell transcriptome by the presence of a conceptus must be acknowledged. We observed down-regulation of 10 DEGs, including that of the apoptosis regulator XIAP associated factor-1 (XAF1) in epithelial cells of the isthmus in FP versus LP groups, whose expression has been reported to be increased by the addition of a conceptus to cultures of primary bovine oviductal epithelial cells [125].

Gene ontology classification of up-regulated DEGs within epithelial cells of the isthmus in the FP versus the LP revealed 97 significant biological processes with top biological processes being protein folding, cell cycle, cell division, mitosis, and electron transport chain ( $P < 0.05$ ). Similar to the ampulla, there were 57 significant cellular components affected by stage of the cycle within epithelial cells of the isthmus, including endoplasmic reticulum lumen and membrane, cytoplasm, and mitochondrion and 46 significant molecular functions. Gene ontology analysis of the down-regulated DEGs within epithelial cells of the isthmus revealed 101 significant biological processes, 26 significant cellular components, and 45 significant molecular functions ( $P < 0.05$ ). Top biological processes were negative regulation of fibroblast growth factor receptor signaling pathway, calcium-independent cell-cell adhesion, inactivation of MAPK activity, brown fat cell differentiation, and SMAD protein signal transduction. Top cellular components were similar to those observed within the ampulla and included cytoplasm, plasma membrane cytosol, extracellular region, and tight junction.

Again, QIAGEN'S Ingenuity Pathway Analysis (IPA, QIAGEN, Redwood City, [www.qiagen.com/ingenuity](http://www.qiagen.com/ingenuity)) was used to identify the canonical pathways affected

by stage of the cycle within epithelial cells of the isthmus. Up-regulated DEGs within epithelial cells of the isthmus in FP versus LP were oxidative phosphorylation, mitochondrial dysfunction, superpathway of cholesterol biosynthesis, superpathway of geranylgeranyldiphosphate biosynthesis I (via mevalonate), and mevalonate pathway I ( $P < 0.05$ , Supplementary Figure 4A). Similar to that observed in the ampulla, cholesterol biosynthesis stands out as a key pathway with gene expression increased under an estrogen dominant environment. Consistency in response was also observed among down-regulated DEGs. Top pathways for down-regulated DEGs included molecular mechanisms of cancer, basal cell carcinoma signaling, role of osteoblasts, osteoclasts and chondrocytes in rheumatoid arthritis, Role of Macrophages, Fibroblasts and Endothelial Cells in Rheumatoid Arthritis, and Corticotropin Releasing Hormone Signaling ( $P < 0.05$ , Supplementary Figure 4B).

## **Conclusions**

At the genome level, estrous cycle stage-dependent effects on epithelial cell gene expression are not well defined. The current study therefore investigated changes in the expression of mRNA within the epithelium of the ampulla and isthmus of the bovine oviduct during the luteal and follicular phases of the estrous cycle. This transcriptomal profiling analysis was performed to increase our understanding of gene expression and potentially epithelial cell processes important for oviductal function and fertility, and to identify novel mRNA that may prove critical for fertility after analysis in the future.

## CHAPTER 5.

# REGULATION OF OVIDUCTAL FUNCTION THROUGH ESTROGEN-RECEPTOR ALPHA (ESR1): A TRANSCRIPTOMAL ANALYSIS USING TRANSGENIC MICE

### Abstract

The oviduct provides the microenvironment necessary for gamete storage and maturation, fertilization, and early development of the conceptus. Within the oviduct, ESR1 is the predominant estrogen receptor expressed mediating the effects of estrogens on a variety of oviductal functions. Specifically, transcriptional regulation whereby hormone bound receptors target the estrogen responsive element (ERE) on DNA gene sites to either enhance or repress transcription. Considering the early reproductive events that occur in the oviduct during the estrogen dominant phase, ESR1 is essential for reproductive success. The objective of this study was to determine ESR1-dependent changes in gene expression in the oviducts of mice using the Affymetrix Genechip Mouse Genome 430-2.0 arrays (Affymetrix Inc., CA). Whole oviducts were collected from immature mice with a global deletion of ESR1 (ESR1KO) and their wild-type (WT) littermates at 23 days of age or 48 hr after treatment of ESR1KO or WT littermates with 5 IU of PMSG. Stimulation with PMSG and collection of oviducts 48 hr later is an established protocol in which to induce follicular development and production of estradiol. Oviducts from 3-4 mice were pooled for each genotype and time point and total RNA extracted and purified using TRIzol and RNeasy columns. Three independent

replicates were collected for microarray analysis. Following microarray hybridization, the resulting dataset was analyzed using Partek Genomics Suite 6.6 (Partek Inc., MO). GC-RMA, quantile normalization, and Median Polish were applied for GeneChip background correction, log base2 transformation, conversion of expression values and probeset summarization. Statistical 2-way ANOVA revealed 2428 genes affected by genotype and treatment ( $P < 0.01$ , FDR  $< 0.13$ ) and a pairwise comparison of ESR1KO PMSG treatment versus WT PMSG treatment identified 496 significantly up-regulated genes and 690 significantly down-regulated genes with at least a 2 fold difference between groups ( $P < 0.01$ ). Differentially expressed genes from the pairwise comparison were subjected to pathway analysis using Fischer's exact test to determine significant pathways. Up-regulated genes were found to be involved in immune response and cell signaling pathways, while down-regulated genes were found in pathways related to cholesterol biosynthesis and reflected functions such as cellular hypertrophy, lipid metabolism, molecular transport, and cellular morphology. These results indicate many biological processes regulated by ESR1 and may reveal the identity of novel genes involved in oviduct function for future analysis.

## Introduction

Reproductive success depends on a functional oviduct for gamete storage, maturation, fertilization, and early-conceptus development. Ovarian-derived estradiol is a known regulator of oviductal function with the transcription factor, estrogen receptor- $\alpha$  (ESR1) being the predominant estrogen receptor expressed in the oviduct [135, 136]. ESR1 is essential for reproductive function and plays a diverse role such as, transcriptional regulation, whereby hormone bound receptors target the estrogen responsive element (ERE) on DNA gene sites to either enhance or repress transcription [137, 138]. The expression of ESR1 in the oviduct has been localized to ciliated and secretory epithelial cells, stromal cells, and muscle cells throughout the estrous cycle with cyclic changes in circulating concentrations of estradiol regulating ESR1 protein expression [19, 21, 25]. Several studies have described the morphological and functional dependence of the oviduct on estrogens and ESR1 [21, 83]. For example, long term administration of exogenous estradiol leads to cellular hypertrophy and increased protein synthesis in secretory epithelial cells from the mouse oviduct in vivo [21]. Furthermore, our lab has previously reported a proposed regulator of inflammation within the oviduct, hematopoietic form of prostaglandin D synthase (HPGDS), which was found to be dependent upon ESR1 expression [23]. However, genome-wide reports on estradiol and ESR1 regulation of oviductal function remain limited.

The development of estrogen receptor knockout mouse models has advanced our understanding of the physiological role of ESR1 in reproductive tissues.

Estrogens are known to stimulate epithelial cell proliferation and differentiation in the uterus and ESR1KO mice are infertile due to underdeveloped and hyperplastic uteri [139]. ESR1KO females also develop cystic ovaries due to elevated concentrations of estradiol leading to aberrant regulation of the hypothalamic-pituitary axis [139, 140].

Given that the incidence of tubal dysfunction is comparable to endometriosis and impaired ovarian function and as a reason for woman to seek treatment for infertility, our objective herein was to identify estradiol and ESR1-dependent changes in mRNA expression in the oviduct. Specifically, microarray-based transcriptional profiling was performed using oviducts collected from mice bearing a global deletion of ESR1 (ESR1KO) and their control littermates (WT). Global gene expression profiles were also determined in oviducts collected from ESR1KO and WT controls after ovarian estradiol production was stimulated by treatment with PMSG. Given the size of the dataset generated by this analysis, our approach is not to provide a detailed discussion of genes or processes affected by genotype, but to summarize the results and provide our bioinformatics analysis (as Tables and Supplementary Tables) and make our data available for further analysis by others. In addition, the differentially expressed gene list generated from, PMSG-treated ESR1KO versus PMSG-treated WT mice was subjected to gene ontology and pathway analysis to increase our understanding of oviductal processes dependent on estradiol and ESR1 that may be identified as key regulators of fertility in the future.

## Methods

### *Animals and Tissue Collection*

All animal procedures were approved by the University of Kentucky Institutional Care and Use Committee. Mice with a global deletion of ESR1 (ESR1KO) on a C57BL/6 background were generated as previously described [23, 141]. Briefly, two transgenic mouse lines were used, male ESR1<sup>fllox/fllox</sup> were bred with female Zp3<sup>cre</sup> to produce a line expressing cre recombinase in the oocyte. The F1 heterozygotes (ESR1<sup>fllox/+</sup>Zp3<sup>cre</sup>) were bred with ESR1<sup>fllox/fllox</sup> resulting in ESR1<sup>fllox/fllox</sup>Zp3<sup>cre</sup> mice, where females produce oocytes that are ESR1<sup>-</sup>. The ESR1<sup>-</sup> oocytes were then fertilized with sperm from ESR1<sup>fllox/fllox</sup> males resulting in ESR1<sup>fllox/-</sup> progeny. Inbreeding of two ESR1<sup>fllox/-</sup> mice produces a litter where one fourth of progeny are ESR1<sup>-/-</sup>. Female littermates that expressed ESR1 served as wild-type (WT) controls. Genomic DNA was extracted from ear punches using the Easy DNA kit (Invitrogen, Carlsbad CA) to confirm genotypes, as previously described [23, 141]. Whole oviducts were collected for extraction of RNA from immature female mice (ESR1KO and WT) killed at 23 days of age, or ESR1KO and WT mice treated with 5 IU PMSG at 23 days of age and killed 48 h later.

### *RNA Extraction and Analysis*

Oviducts were pooled from 3-4 mice per treatment group and total RNA was extracted using TRIzol Reagent (Invitrogen, Carlsbad, CA) and purified through RNeasy columns (Qiagen, Valencia, CA), as described before [23]. RNA was analyzed for quality and quantified by spectrophotometry using an Eppendorf BioPhotometer Plus (Eppendorf, Hamburg, Germany) with a mean 260/280 ratio of  $1.75 \pm 0.10$  among all samples. Aliquots of the same total RNA were used for both microarray and real-time reverse-transcription PCR (real-time RT-PCR).

### *Microarray Hybridization and Analysis*

A total of 12 microarray hybridizations were performed using the Affymetrix Genechip Mouse Genome 430-2.0 arrays (GeneChip, Affymetrix, Inc., Santa Clara, CA) according to the manufacturer's instructions at the University of Kentucky Microarray Core Facility, as described before [142]. Three replicates using different mice were generated for each treatment group.

Microarray data were analyzed by importing raw expression intensity values (\*.cel files) into Partek Genomics Suite 6.6 (Partek Inc., St. Louis, MO), where the GC-Robust Multiarray Analysis algorithm (GC-RMA), quantile normalization, and Median Polish was applied for GeneChip background correction, log base 2 transformation, conversion of expression values and probeset summarization. Annotation was performed using NetAffx annotation database (Release 34) on

December 3<sup>rd</sup>, 2014. Quality of data was assessed using light intensity expression values on a per chip and per gene basis and visualized as box plots (Figure 5.1).

Principal component analysis (PCA) was conducted to determine the quality of the microarray hybridization and visualize the general data variation among the chips (Figure 5.2), as previously described [106].

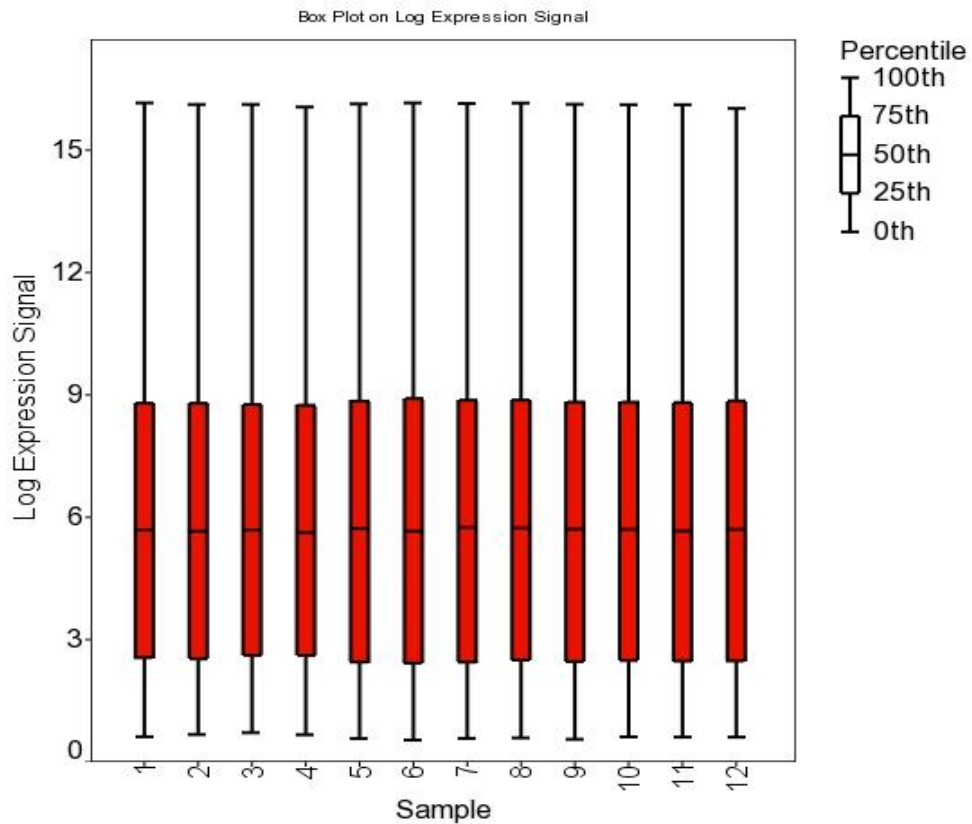


**Figure 5.1.** Box plot of the  $\log_2$  expression signal for each sample (microarray chip).

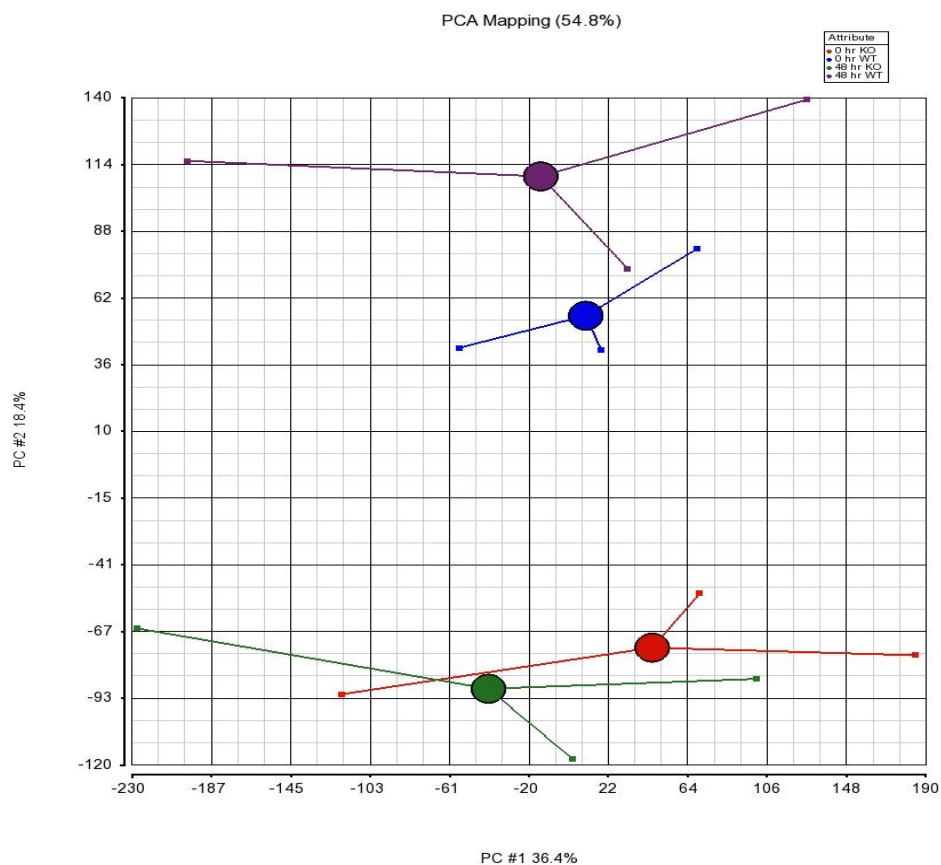


**Figure 5.2.** Principal component analysis of microarray transcriptome results of oviducts collected from ESR1KO and WT littermates with or without PMSG treatment. Red: 0 hr ESR1KO, Blue: 0 hr WT, Green: PMSG-treated ESR1KO, Purple: PMSG-treated WT mice.

For statistical analysis, to detect differentially expressed genes (DEG's) and the interaction between genotype and PMSG treatment, the normalized and background adjusted microarray data were imported into Partek Genomics suite 6.6 (Partek, Inc.) and a two-way ANOVA performed with factor 1 being genotype and factor 2 being PMSG treatment. Statistical significance of difference for each gene was set to P-value <0.01 with Benjamini-Hochberg multiple testing correction for false discovery rate (FDR) < 0.13. Genes considered significant in the overall model

( $P < 0.01$ , FDR  $< 0.13$ ) were then subjected to pairwise comparisons using Fischer's Least Significant Difference (LSD) test to estimate the significance of difference for each gene in each comparison. Genes showing a mean difference in signal intensity of at least 2-fold change and a P-value  $< 0.01$  were considered differentially expressed.

All the microarray raw data (13 \*.cel files) collected and GCRMA-normalized and  $\log_2$  transformed intensity values will be deposited into the Gene Expression Omnibus (National Center for Biotechnology Information, <http://www.ncbi.nlm.nih.gov/geo>).

#### *Gene Ontology Analysis*

The DEG list (1185 DEG's) from, PMSG-treated ESR1KO versus PMSG-treated WT mice was subjected to gene ontology and pathway analysis. Differentially expressed genes were interrogated for their gene ontology (GO) classes using Partek Genomics Suite 6.6 (Partek, Inc.). Partek derives gene ontology classifications from geneontology.org and/or the affymetrix database. GO hierarchies leads to the division of the gene list into significant classifications when the observed number of differentially expressed genes in a GO category is greater than expected. Statistical analysis for significant classifications was performed using Fischer's exact test, right-tailed. A P-value  $< 0.01$  is suggestive of an over representation of genes from within a particular GO category, indicative of a functional effect.

### *Pathway Analysis*

The list of DEG's from PMSG-treated ESR1KO versus PMSG-treated WT mice was then subjected to Ingenuity Pathway Analysis (IPA®, QIAGEN Redwood City, [www.qiagen.com/ingenuity](http://www.qiagen.com/ingenuity)) which uses multiple databases to extrapolate significant pathways based on the number of significant genes within our list and known to be involved in a particular pathway. To determine significant pathways in the oviducts of PMSG-treated ESR1KO versus PMSG-treated WT treated mice, a Fischer's exact test was performed with significance set to P-value < 0.05.

### *Real-time RT-PCR Analysis*

Pathway analysis revealed that the most significant pathways were reflective of immune responses. Therefore, to validate the microarray analysis, real-time RT-PCR for a selection of mRNA known to be involved in immune response pathways was performed using an Eppendorf Mastercycler ep *realplex*<sup>2</sup> system (Eppendorf) using iQ SYBR Green Supermix (Bio-RAD, Hercules, CA), as described before [23]. Briefly, cDNA was synthesized using the SuperScript III 1<sup>st</sup> Strand Synthesis System (Invitrogen), with 0.5 µg of RNA used for each reverse transcription reaction. Real-time RT-PCR was performed with a total volume of 25 µl per reaction, with each reaction containing 5 µL of cDNA, 1 µL of a 10 µM stock of each primer (forward and reverse), 12.5 µL of 2× SYBR Green PCR Master Mix, and 5.5 µL of nuclease-free water. Gene expression was analyzed by the 2<sup>-ΔΔCT</sup> method [111]. The typical

dissociation curves of these cDNA, plus *Gapdh* as the housekeeping gene was confirmed. The following oligonucleotide primer pairs were used: *Ccl5*: F: CCT CAC CAT ATG GCT CGG AC and R: ACG ACT GCA AGA TTG GAG CA; *Cyp26a1*: F: AGC TCC TGA TTG AGC ACT CG and R: GGA GGA TTC AAT CGC AGG GT; *Hpgds*: F: CAC TAG TTT CCT GGC TAG GGT and R: TGT CAC AGC TCC TTT CCT TGT; *Il18rap*: F: TGC AAT GAA GCG GCA TCT GT and R: CCG GTG ATT CTG TTC AGG CT; *Lrat*: F: GTC GCC CAT CTA ATG CCT GA and R: CTG TGG ACT GAT CCG AGA GC; *Ptgs2*: F: CAT CCC CTT CCT GCG AAG TT and R: CAT GGG AGT TGG GCA GTC AT; *S100a8*: F: CTT TCG TGA CAA TGC CGT CTG and R: AGA GGG CAT GGT GAT TTC CT; *Upk1a*: F: TGA GCA AGA GTG TTG TGG CA and R: CAC GAT ATG CCC CAC GTG TA; *Gapdh*: F: CCC CCA ATG TGT CCG TCG TGG and R: TGA GAG CAA TGC CAG CCC CG.

For statistical analysis of real-time RT-PCR results, datasets were first tested for normality and equal variance. When appropriate, data were transformed before statistical analysis. A one-way ANOVA using SigmaStat 3.5 (Systat Software, Inc., Point Richmond, CA, USA) was used to determine differences in levels of mRNA. When differences were detected a Fischer's Least Significant Difference (LSD) test was used to determine which genes differed.

## Results

### *Real-time RT-PCR Analysis of Selected mRNA*

The expression of mRNA for Ccl5, Cyp26a1, Hpgds, Il18rap, Lrat, Ptgs2, S100a8, and Upk1a in the oviducts of PMSG-treated ESR1KO versus PMSG-treated WT mice was determined by real-time RT-PCR. A comparison of the results obtained by real-time RT-PCR and microarray analysis is presented in Table 5.1. Overall, real-time RT-PCR revealed the same directional trends in gene expression that were observed by microarray analysis.

**Table 5.1.** Comparison of gene expression for selected mRNA by Microarray and Real-time RT-PCR in oviducts collected from PMSG-treated ESR1KO versus PMSG-treated WT mice.

<b>ESR1 KO + PMSG trt vs. WT + PMSG trt</b>				
<b>Gene Symbol</b>	<b>Microarray</b>		<b>Real-time RT-PCR</b>	
	<b>Fold-Change</b>	<b>P-value</b>	<b>Fold-Change</b>	<b>P-value</b>
Ccl5	2	0.166	4.2	< 0.001
Cyp26a1	-131.1	< 0.001	-27.4	< 0.001
Hpgds	-73.4	< 0.001	-13.4	< 0.001
Il18rap	1	0.22	6.2	< 0.001
Lrat	-53.5	< 0.001	-21.8	< 0.001
Ptgs2 (Cox2)	1.57	0.24	2.19	< 0.001
S100a8	20.7	0.0006	18.02	< 0.001
Upk1a	-77.1	< 0.001	-38.9	< 0.001

Fold-Change in gene expression and P-values are indicated after analysis by microarray and by independent real-time RT-PCR.

### *Detection of differentially expressed genes by Microarray Analysis*

After chip normalization, a statistical two-way ANOVA and pairwise comparison (LSD test) was performed to generate a list of 2428 differentially expressed genes (Table 5.2,  $P < 0.01$ ,  $FDR < 0.13$ ). Genotype affected the expression of 2215 genes, PMSG affected the expression of 465 genes, and Genotype x PMSG affected the expression of 438 genes. Following removal of unannotated and duplicate probesets, DEGs were further subdivided between up- and down-regulated genes.

**Table 5.2.** Number of genes differentially regulated in whole oviducts from ESR1KO and WT mice.

<b>Parameter</b>	<b>Total differentially regulated genes</b>		
Model	2428		
Genotype	2215		
PMSG treatment	465		
Genotype by PMSG interaction	438		
	<b>Pairwise comparisons</b>	<b>Up-regulated</b>	<b>Down-regulated</b>
KO PMSG vs. KO no PMSG	37	31 (84%)	6 (16%)
WT PMSG vs. WT no PMSG	318	164 (52%)	154 (48%)
KO PMSG vs. WT PMSG	1185	689 (58%)	496 (42%)
KO no PMSG vs. WT no PMSG	664	328 (49%)	336 (51%)

Significance set to P-value < 0.01 with FDR < 0.13. Total numbers reflect unannotated and duplicate probe set removal from gene lists. For pairwise comparisons only genes with at least a 2-fold change were considered differentially expressed.

In PMSG-treated ESR1KO versus PMSG-treated WT oviducts, the identity of most highly up- and down-regulated genes is provided in Table 5.3 and the total differentially regulated genes from this pairwise comparison are provided as Supplementary Table 1.

**Table 5.3.** Most highly up- and down-regulated genes from PMSG-treated ESR1KO versus PMSG-treated WT mouse oviducts. Significance set to  $P < 0.01$ . Cutoff is 2 fold-change in expression.

<b>Gene Symbol</b>	<b>Gene Description</b>	<b>P-value</b>	<b>Fold-Change</b>
BC048679	cDNA sequence BC048679	<0.001	222.15
Apod	apolipoprotein D	<0.001	98.02
Cdh16	cadherin 16	<0.001	50.13
Chodl	Chondrolectin	<0.001	48.14
Sult1e1	sulfotransferase family 1E, member 1	<0.001	46.32
G6pc2	glucose-6-phosphatase, catalytic, 2	<0.001	42.88
Pla2g10	phospholipase A2, group X	<0.001	40.8
Fgf18	fibroblast growth factor 18	<0.001	38.17
Avpr1a	arginine vasopressin receptor 1A	<0.001	35.78
Aldh1a3	aldehyde dehydrogenase family 1, subfamily A3	<0.001	34.76
Lrrtm1	leucine rich repeat transmembrane neuronal 1	<0.001	29.44
Serpina1b	serine (or cysteine) prepeptidase inhibitor, clade A, member 1B	<0.001	27.57
Ager	advanced glycosylation end product-specific receptor	<0.001	22.77
Synpr	Synaptoporin	<0.001	22.32
S100a8	S100 calcium binding protein A8 (calgranulin A)	<0.001	20.77
Adamts16	a disintegrin-like and metallopeptidase (reprolysin type) with thrombospondin type 1 mo	<0.001	19.82
Il18r1	interleukin 18 receptor 1	<0.001	19.45
S100a9	S100 calcium binding protein A9 (calgranulin B)	0.0015	17.86
Atp6v1b1	ATPase, H <sup>+</sup> transporting, lysosomal V1 subunit B1	<0.001	17.8

**Table 5.3.** (Continued)

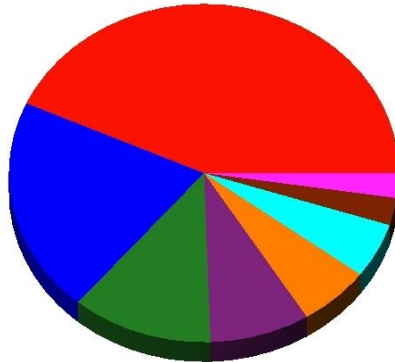
Wnt7a	wingless-related MMTV integration site 7A	<0.001	17.49
Dcpp3	demilune cell and parotid protein 3	<0.001	-770.92
2300002M23Rik	RIKEN cDNA 2300002M23 gene	<0.001	-524.94
Cyp26a1	cytochrome P450, family 26, subfamily a, polypeptide 1	<0.001	-131.13
Tshr	thyroid stimulating hormone receptor	<0.001	-121.71
Dcpp1/2/3	demilune cell and parotid protein 1/2/3	<0.001	-106.94
Syn2	synapsin II	<0.001	-91.45
Slc6a2	solute carrier family 6 (neurotransmitter transporter, noradrenalin), member 2	<0.001	-77.2
Upk1a	uroplakin 1A	<0.001	-77.14
Hpgds	hematopoietic prostaglandin D synthase	<0.001	-73.37
Klk1b24	kallikrein 1-related peptidase b24	<0.001	-73.19
Greb1	gene regulated by estrogen in breast cancer protein	<0.001	-64.6
Klk1b1	kallikrein 1-related peptidase b1	<0.001	-62.94
Klk1b21	kallikrein 1-related peptidase b21	<0.001	-53.58
Lrat	lecithin-retinol acyltransferase (phosphatidylcholine-retinol-O-acyltransferase)	<0.001	-53.53
Gria1	glutamate receptor, ionotropic, AMPA1 (alpha 1)	<0.001	-46.45
Akr1c14	aldo-keto reductase family 1, member C14	<0.001	-45.65
Stat5a	signal transducer and activator of transcription 5A	<0.001	-44.22
Col6a4	collagen, type VI, alpha 4	<0.001	-43.1
Rasd1	RAS, dexamethasone-induced 1	<0.001	-42.74
Adh7	alcohol dehydrogenase 7 (class IV), mu or sigma polypeptide	<0.001	-42.46

*Gene Ontology and Ingenuity Pathway Analysis of DEG's in the oviducts of PMSG-treated ESR1KO versus PMSG-treated WT mice*

To determine the molecular functions, cellular components, and biological processes of DEG's expressed in the oviducts of PMSG-treated ESR1KO versus PMSG-treated WT mice, Gene Ontology and Ingenuity Pathway Analyses were performed with significance set to enrichment P-value < 0.01. The significantly enriched molecular function categories using GO are indicated in Figure 5.3A. The five categories with the highest enrichment score within molecular functions were binding, protein binding, receptor binding, catalytic activity, and calcium ion binding. Significantly enriched cellular component categories are indicated in Figure 5.3B. The most highly enriched cellular component categories were extracellular region, extracellular region part, extracellular space, extracellular matrix, and membrane. Significantly enriched biological processes are indicated in Figure 5.3C, with the most highly enriched categories being single organism process, positive regulation of biological process, single organism cellular process, regulation of multicellular organismal process, and positive regulation of cellular process.

Molecular Function

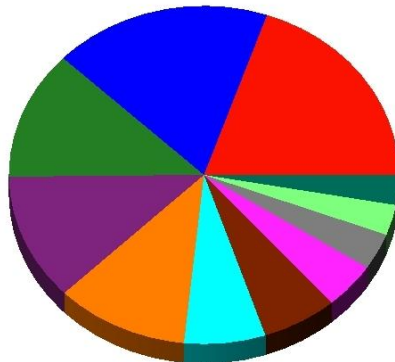
A.



- 43.23% binding (86.71)
- 20.60% catalytic activity (41.33)
- 11.71% transporter activity (23.49)
- 8.29% receptor regulator activity (16.63)
- 5.95% enzyme regulator activity (11.93)
- 5.24% antioxidant activity (10.52)
- 2.62% electron carrier activity (5.25)
- 2.36% channel regulator activity (4.73)

Cellular Component

B.



- 19.76% extracellular region (105.78)
- 18.09% extracellular region part (96.84)
- 12.31% extracellular matrix (65.91)
- 12.14% membrane (64.99)
- 11.05% cell part (59.17)
- 6.74% membrane part (36.10)
- 6.24% extracellular matrix part (33.43)
- 4.42% cell junction (23.64)
- 3.48% organelle (18.62)
- 2.90% synapse (15.53)
- 2.86% synapse part (15.30)

C.

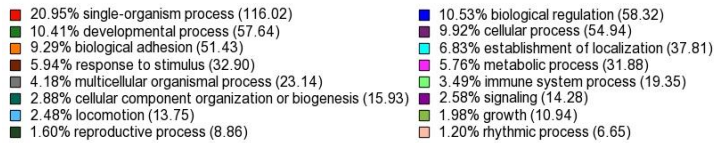
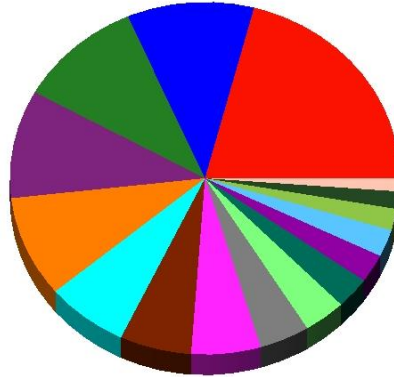


**Figure 5.3.** Gene ontology analysis from PMSG-treated ESR1KO versus PMSG-treated WT mice. Significance of gene enrichment set to P-value < 0.01.

Canonical pathway analysis of DEG's from PMSG-treated ESR1KO versus PMSG-treated WT mice was performed using QIAGEN'S Ingenuity Pathway Analysis (IPA, QIAGEN, Redwood City, [www.qiagen.com/ingenuity](http://www.qiagen.com/ingenuity)). The six most significant pathways identified by Ingenuity Pathway Analysis software are provided in Figure 5.4, all are reflective of ESR1-regulation of the immune response (P<0.05).

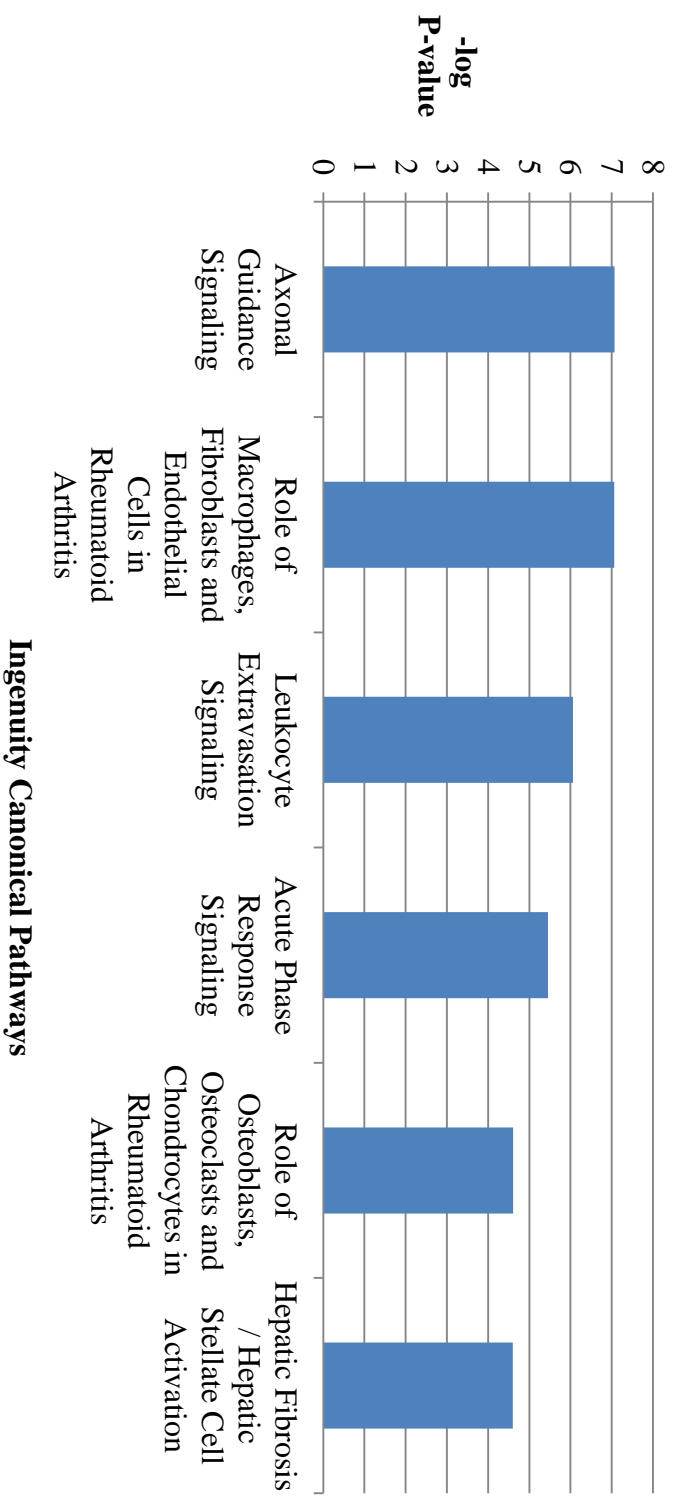


**Figure 5.4.** The six most significant pathways identified by Ingenuity Pathway Analysis software from the 1185 DEGs identified in PMSG-treated ESR1KO versus PMSG-treated WT mice ( $P < 0.05$ ).

## Discussion and Conclusions

A normally functioning oviduct is essential for gamete maturation and transport, fertilization, and early conceptus development. Although immune responses and inflammation in the oviduct is a required physiological occurrence, aberrant inflammation can lead to oviductal disease and/or ectopic pregnancy necessitating woman to seek treatment for infertility. Estradiol is a known regulator of oviductal function with estrogen receptor alpha (ESR1) expression abundant in the epithelial mucosa; however, estradiol and ESR1-dependent changes in mRNA expression in the oviduct have yet to be fully elucidated. Furthermore, increasing our understanding of the role of estradiol and ESR1 in immune responses may lead to the development of novel treatment options that specifically target inflammatory responses. The objective of this study was to identify estradiol and ESR1 dependent differences in gene expression between whole oviducts collected from ESR1 knockout and wild-type littermates at 0 hr as well as 48 hr after treatment with PMSG using Affymetrix Mouse 430-2.0 genome arrays. Overall, 2428 genes were differentially regulated within our model with significance set to  $P < 0.01$ . Real-time RT-PCR performed on selected mRNA confirmed expression results obtained by microarray.

For the purposes of this study and of physiological importance we evaluated gene expression changes between ESR1KO and WT littermates 48 hr after PMSG treatment. The present study utilized immature mice because abnormal ovarian histology is not observed in ESR1KO females until after puberty and the

steroidogenic capacity of mature WT mice will clearly have an effect on gene expression. After the 2428 DEGs from our model were identified a pairwise comparison of PMSG treated ESR1KO and WT mice was performed and revealed 1185 differentially regulated genes with at least a 2 fold-change in signal intensity and a P-value < 0.01.

Our objective herein is not to discuss the role of individual genes identified as differentially regulated in detail, but rather provide examples of consistency among our profiling results with previous targeted analyses performed by others. Several of the top up-regulated DEGs were found to be involved in the inflammatory response with specific functions associated with chemotaxis and activation of immune cells. Understanding the molecular mechanisms of the immune response within the oviduct is of particular interest as aberrant inflammation is one of the major causes of pelvic inflammatory disease in women [143]. For example, S100 calcium binding protein A8 and A9 (S100A8/9) were found to increase 21- and 18-fold, respectively in ESR1KO mice when compared to WT after PMSG treatment. The S100 calcium binding proteins have been implicated in the regulation of cell growth and differentiation, but more interestingly are associated with many chronic inflammatory diseases [142]. As reviewed by Passey et al., 1999, S100A8/9 have pro- and anti-inflammatory properties depending on cellular expression and physiological condition however, the specific role of these proteins is unclear but have been suggested to modulate leukocyte trafficking [144, 145]. Also of note is the 19-fold increased expression of interleukin 18 receptor 1 (Il18r1) in PMSG-treated ESR1KO mice. The Il-18 receptor consists of two subunits with the Il18r1

subunit being involved in ligand binding and mRNA levels have been found to increase during estrus. The ligand for Il18r1 is interleukin-18 (IL-18) which acts as a pro-inflammatory cytokine involved in stimulating Interferon- $\gamma$  (Ifn- $\gamma$ ) during chronic inflammatory conditions [146]. Studies have reported Il-18 expression in the uterus [147] and ovaries [148] of mice and down-regulation by estrogen has been noted [147, 149]. Our study did not identify Il-18 as differentially regulated however, Otsuki et al., 2007, reported increases in Il18r1 mRNA expression in the mouse endometrium after ovariectomy and estradiol-17 $\beta$  reversed this effect [150]. The findings of the current study support the regulation of Il18r1 by estrogen and ESR1 expression in the oviduct.

Of the 1185 DEGs in PMSG-treated ESR1KO versus PMSG-treated WT mice, 496 (42%) were down-regulated. The hematopoietic form of prostaglandin D synthase (HPGDS) was recently localized to the oviduct's epithelium and a dependence of HPGDS expression on ESR1 is reported [23]. This synthase is hypothesized to be a regulator of oviductal inflammation and our current data supports this hypothesis as a 73 fold decrease in HPGDS mRNA expression was observed in our dataset. Of interest are the demilune cell and parotid protein 1/2/3 (Dcpp1/2/3) genes which were found to decrease significantly in our study.

Previously, Dcpp expression has been localized to the oviduct epithelium and are suggested estrogen responsive genes as expression increasing during estrus and is up-regulated in ovariectomized mice treated with estrogen [151]. The specific functions of Dcpp in the oviduct are not clear, but Dcpp immunostaining has been described in mouse embryos and the presence of embryos is reported to modulate Dcpp expression in the mouse oviduct suggesting a role of this gene in embryogenesis [151].

Gene ontology classification of the 1185 DEGs from PMSG-treated ESR1KO versus PMSG-treated WT mice revealed an over representation of genes associated with binding from within the GO Category “molecular functions” and the extracellular region in the GO category “cellular compartment”. Taken together an enrichment of gene products associated with binding activities and localized to the extracellular region in the PMSG-treated ESR1KO mice may be reflective of gene product transport and release into the oviduct lumen. Furthermore, gene enrichment for the GO category “biological process” depicts the response of the oviduct to stimuli, such as steroid hormones.

To further understand the biological roles of ESR1 in the mouse oviduct, the 1185 DEGs from PMSG-treated ESR1KO versus PMSG-treated WT mice was analyzed using Ingenuity Pathway Analysis (IPA®, QIAGEN), which uses multiple databases to extrapolate significant canonical pathways based on the number of genes expected to be expressed within each pathway. The top canonical pathway, axonal guidance signaling, relates to functions associated with cell morphology, cellular assembly and organization, cellular function and maintenance. Previous

studies have reported normal oviduct morphology in immature ESR1KO mice [23], however the current results warrant further investigation in to the potential morphological differences between ESR1KO and WT mouse oviducts. Several pathways associated with the immune response were significant in our dataset including leukocyte extravasation signaling which is the process of leukocyte migration from blood to tissue during the inflammatory response. Adult ESR1KO mice are known to display altered hormone profiles including elevated testosterone and luteinizing hormone levels which could in itself affect the immune response [152]. The current study, however utilized immature mice to reduce these affects suggesting ESR1 dependent mechanisms involved in modulating the immune response within the oviduct.

To conclude, these results give us further insights into the genes regulated by estrogen and ESR1 expression. Pathway analysis underline the complex role of estrogens in regulating the immune response within the oviduct and potential ESR1 dependent molecules involved.

## CHAPTER 6.

### INTRAPERITONEAL ADMINISTRATION OF LIPOPOLYSACCHARIDE INDUCES DIFFERENTIAL EXPRESSION OF mRNA ENCODING INFLAMMATORY MEDIATORS IN THE OVIDUCTS OF MICE

#### Abstract

Infection with gram-negative bacteria is a major cause of aberrant inflammation in the oviduct; consequences can include tubal infertility and/or ectopic pregnancy in women. Understanding inflammatory responses due to bacterial infection is necessary for the development of novel treatment options that specifically target inflammatory responses. Our objective was to test the hypothesis that intraperitoneal (IP) administration of *E. Coli* -derived lipopolysaccharide (LPS) induces the expression of inflammatory mRNAs in the mouse oviduct. On the day of estrus, 6-8 week old CD1 mice (n=4/treatment) were treated IP with 0 (control), 2 ug (low dose) or 10 ug (high dose) of LPS from *E. Coli* serotype 055:B5 in 100 ul PBS. Mice were killed 24 h later and the oviducts collected for determination of inflammatory gene expression by a targeted nanostring approach using the nCounter GX Mouse Inflammation Kit (Nanostring Technologies, Seattle, Wa). Real-time PCR was used to validate selected mRNAs. The effect of LPS was evaluated by one-way ANOVA and treatment means of differentially expressed mRNA ( $P < 0.05$ ) were separated using a post-hoc LSD test. 56/179 targeted genes were affected by treatment ( $P < 0.05$ ). Pairwise comparison revealed 8 mRNA differentially expressed in control vs low dose, 50 mRNAs in control vs high dose and 43 mRNAs in low vs

high dose ( $P < 0.05$ ). These results indicate that systemic treatment with LPS induces inflammation in the oviducts of mice and provides evidence of a new model to investigate the regulation of oviductal inflammation in the future.

## Introduction

Infection with gram-negative bacteria is a major cause of aberrant inflammation in the reproductive tract of animals and humans. If left untreated the bacteria can ascend to and infect the oviduct; consequences can include pelvic inflammatory disease (PID), oviduct epithelial cell death, tubal infertility and/or ectopic pregnancy [2, 153]. Knowledge of gene expression patterns involved with inflammatory response mechanisms in the oviduct is not as extensive compared to other regions of the reproductive tract. Understanding inflammatory responses due to bacterial infection is necessary for the development of novel treatment options that specifically target inflammatory responses.

When bacteria are introduced, Toll-like receptors present on immune cells recognize and bind LPS, initiating a pro-inflammatory response with the production of cytokines and chemokines [154-156]. A systemic and local LPS induced immune response has been described previously for *in vitro* and *in vivo* models investigating implantation, conceptus viability, and pregnancy loss [157-160]. Recently, Brecchia et al., 2014, described an *in vivo* rabbit model of systemic inflammation by intra-peritoneal administration of LPS and assessed the effects on uterine and oviductal function. The results showed that IP-LPS treatment in female rabbits negatively affected reproductive function [161].

However, few *in vivo* studies specifically target oviductal inflammatory gene expression in response to systemic administration of LPS. Considering the oviduct plays a critical role in gamete transport and maturation, fertilization, and early

conceptus development, there is a need for a reliable and repeatable animal model that allows for the study of inflammatory mechanisms in the oviduct. Using LPS as an independent inflammatory insult, the objective of this study was to provide evidence for a model of systemic inflammation and determine expression changes of inflammatory mRNAs in the oviducts of mice following IP injection with 0 (control), 2 ug (low dose) or 10 ug (high dose) of LPS from *E. Coli* in 100 ul PBS.

## **Methods**

### *Animals and Tissue Collection*

Animal procedures involved in this study were approved by the University of Kentucky Animal Care and Use Committee. Prior to treatment, normal estrous cycle was confirmed in 6-8 week old CD1 mice by analysis of vaginal cytology, as described previously [142]. Briefly, vaginal smears were collected daily, at the same time each day, using PBS and a bent, blunted borosilicate glass pipette. Vaginal cytology's were evaluated under a Motic AE21 inverted microscope (Motic Instruments, Richmond, British Columbia, Canada) and classified according to well-established morphological criteria and digital images recorded for later reference [162]. On the day of estrus, mice were treated with 0 (control), 2 ug (low dose) or 10 ug (high dose) of LPS from *E. Coli* serotype 055:B5 in 100 ul PBS (Sigma-Aldrich, Saint Louis MO) via intraperitoneal (IP) injection (n=4/treatment). Twenty four hours later, vaginal smears were collected to determine whether treatment affected

estrous cycle progression and mice were killed for collection of oviducts. Tissues for gene expression analysis were snap-frozen for later extraction of RNA.

#### *RNA Extraction and Analysis*

Total RNA was extracted from single oviducts using Trizol reagent (Invitrogen Corporation, Carlsbad, CA, USA) and purified with RNeasy columns (Qiagen, Valencia, CA, USA) according to manufacturer's instructions. RNA quality was analyzed by determining the RNA integrity number (RIN) using an Agilent 2100 Bioanalyzer (Agilent Technologies, Palo Alto, CA) at the University of Kentucky Microarray Core Facility. RNA integrity numbers were greater than 9.7 and 28S/18S rRNA absorbance ratios greater than 2.0 for all samples and all samples passed the quality control measurements required for this platform.

#### *NanoString nCounter® Gene Expression Profiling*

Nanostring analysis was performed using the nCounter® GX Mouse Inflammation Kit (Nanostring Technologies, Seattle, Wa) which consists of 179 inflammation related genes and six internal reference genes. Analysis was performed according to the manufacturer's instructions at the University of Kentucky Microarray Core Facility as described previously [163]. The Digital multiplexed NanoString nCounter analysis system uses molecular barcodes to detect and count transcripts. Briefly, 100 ng of total RNA from each sample was hybridized

with reporter and capture probes which hybridize directly to target molecules. After hybridization sample processing allows for probe/target complexes to be immobilized on the nCounter cartridge and unbound probes removed. After sample processing digital data acquisition allows for barcodes on reporter probes to be tabulated for each target molecule. The raw reported code count data generated from the nCounter Digital Analyzer was exported to nSolver software (NanoString Technologies) for normalization, background assessment, and molecule count summarization as previously described [164]. For NanoString nCounter data, positive control normalization is used to reduce sources of variation associated with hybridization, purification, and binding efficiency. This is accomplished through positive spike-in RNA hybridization controls to estimate the experimental variables based on a calculated positive control scaling factor. Gene normalization was performed to correct for differences in sample input between assays by using the geometric mean of 3 reference genes (Gapdh, Pgk1, Tubb5), which expression values did not differ between treatments. Negative control probes are also included in the assay which is used to assess background counts and decrease false discovery rate by determining the presence or absence of target molecules.

Following normalization procedures, background adjustment, and count summarization, the resulting data were imported into Partek Genomics Suite 6.6 (Partek Inc., St. Louis, MO, USA) for statistical analysis. One-way ANOVA was used to determine differences in relative molecule count and significance was set to P-value < 0.05. If differences were detected, treatment means were separated using Fischer's Least Significance difference (LSD) test to determine which means differed [107, 108]. An expression difference between treatments of P-value < 0.05 was considered statistically significant.

### *Real-time RT-PCR Analysis*

Real-time PCR was performed to validate expression of mRNAs for Chemokine (C-C motif) ligand 5 (Ccl5), Chemokine (C-X-C motif) ligand 1 (Cxcl1), Chemokine (C-X-C motif) ligand 10 (Cxcl10), Chemokine (C-X-C motif) receptor 2 (Il8rb), Interleukin 18 receptor accessory protein (Il18rap) using an Eppendorf Mastercycler ep *realplex*<sup>2</sup> system (Eppendorf, Hamburg, Germany) with iQ SYBR Green Supermix (Bio-RAD, Hercules, CA USA), as described before [23]. The following oligonucleotide primer pairs were used: Ccl5, F: CCT CAC CAT ATG GCT CGG AC and R: ACG ACT GCA AGA TTG GAG CA; Cxcl1, F: ACT CAA GAA TGG TCG CGA GG and R: GTG CCA TCA GAG CAG TCT GT; Cxcl10, F: CTA TCC TGC CCA CGT GTT GA and R: TCC ACT GGG TAA AGG GGA GT; Il8rb, F: CTT AGC CAA GGA GGG AAG GC and R: GGG CTC TGC TAA GAA CGGT GA; Il18rap, F: TGG AAT GAA GCG GCA TCT GT and R: CCG GTG ATT CTG TTC AGG CT; Gapdh, F: CCC CCA ATG TGT CCG TCG TGG and R: TGA GAG CAA TGC CAG CCC CG.

Briefly, cDNA was synthesized using the SuperScript III 1<sup>st</sup> Strand Synthesis System (Invitrogen), with 0.5 µg of RNA used for each reverse transcription reaction. Real-time RT-PCR was performed with a total volume of 25 µL per reaction, with each reaction containing 5 µL of cDNA, 1 µL of a 10 µM stock of each primer (forward and reverse), 12.5 µL of 2× SYBR Green PCR Master Mix, and 5.5 µL of nuclease-free water. The typical dissociation curves of these cDNA, plus Gapdh as the housekeeping gene was confirmed and gene expression was analyzed by the 2<sup>ΔΔCT</sup> method [111]. For real-time RT-PCR analysis, expression values within a

transcript were tested for normality and homogeneity of variance and, when appropriate (Il18rap, Il8rb), a natural log transformation was conducted to normalize variation before statistical analysis of LPS treatment effects by one-way ANOVA using SigmaStat 3.5 (Systat Software, Inc., Point Richmond, CA). When affected ( $P < 0.05$ ), the treatment means were separated using Fischer's LSD test.

## **Results**

### *Real-time RT-PCR Analysis of Selected Transcripts*

To test the hypothesis that IP injected *e.coli* derived LPS effects inflammatory mRNAs in the oviduct, gene expression analysis using the NanoString nCounter GX Mouse Inflammation Kit (Nanostring Technologies) was performed. The expression of selected mRNAs as described in the materials and methods were reevaluated by independent real-time RT-PCR. The results obtained by NanoString and real-time RT-PCR were consistent (Table 6.1).

**Table 6.1.** Comparison of gene expression for selected mRNA by NanoString and Real-time RT-PCR.

Gene	Low dose vs. Control			High dose vs. Control			High dose vs. Low dose		
	Fold-Change	P-value	Real-time RT-PCR	Fold-Change	P-value	Real-time RT-PCR	Fold-Change	P-value	Real-time RT-PCR
Ccl5	18.8	0.08	0.03	27.2	0.02	<0.001	1.4	0.38	<0.001
Cxcl1	1.5	0.69	0.24	7.1	0.001	<0.001	4.6	0.002	<0.001
Cxcl10	3.4	0.22	0.65	15.5	<0.001	<0.001	4.6	<0.001	<0.001
Il8rb	5	0.02	<0.001	10.8	<0.001	<0.001	2.2	0.002	<0.001
Il18rap	1.9	0.06	0.01	3	0.001	0.002	1.6	0.03	0.41

mRNA for Real-time RT-PCR analysis were selected based on their known involvement in the inflammatory response in the oviducts of mice.

*NanoString nCounter Gene Expression Analysis*

Of the 179 targeted genes within the nCounter GX Mouse Inflammation Kit, 56 were affected by treatment with LPS ( $P < 0.05$ ). As depicted in the venn diagram (Figure 6.1), two genes (*Il8rb* and *Ccl8*) overlapped between the contrasts. In oviducts collected from mice treated with low dose (2 ug) LPS, the expression of mRNA encoding 6 inflammation related genes increased and 2 genes decreased compared to mice treated with PBS only (Table 6.2,  $P < 0.05$ ).

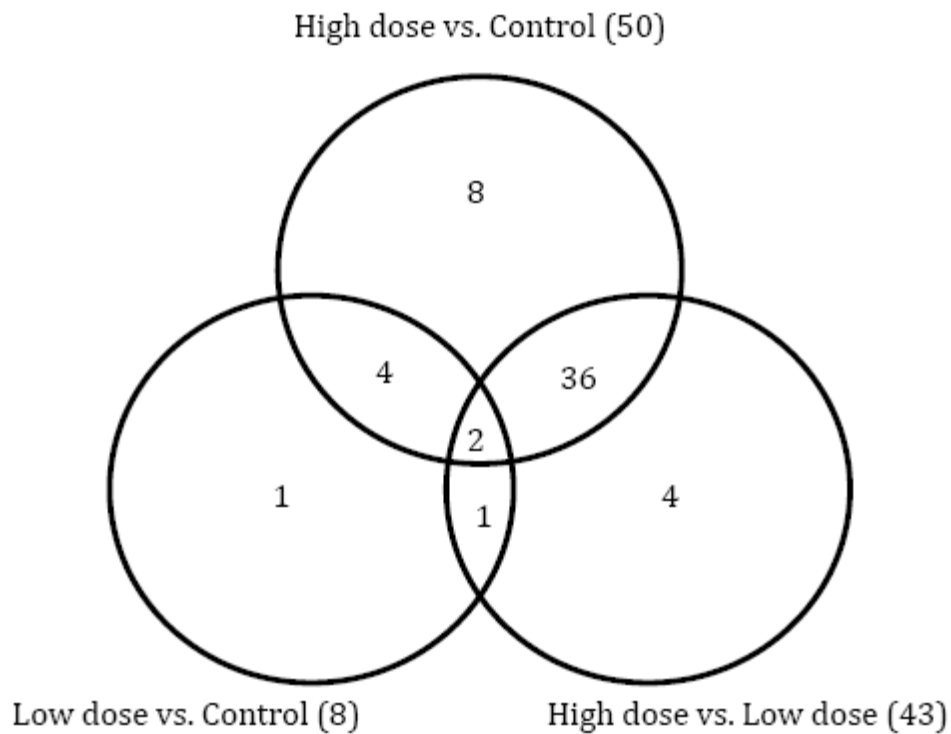


**Figure 6.1.** Venn diagram depicting the number of differentially genes between high dose (10 ug LPS), low dose (2 ug LPS) and control oviducts collected from CD1 mice.

**Table 6.2.** Differentially expressed transcripts between low dose (2 ug LPS) and control (PBS only) oviducts collected from CD1 mice (P < 0.05).

<b>Gene Symbol</b>	<b>Gene Description</b>	<b>Fold-change</b>	<b>P-value</b>
Ccl22	Chemokine (C-C motif) ligand	0.62	0.01
Shc1	src homology 2 domain-containing transforming protein C1 (Shc1), transcript variant 2	0.90	0.01
Il8rb	chemokine (C-X-C motif) receptor 2	4.95	0.02
C3ar1	complement component 3a receptor 1	1.86	0.03
Ccl8	Chemokine (C-C motif) ligand	4.76	0.03
C1qa	complement component 1, q subcomponent, alpha polypeptide	2.21	0.04
C1qb	complement component 1, q subcomponent, beta polypeptide	1.96	0.04
Ccr7	chemokine (C-C motif) receptor 7	3.51	0.05

In oviduct samples collected after treatment with high dose (10 ug) LPS, the expression of mRNA encoding 50 inflammation related genes were differentially expressed (P < 0.05) with expression of all mRNA increasing compared to controls (Table 6.3). Mean values of significant mRNA (P<0.05) in oviducts collected from high dose (10 ug) LPS versus low dose (2 ug) LPS were separated using Fischer's LSD test and revealed 43 mRNA differentially expressed with only the expression of one mRNA (Pik3c2g) decreasing in the high dose when compared to the low dose (Table 6.4).

**Table 6.3.** Differentially expressed transcripts between high dose (10 ug LPS) and control (PBS only) oviducts collected from CD1 mice (P < 0.05).

<b>Gene Symbol</b>	<b>Gene Description</b>	<b>Fold-change</b>	<b>P-value</b>
Ccl7	Chemokine (C-C motif) ligand	17.69	< 0.001
C1r	complement component 1, r subcomponent A	4.33	< 0.001
Cxcl10	Chemokine (C-X-C motif) ligand	15.50	< 0.001
Ccl2	Chemokine (C-C motif) ligand	13.87	< 0.001
C1s	complement component 1, s subcomponent	4.55	< 0.001
Il8rb	chemokine (C-X-C motif) receptor 2 (Cxcr2)	10.81	< 0.001
Cd40	tumor necrosis factor receptor superfamily member 5	2.82	< 0.001
C3	complement component 3	3.91	< 0.001
Tlr2	toll-like receptor 2	2.87	< 0.001
Cfb	complement factor B	26.94	< 0.001
Il15	Interleukin 15	1.81	< 0.001
Ccl8	Chemokine (C-C motif) ligand	9.00	< 0.001
Csf1	colony stimulating factor 1	1.93	< 0.001
C4a	complement component 4A	3.53	< 0.01
Cxcl9	Chemokine (C-X-C motif) ligand	45.79	< 0.01
Tnfsf14	tumor necrosis factor (ligand) superfamily, member 14	2.43	< 0.01
Stat1	signal transducer and activator of transcription 1	3.35	< 0.01
Il18rap	interleukin 18 receptor accessory protein	3.05	< 0.01
Il23r	interleukin 23 receptor	2.84	< 0.01
Ccl4	Chemokine (C-C motif) ligand 4	3.47	< 0.01
Cxcl1	Chemokine (C-X-C motif) ligand	7.07	< 0.01
C2	complement component 2	2.33	< 0.01
C3ar1	complement component 3a receptor 1	2.41	< 0.01
Ly96	Lymphocyte Antigen 96	1.38	< 0.01
C1qb	complement component 1, q subcomponent, beta polypeptide	2.70	< 0.01
Il1b	interleukin 1 beta	2.45	< 0.01
Tgfb1	transforming growth factor, beta 1	1.44	< 0.01
Ccl19	Chemokine (C-C motif) ligand 19	2.71	< 0.01
C1qa	complement component 1, q subcomponent, alpha polypeptide	2.91	< 0.01
Ltb	lymphotoxin B	2.08	< 0.01
Tnf	tumor necrosis factor	4.14	0.01
Mapkap k2	MAP kinase-activated protein kinase 2	1.20	0.01
Itgb2	integrin beta 2	2.42	0.01

**Table 6.3.** (Continued)

Nfkb1	nuclear factor of kappa light polypeptide gene enhancer in B cells 1	1.25	0.01
Ccl3	Chemokine (C-C motif) ligand	3.36	0.01
Mafk	v-maf musculoaponeurotic fibrosarcoma oncogene family, protein K	1.41	0.01
Ccr1	chemokine (C-C motif) receptor 1	1.97	0.01
Cebpb	CCAAT/enhancer binding protein (C/EBP), beta	1.32	0.01
Maff	v-maf musculoaponeurotic fibrosarcoma oncogene family, protein F	1.67	0.01
Nos2	nitric oxide synthase 2, inducible	1.94	0.01
Ccr7	chemokine (C-C motif) receptor 7	4.45	0.01
Cxcl5	Chemokine (C-X-C motif) ligand	6.56	0.01
Gusb	glucuronidase, beta	1.19	0.01
Ripk2	receptor (TNFRSF)-interacting serine-threonine kinase 2	1.50	0.02
Cxcl2	Chemokine (C-X-C motif) ligand	4.57	0.02
Il1rn	interleukin 1 receptor antagonist	2.29	0.02
Ccl17	Chemokine (C-C motif) ligand	1.73	0.02
Ccl5	Chemokine (C-C motif) ligand	27.21	0.02
Prkcb1	protein kinase C, beta 1	1.30	0.03
Il7	Interleukin	1.29	0.03

**Table 6.4.** Differentially expressed transcripts between high dose (10 ug LPS) and low dose (2 ug LPS) oviducts collected from CD1 mice ( $P < 0.05$ ).

<b>Gene Symbol</b>	<b>Gene Description</b>	<b>Fold-Change</b>	<b>P-value</b>
Ccl7	Chemokine (C-C motif) ligand	8.58	< 0.001
C1r	complement component 1, r subcomponent A	2.54	< 0.001
Ccl2	Chemokine (C-C motif) ligand	5.73	< 0.001
Cxcl10	Chemokine (C-X-C motif) ligand	4.59	< 0.001
C1s	complement component 1, s subcomponent	2.50	< 0.001
Cd40	tumor necrosis factor receptor superfamily member 5	2.00	< 0.001
Csf1	colony stimulating factor 1	1.91	< 0.001
C3	complement component 3	2.30	< 0.001
Tlr2	toll-like receptor 2	2.03	< 0.01
Il23r	interleukin 23 receptor	2.39	< 0.01
Il8rb	chemokine (C-X-C motif) receptor 2	2.18	< 0.01
Cxcl1	Chemokine (C-X-C motif) ligand	4.62	< 0.01
Cfb	complement factor B	3.16	< 0.01
Il15	Interleukin	1.47	< 0.01
C4a	complement component 4A	2.27	< 0.01
Stat1	signal transducer and activator of transcription 1	2.42	< 0.01
Cxcl9	Chemokine (C-X-C motif) ligand	3.97	< 0.01
Tgfb1	transforming growth factor, beta 1	1.37	0.01
Ccl4	Chemokine (C-C motif) ligand	1.97	0.01
C2	complement component 2	1.66	0.01
Cebpb	CCAAT/enhancer binding protein (C/EBP), beta	1.32	0.01
Daxx	Fas death domain-associated protein	1.23	0.01
Ripk1	receptor (TNFRSF)-interacting serine-threonine kinase 1	1.23	0.01
Tnfsf14	tumor necrosis factor (ligand) superfamily, member 14	1.58	0.01
Pik3c2g	phosphatidylinositol 3-kinase, C2 domain containing, gamma polypeptide	0.42	0.01
Il7	Interleukin	1.36	0.01
Mafk	v-maf musculoaponeurotic fibrosarcoma oncogene family, protein K	1.35	0.01
Ccl8	Chemokine (C-C motif) ligand	1.89	0.01
Il1b	interleukin 1 beta	1.75	0.01
Tnf	tumor necrosis factor	2.62	0.02
Hspb2	heat shock protein 2	1.52	0.02
Ccl19	Chemokine (C-C motif) ligand	1.87	0.02
Ccr1	chemokine (C-C motif) receptor 1	1.70	0.02

**Table 6.4.** (Continued)

Ly96	Lymphocyte Antigen 96	1.22	0.02
Cxcl5	Chemokine (C-X-C motif) ligand	4.11	0.02
Il18rap	interleukin 18 receptor accessory protein	1.58	0.03
Il1rn	interleukin 1 receptor antagonist	2.06	0.03
Ccl22	Chemokine (C-C motif) ligand	1.44	0.03
Prkcb1	protein kinase C, beta 1 (Prkcb1)	1.27	0.03
Ltb	lymphotoxin B	1.51	0.04
Ccl17	Chemokine (C-C motif) ligand	1.55	0.04
Nos2	nitric oxide synthase 2, inducible	1.53	0.05
Maff	v-maf musculoaponeurotic fibrosarcoma oncogene family, protein F	1.40	0.05

## Discussion and Conclusions

We hypothesized that systemic treatment with LPS would lead to an increase in inflammatory mediators in the oviduct. Similar to studies of the mouse ovary and uterus [158, 165], treatment of LPS as an independent inflammatory insult resulted in an increase in inflammatory mRNAs in the oviduct. Using NanoString nCounter technology, our results revealed that IP treatment with *E.coli* derived-LPS induced changes in mRNA encoding inflammation related genes in the oviduct of mice.

In agreement with a previous in vitro study by Ibrahim et al., 2015, on the effects of LPS on bovine oviductal epithelial cells, increases in gene expression for Csf1, Il1b, and Tgfb1 were observed in treated animals compared to controls suggesting that the use of IP administered LPS could be a useful in vivo model for understanding inflammatory mechanisms in the oviduct [166]. Furthermore, mRNA encoding Ccl5, Cxcl1, Cxcl10, Il8rb, and Il18rap were found to increase in treated animals compared to controls and was confirmed by independent real-time RT-PCR. Of note, mRNA encoding Ccl5 has been reported to increase in the oviducts of

*Chlamydia trachomatis* infected woman [167] and mice [73] and is a chemoattractant for monocytes and Th1 cells. Prolonged production of Ccl5 is also associated with tubal damage and scarring after repeated exposure to *Chlamydia trachomatis* [167]. Similar to Ccl5, mRNA levels for the C-X-C motif chemokine Cxcl1 increased significantly in both the high and low dose animals and is associated with gram-negative bacterial infections. Cxcl1 exerts its neutrophil attractant activity through the chemokine receptor Il8rb [168]. Interestingly, increases in the expression of Il8rb have been suggested to be associated with inflammation induced tubal ectopic pregnancies in woman; however, it has not been determined whether Il8rb expression plays a role in the development of ectopic pregnancy or is induced by ectopic pregnancy [169].

In conclusion, understanding regulators of inflammation in the oviduct can aid in improving the reproductive health of woman. The results of this study provide evidence of a useful model to further investigate inflammation in the oviduct.

## CHAPTER 7.

### CONCLUSIONS AND IMPLICATIONS

Genomic based studies are an increasingly important area in discovery based research to understand and analyze the function of biological systems. In this dissertation the oviduct is of interest because this complex organ has received less attention in terms of whole genome investigation than other areas of the reproductive tract such as the uterus and the ovary. With advances in bovine specific microarray technology, transgenic mouse models, and targeted NanoString nCounter technology it is possible to investigate the function of the oviduct at the transcriptional level to increase our knowledge and generate data which will serve as a base for future studies.

The objective of this dissertation was to delineate steroid dependent gene expression changes in the oviduct using bovine and mouse models and to further analyze the inflammatory response of this organ. In Chapter 4, bovine oviductal epithelial cells were isolated from sections of the ampulla and isthmus during the follicular or luteal phase of the estrous cycle to gain a better understanding of the in vivo conditions of the oviduct. Investigating gene expression changes during these two phases gives us a baseline for understanding mechanisms regulating oviductal function. In addition, through bioinformatic analyses, important pathways related to oviduct function were identified. For example, pathways upregulated in the oviduct during the follicular phase were representative of cholesterol biosynthesis which is necessary for the oviduct to prepare for gametes. In addition, the oxidative

phosphorylation pathway was among the most highly upregulated pathways during the follicular phase which is indicative of the energy requirements needed for cellular processes related to epithelial cell secretions. Previous bovine studies of gene expression changes in the bovine oviduct have largely focused on targeted evaluations of gene expression. The results of the current study not only provided support to previous targeted studies, but also identified numerous novel genes which may be revealed as mediators of oviductal function in the future. For example, further localizing characterizing novel genes like binder of sperm 3 (BSP3) in the oviduct, which is previously described to be secreted by seminal vesicles in males and thought to be involved in the formation of the sperm reservoir in the oviduct. The approach in this study utilized young, normally cycling females therefore, the data generated could be used as a comparison tool for gene expression studies of the oviduct from sub-fertile animals or females undergoing estrous cycle manipulation to determine candidate genes which could be used as biomarkers of fertility. Overall, this study provides global oviductal epithelial cell gene expression profiles in young, normally cycling heifers.

It is well known that the function of the oviduct is dependent on the ovarian-derived steroid hormones progesterone and estradiol. The study reported in Chapter 5 investigated gene expression in the mouse oviduct collected from ESR1 mutant mice and WT littermates after treatment of PMSG to identify candidate genes and biomolecular processes that may be dependent on ESR1 expression. Similar to the transcriptomal study conducted with the bovine oviductal epithelial cells in Chapter 4, this study aimed to give insight into ESR1 dependent mechanisms

through gene profile lists and bioinformatics analyses. The implications of the data generated identify biological processes that are likely regulated by ESR1 such as cell proliferation and differentiation and genes associated with the inflammatory response. In summary, the results indicate many genes and processes regulated by ESR1 and may be targets for future analysis for the management of fertility and/or oviductal disease.

The objective of Chapter 6 was to evaluate an in vivo mouse model of systemic inflammation by intra-peritoneal administration of LPS to investigate the response of the oviduct regarding inflammatory mediators. The hypothesis stated in Chapter 6 was generated after the gene expression evaluation reported in Chapter 5 and appendix 1. Many genes associated with inflammation were differentially regulated in the ESR1 transgenic mouse model leading to the necessity to continue to evaluate inflammatory mediators in the oviducts in vivo. Furthermore, the study reported in Appendix 1 involved the use of a mouse model of genital infection by *C. trachomatis*; however, the variability in results observed in Appendix 1 confirms previous reports with regards to the genetic component of susceptibility to *C. trachomatis* infection in mice. Considering the importance of the oviduct in early reproductive events and infection with gram-negative bacteria is a major cause of aberrant inflammation in animals and humans it is necessary to establish a repeatable and reliable in vivo model. Using a targeted NanoString approach, the results of chapter 6 indicated an increased expression of pro-inflammatory molecules after treatment with LPS suggesting that the use of IP administered LPS could be a useful model for understanding the mechanisms of

inflammation in the oviduct. Moreover, future studies are planned to investigate the potential regulatory miRNAs induced by LPS treatment.

The translational impact of these genomic studies has the potential to identify target molecules and processes to improve production animal and human fertility. By understanding how the oviduct responds to steroidogenesis and pathogens, strategies and methodologies to improve reproductive efficiency can be explored in the future. Furthermore, this dissertation provides evidence of a model for oviductal dysfunction, which could have widespread impacts to the development of treatment options that targets pro-inflammatory molecules.

## APPENDIX 1.

### DIFFERENTIAL EXPRESSION OF MRNA ENCODING CYTOKINES AND CHEMOKINES IN THE REPRODUCTIVE TRACT AFTER INFECTION OF MICE WITH *CHLAMYDIA TRACHOMATIS*.

#### Abstract

Infection with *Chlamydia trachomatis* targets epithelial cells within the genital tract which respond by secreting chemokines and cytokines. Persistent inflammation can lead to fibrosis, tubal infertility and/or ectopic pregnancy; many infections are asymptomatic. Most studies have investigated the inflammatory response in the initial stages of infection, less is known about the later stages of infection, especially with a low, potentially asymptomatic, bacterial load. Our objective was to determine the inflammatory mediators involved in clearance of low-grade infection and the potential involvement in chronic inflammation. Six to eight week old C3H/HeJ mice were pretreated with 2.5 mg medroxyprogesterone acetate on day -10 and -3 before infection. Mice (n=3 for 28 d, n=3 for 35 d) were infected with  $5 \times 10^2$  inclusion-forming units of *C. trachomatis*, serovar D; vaginal cultures were obtained weekly to monitor infection. Control mice (n=3 for 28 d, n=3 for 35 d) were sham infected. Mice were killed on day 28 (experiment 1) and day 35 (experiment 2) post-infection and vaginal tissue, uterine horns and oviducts collected for analysis of mRNAs encoding inflammatory cytokines and chemokines. Total RNA was isolated and a superarray analysis performed using mouse Cytokines and Chemokines PCR arrays (Qiagen, Valencia, CA). Statistical differences in gene

expression were determined using a paired Students t-test. At 28 days after infection, the expression of mRNA encoding 6, 35 and 3 inflammatory genes differed from controls in vaginal, uterine and oviductal tissues, respectively ( $P < 0.05$ ). At 35 days after infection, the expression of mRNA encoding 16, 38 and 14 inflammatory genes differed from controls in vaginal, uterine and oviductal tissues, respectively ( $P < 0.05$ ). Understanding the mechanisms involved in the inflammatory response at later stages of infection should aid in the development of treatment options that minimize the development of asymptomatic, chronic inflammation-induced infertility.

## Introduction

*Chlamydia trachomatis* is an obligate intracellular pathogen and the most frequently reported sexually transmitted bacteria in the United States [170]. *C. trachomatis* targets epithelial cells within the genital tract initiating an immune response. Infectious load is correlated to clinical pathogenesis [171, 172]; infection with *C. trachomatis* is often asymptomatic. If left untreated the bacteria can ascend to and infect the oviducts [73, 173]. Untreated *C. trachomatis* infection can lead to persistent or recurrent inflammation, fibrosis, scarring, pelvic inflammatory disease (PID), tubal infertility, and/or an increased susceptibility to ectopic pregnancy [174, 175].

Upon infection, *C. trachomatis* elementary bodies (EBs) invade host epithelial cells in the genital tract. Within the host cells, EBs differentiate into reticulate bodies (RBs) which actively replicate within the host cell cytoplasm and then reorganize back into infectious EBs. This biphasic life cycle as well as adaptation to evade the immune response allows *C. trachomatis* to persist for extended periods within host epithelial cells, inducing a chronic inflammatory response [72, 74, 176-178].

Previous studies have investigated the inflammatory response of *C. trachomatis* in the initial stages of infection, including regulation by cytokines, chemokines and inflammatory mediators involved in the recruitment of immune cells [72-74, 179, 180]. For example, Rasmussen et. al, [72] demonstrated that once *C. trachomatis* has established infection within epithelial cells, the innate immune

response allows for the production of pro-inflammatory cytokines such as interleukins 1, 6, 8 (Il-1, Il-6, Il-8), tumor necrosis factor-alpha (Tnf- $\alpha$ ), and colony stimulating factor 2 (Csf2). Secretion of these cytokines and chemokines recruit immune cells such as natural killer (NK) cells and phagocytes. Following an established intracellular infection, the T-cell mediated immune response then becomes the critical element required for clearance [181]. However, evidence suggests that this T-cell response also contributes to the pathology following infection. Th1 cells limit replication of *C. trachomatis*, but Th2 cells inhibit Th1 responses leading to continued production of pro-inflammatory cytokines which can lead to fibrosis [75]. *C. trachomatis* also induces production of Tnf- $\alpha$ , which promotes apoptosis of infected and bystander cells [182]. Overall, understanding cytokine and chemokine regulation during both acute and chronic phases of infection may contribute to the development of treatment options that will minimize the long-term inflammatory consequences attributed to this disease.

Limited investigation of the later stages of infection has been performed, especially after infection with a low bacterial load. Maxion and Kelly [73] reported that cytokine and chemokine expression differs in anatomically distinct regions of the genital tract; these authors investigated the expression of chemokines associated with Th1 and Th2 responses in the oviducts and cervical-vaginal regions of the reproductive tract during the induction phase (0-14 days) and resolution phase (14-35 days) of infection. Spatially distinct regulation was noted; however, the authors focused their experiments on the evaluation of chemokine expression related to Th1 and Th2 responses using the mouse pneumonitis biovar of *C.*

*trachomatis*. Our objective was to determine within the reproductive tract the concurrent level of expression of mRNA encoding inflammatory mediators during the later phases of infection using a relatively low infectious load of *C. trachomatis* biovar, serovar D, one of the most prevalent serovars involved in urogenital infections of humans [183]. Two separate experiments were performed, with tissues collected at 4 and 5 weeks after infection (experiment 1 and 2, respectively). Our hypothesis was that mRNA encoding pro-inflammatory cytokines and chemokines will be differentially expressed in the female reproductive tract of mice infected with *C. trachomatis* at both 28 and 35 days post-infection compared to controls.

## **Methods**

### *Animals and Tissue Collection*

All animal experiments were performed according to the guidelines and protocol approved by the University of California Irvine Institutional Animal Care and Use Committee (protocol # 2009-2868). Using a previously described model of confirmed genital infection by *C. trachomatis*, serovar D, female C3H/HeJ mice, 6 -to 8 -week old, (Jackson Laboratories, Sacramento, CA) were pretreated with 2.5 mg medroxyprogesterone acetate (SICOR Pharmaceuticals) on Days -10 and -3 before infection [184, 185]. In both experiments mice were infected via vaginal challenge with  $5 \times 10^2$  inclusion-forming units (IFUs) of *C. trachomatis*, serovar D in 0.01 mL of

Eagle Minimal essential media (MEM, Gibco) on Day 0, as previously described [184, 185]. Control mice were also pretreated with medroxyprogesterone acetate, but were sham infected with Eagle Minimal essential media (MEM, Gibco) alone. Vaginal swabs were obtained twice weekly after infection and cell cultures were performed to monitor infection as previously described [184-186]. Mice were killed on day 28 (n = 3 for control and infected) in experiment 1 and day 35 (n = 3 for control and infected) in experiment 2. Immediately before being sacrificed vaginal cultures were obtained and all mice inoculated vaginally with *C. trachomatis* remained culture positive but at a significantly lower level than that obtained throughout the first two weeks of infection. Results of vaginal cultures following infection with this strain/dose of *C. trachomatis*, serovar D have been reported, including number of IFUs recovered [185]. Vaginal tissue, uterine horns and the oviducts were collected and snap-frozen for later extraction of RNA.

### *RNA Extraction and Analysis*

Total RNA was extracted from each tissue sample using TRIzol reagent (Invitrogen, Carlsbad, CA) and purified through RNeasy columns (Qiagen, Valencia, CA). To determine the effect of treatment on the expression of genes involved in the inflammatory response, a targeted real-time PCR SuperArray analysis was performed using RT<sup>2</sup> Profiler PCR arrays for mouse Cytokines and Chemokines (Qiagen), as previously described [23]. Real-time PCR were performed on an Eppendorf Mastercycler ep *realplex*<sup>2</sup> system (Eppendorf, Hamburg, Germany). Gene expression was standardized against GAPDH as a housekeeping gene and analyzed by the  $2^{-\Delta\Delta CT}$  method [111]. Statistical differences in the expression of mRNA were determined using a paired Students t-test.

## Results

*Experiment 1: Expression of mRNA encoding inflammatory genes in vaginal, uterine and oviduct tissues at 28 days post-infection*

Gene expression analysis was used to determine the effect of infection on the expression of inflammatory mRNAs at 28 days post-infection. In vaginal tissue collected at 28 days after infection, the expression of mRNA encoding 6 inflammatory genes increased and no genes decreased when compared to controls (Table A1.1).

**Table A1.1.** Effect of treatment on the expression of mRNAs in the vagina at 28 and 35 days post-infection.

<b>28 day infected vs control</b>				
Gene Symbol	Control Avg. $\Delta$ Ct $\pm$ SEM	Infected Avg. $\Delta$ Ct $\pm$ SEM	Fold change	p-value
Ccl24	12.79 $\pm$ 0.76	10.62 $\pm$ 0.53	4.5	0.007
Ccl3	10.18 $\pm$ 0.54	7.81 $\pm$ 1.00	5.5	0.025
<i>Ccl4*</i>	9.03 $\pm$ 0.59	6.28 $\pm$ 0.44	6.7	0.036
Cd40lg	14.01 $\pm$ 0.30	11.05 $\pm$ 0.36	7.8	0.011
Cxcl1	9.00 $\pm$ 0.25	6.18 $\pm$ 0.24	7.1	0.028
Il22	15.96 $\pm$ 0.37	15.03 $\pm$ 0.39	1.9	0.024
<b>35 day infected vs control</b>				
Gene Symbol	Control Avg. $\Delta$ Ct $\pm$ SEM	Infected Avg. $\Delta$ Ct $\pm$ SEM	Fold change	p-value
Bmp7	6.43 $\pm$ 0.17	6.51 $\pm$ 0.25	0.5	0.032
Csf3	4.88 $\pm$ 0.05	5.47 $\pm$ 0.06	0.5	<0.001
Ccl4*	9.03 $\pm$ 0.58	6.28 $\pm$ 0.23	4.2	0.019
Ctf1	6.67 $\pm$ 0.15	7.19 $\pm$ 0.12	0.6	0.023
Hprt	1.65 $\pm$ 0.14	1.81 $\pm$ 0.04	0.6	0.022
Ifna2	11.3 $\pm$ 0.19	11.41 $\pm$ 0.24	0.4	0.014
Ifng	13.04 $\pm$ 0.54	9.68 $\pm$ 0.43	8.5	0.035
Il10	9.94 $\pm$ 0.38	8.35 $\pm$ 0.32	2.8	0.048
Il11	11.76 $\pm$ 0.07	10.52 $\pm$ 0.23	2.3	0.03
Il18	5.86 $\pm$ 0.22	6.54 $\pm$ 0.06	0.4	0.014
Il1a	7.13 $\pm$ 0.09	5.97 $\pm$ 0.04	1.4	0.007
Il1rn	6.36 $\pm$ 0.37	5.95 $\pm$ 0.13	1.9	0.042
Mif	0.43 $\pm$ 0.12	0.76 $\pm$ 0.08	0.7	0.045
Pf4	5.15 $\pm$ 0.19	5.26 $\pm$ 0.06	0.6	0.031
Thpo	12.95 $\pm$ 0.6	13.76 $\pm$ 0.16	3.7	0.019
Tnf	8.4 $\pm$ 0.19	6.86 $\pm$ 0.09	2.4	0.002

The normalized average  $\Delta$  Ct value was calculated using GAPDH as the house-keeping gene. Fold change values (infected over control) in gene expression are presented as average fold change ( $2^{-(\text{average } \Delta\Delta\text{Ct})}$ ) for differentially expressed mRNAs ( $P < 0.05$ ).

In uterine samples collected at 28 days after infection, the expression of mRNA encoding 32 inflammatory genes increased and 3 genes decreased when compared to controls (Table A1.2). Of the 6 inflammatory mRNAs that increased within vaginal tissue after infection, 4 were also differentially affected by treatment in uterine samples.

**Table A1.2.** Effect of treatment on the expression of mRNAs in the uterus at 28 days post-infection.

<b>28 day infected vs control</b>									
Gene Symbol	control Avg. $\Delta$ Ct $\pm$ SEM	Infected Avg. $\Delta$ Ct $\pm$ SEM	Fold change	p-value	Gene Symbol	control Avg. $\Delta$ Ct $\pm$ SEM	Infected Avg. $\Delta$ Ct $\pm$ SEM	Fold change	p-value
Ccl1*	13.84 $\pm$ 0.32	12.03 $\pm$ 0.32	3.5	0.040	Il16*	7.41 $\pm$ 0.17	6.24 $\pm$ 0.27	2.2	0.045
Ccl17*	9.56 $\pm$ 0.11	7.76 $\pm$ 0.21	3.5	0.009	Il27*	11.83 $\pm$ 0.11	9.70 $\pm$ 0.15	4.4	0.002
Ccl2*	7.31 $\pm$ 0.29	4.53 $\pm$ 0.35	6.8	0.025	Lta*	11.01 $\pm$ 0.21	9.01 $\pm$ 0.37	4	0.037
Ccl22*	9.18 $\pm$ 0.13	7.45 $\pm$ 0.31	3.3	0.025	Ltb*	6.85 $\pm$ 0.16	3.58 $\pm$ 0.29	9.6	0.009
Ccl24*	11.64 $\pm$ 0.13	12.81 $\pm$ 0.30	0.4	0.018	Tgfb2*	0.67 $\pm$ 0.04	2.57 $\pm$ 0.76	0.3	0.030
Ccl3*	11.52 $\pm$ 0.34	8.49 $\pm$ 0.13	8.2	0.001	Tnf*	9.77 $\pm$ 0.22	6.93 $\pm$ 0.30	7.2	0.013
Ccl4*	9.73 $\pm$ 0.39	6.41 $\pm$ 0.15	10	0.001	Tnfsf11*	10.44 $\pm$ 0.47	8.68 $\pm$ 0.28	3.4	0.029
Ccl5*	5.80 $\pm$ 0.05	1.75 $\pm$ 0.27	16.6	0.008	Xcl1*	7.00 $\pm$ 0.19	5.29 $\pm$ 0.23	3.3	0.016
Cd40lg*	14.40 $\pm$ 0.61	8.19 $\pm$ 0.35	74	0.016	Ccl12	7.01 $\pm$ 0.25	3.70 $\pm$ 0.30	9.9	0.015
Csf2*	12.12 $\pm$ 0.45	9.31 $\pm$ 0.17	7	0.002	Ccl7	6.68 $\pm$ 0.33	3.63 $\pm$ 0.36	8.3	0.027
Cxcl10*	8.91 $\pm$ 0.06	4.99 $\pm$ 0.31	15.1	0.012	Cxcl5	10.50 $\pm$ 0.10	5.42 $\pm$ 0.46	34	0.049
Cxcl13*	7.80 $\pm$ 0.73	4.10 $\pm$ 0.13	13	0.001	Gusb	2.88 $\pm$ 0.09	2.27 $\pm$ 0.15	1.5	0.035
Cxcl16*	5.19 $\pm$ 0.15	3.27 $\pm$ 0.20	3.8	0.008	Il12a	12.98 $\pm$ 0.35	11.79 $\pm$ 0.26	2.3	0.045
Cxcl9*	8.26 $\pm$ 0.21	2.47 $\pm$ 0.18	55.3	0.001	Il18	6.87 $\pm$ 0.06	5.92 $\pm$ 0.11	1.9	0.003
Fasl*	10.13 $\pm$ 0.21	6.46 $\pm$ 0.20	12.8	0.002	Il1b	8.29 $\pm$ 0.52	5.55 $\pm$ 0.33	6.7	0.023
Ifna2*	11.25 $\pm$ 0.08	12.23 $\pm$ 0.38	0.5	0.041	Osm	10.42 $\pm$ 0.13	8.05 $\pm$ 0.13	5.2	0.001
Ifng*	11.30 $\pm$ 0.08	7.21 $\pm$ 0.28	17.1	0.006	Tnfsf10*	5.96 $\pm$ 0.13	4.12 $\pm$ 0.29	3.6	0.020
Il12b*	10.68 $\pm$ 0.24	8.07 $\pm$ 0.26	6.1	0.007					

The normalized average  $\Delta$  Ct value was calculated using GAPDH as the house-keeping gene. Fold change values (infected over control) in gene expression are presented as average fold change ( $2^{-\Delta(\text{average } \Delta\Delta\text{Ct})}$ ) for differentially expressed mRNAs ( $P < 0.05$ ).

In oviducts collected at 28 days post-infection, the expression of mRNA encoding 2 inflammatory genes increased and 1 gene decreased (Table A1.3). Of the 3 inflammatory genes affected by treatment within the oviduct, mRNA encoding 1 gene, chemokine (c-c motif) ligand 12 (*Ccl12*), was also increased in uterine samples.

**Table A1.3.** Effect of treatment on the expression of mRNAs in the oviduct at 28 and 35 days post-infection.

<b>28 day infected vs control</b>				
Gene Symbol	Control Avg. $\Delta$ Ct $\pm$ SEM	Infected Avg. $\Delta$ Ct $\pm$ SEM	Fold change	p-value
<i>Ccl12</i>	6.81 $\pm$ 0.37	4.39 $\pm$ 0.51	5.3	0.045
<i>Il13</i>	10.45 $\pm$ 0.21	11.69 $\pm$ 0.28	0.4	0.029
<i>Il23a</i>	11.43 $\pm$ 0.10	10.96 $\pm$ 0.08	1.4	0.021
<b>35 day infected vs control</b>				
Gene Symbol	Control Avg. $\Delta$ Ct $\pm$ SEM	Infected Avg. $\Delta$ Ct $\pm$ SEM	Fold change	p-value
<i>Bmp7</i>	7.97 $\pm$ 0.21	6.99 $\pm$ 0.12	2	0.011
<i>Ccl17</i>	7.11 $\pm$ 0.52	6.19 $\pm$ 0.32	6.1	0.021
<i>Cd40lg</i>	13.02 $\pm$ 0.30	10.40 $\pm$ 0.36	6.2	0.03
<i>Cx3cl1</i>	5.16 $\pm$ 0.21	4.16 $\pm$ 0.18	2	0.025
<i>Cxcl1</i>	12.57 $\pm$ 0.25	9.99 $\pm$ 0.24	6	0.007
<i>Fasl</i>	12.75 $\pm$ 0.66	8.79 $\pm$ 0.34	15.6	0.019
<i>Gpi1</i>	2.71 $\pm$ 0.04	1.56 $\pm$ 0.26	2.2	0.039
<i>Hsp90a</i>	0.53 $\pm$ 0.18	1.98 $\pm$ 0.26	2.7	0.027
<i>Il12b</i>	13.10 $\pm$ 0.24	10.47 $\pm$ 0.17	6.2	0.003
<i>Il1a</i>	11.42 $\pm$ 0.22	9.65 $\pm$ 0.23	3.4	0.011
<i>Il9</i>	7.16 $\pm$ 0.21	8.21 $\pm$ 0.26	0.5	0.044
<i>Lif</i>	10.03 $\pm$ 0.38	8.77 $\pm$ 0.08	2.4	0.016
<i>Mif</i>	1.55 $\pm$ 0.09	0.17 $\pm$ 0.29	2.6	0.044
<i>Osm</i>	11.50 $\pm$ 0.44	9.93 $\pm$ 0.33	3	0.047

The normalized average  $\Delta$  Ct value was calculated using GAPDH as the house-keeping gene. Fold change values (infected over control) in gene expression are presented as average fold change ( $2^{-(\text{average } \Delta\Delta\text{Ct})}$ ) for differentially expressed mRNAs ( $P < 0.05$ ).

*Experiment 2: Expression of mRNA encoding inflammatory genes in vaginal, uterine and oviduct tissues at 35 days post-infection*

In vaginal tissue collected 35 days after infection, the expression of mRNA encoding 8 inflammatory genes was increased and 8 decreased when compared to controls (Table A1.1). In uterine samples collected at 35 days after infection, the expression of mRNA encoding 32 inflammatory genes increased and 6 genes decreased compared to controls (Table A1.4). Of the 16 inflammatory mRNAs affected by treatment in vaginal tissue, 7 were also differentially expressed in uterine samples and 3 in oviduct samples. In oviducts collected at 35 days post-infection, the expression of mRNA encoding 13 inflammatory genes was increased and 1 gene decreased (Table A1.3). Of the 14 inflammatory mRNAs affected by treatment within the oviduct, 5 were also differentially expressed in uterine samples and 3 in vaginal tissue.

**Table A1.4.** Effect of treatment on the expression of mRNAs in the uterus at 35 days post-infection.

<b>35 day infected vs control</b>									
Gene Symbol	control Avg. $\Delta$ Ct $\pm$ SEM	Infected Avg. $\Delta$ Ct $\pm$ SEM	Fold change	p-value	Gene Symbol	control Avg. $\Delta$ Ct $\pm$ SEM	Infected Avg. $\Delta$ Ct $\pm$ SEM	Fold change	p-value
Ccl1	13.26 $\pm$ 0.25	11.66 $\pm$ 0.25	3	0.016	Il27	12.87 $\pm$ 0.30	9.73 $\pm$ 0.27	8.8	0.012
Ccl17	9.41 $\pm$ 0.15	7.97 $\pm$ 0.34	2.7	0.041	Lta	10.67 $\pm$ 0.19	9.22 $\pm$ 0.05	2.7	0.000
Ccl2	6.72 $\pm$ 0.14	5.44 $\pm$ 0.17	2.4	0.007	Ltb	6.92 $\pm$ 0.19	4.28 $\pm$ 0.09	6.2	0.000
Ccl22	8.69 $\pm$ 0.15	7.22 $\pm$ 0.15	2.8	0.005	Tgfb2	1.26 $\pm$ 0.14	3.70 $\pm$ 1.24	0.2	0.021
Ccl24	11.25 $\pm$ 0.08	13.93 $\pm$ 0.94	0.2	0.012	Tnf	9.73 $\pm$ 0.09	6.98 $\pm$ 0.28	6.7	0.013
Ccl3	10.83 $\pm$ 0.31	8.35 $\pm$ 0.08	5.6	0.000	Tnfsf11	9.94 $\pm$ 0.12	9.06 $\pm$ 0.14	1.8	0.013
Ccl4	9.08 $\pm$ 0.23	6.26 $\pm$ 0.04	7	0.000	Xcl1	7.12 $\pm$ 0.19	5.41 $\pm$ 0.40	3.3	0.050
Ccl5	5.47 $\pm$ 0.21	2.32 $\pm$ 0.09	8.9	0.000	Adipoq	11.58 $\pm$ 1.29	6.81 $\pm$ 0.40	27.2	0.034
Cd40lg	13.94 $\pm$ 0.93	8.64 $\pm$ 0.16	39.4	0.001	Cd70	11.19 $\pm$ 0.19	10.38 $\pm$ 0.07	1.7	0.008
Csf2	11.51 $\pm$ 0.29	8.78 $\pm$ 0.16	6.6	0.002	Cntf	7.99 $\pm$ 0.08	8.62 $\pm$ 0.17	0.6	0.023
Cxcl10	9.18 $\pm$ 0.19	5.08 $\pm$ 0.27	17.1	0.005	Csf3	7.55 $\pm$ 0.15	6.56 $\pm$ 0.18	2	0.017
Cxcl13	8.83 $\pm$ 0.27	4.51 $\pm$ 0.36	20	0.017	Cxcl1	11.41 $\pm$ 0.43	7.49 $\pm$ 0.46	15.1	0.029
Cxcl16	5.00 $\pm$ 0.23	3.14 $\pm$ 0.13	3.6	0.002	Cxcl11	12.94 $\pm$ 0.27	6.26 $\pm$ 0.34	102.5	0.018
Cxcl9	8.06 $\pm$ 0.22	2.41 $\pm$ 0.26	50.3	0.006	Il10	11.18 $\pm$ 0.41	8.77 $\pm$ 0.15	5.3	0.003
Fasl	10.25 $\pm$ 0.04	6.92 $\pm$ 0.29	10.1	0.013	Il21	15.24 $\pm$ 0.15	10.55 $\pm$ 0.46	25.8	0.047
Ilma2	10.87 $\pm$ 0.31	12.36 $\pm$ 0.33	0.4	0.037	Il3	15.11 $\pm$ 0.11	14.13 $\pm$ 0.22	2	0.026
Ilng	10.76 $\pm$ 0.16	7.33 $\pm$ 0.09	10.8	0.000	Thpo	11.89 $\pm$ 0.16	13.27 $\pm$ 0.36	0.4	0.020
Il12b	10.31 $\pm$ 0.23	8.46 $\pm$ 0.12	3.6	0.002	Tnfsf10	5.82 $\pm$ 0.18	3.80 $\pm$ 0.19	4	0.004
Il16	7.75 $\pm$ 0.11	6.75 $\pm$ 0.20	2	0.020	Vegfa	4.23 $\pm$ 0.13	4.83 $\pm$ 0.09	0.7	0.023

The normalized average  $\Delta$  Ct value was calculated using GAPDH as the house-keeping gene. Fold change values (infected over control) in gene expression are presented as average fold change ( $2^{-(\text{average } \Delta\Delta\text{Ct})}$ ) for differentially expressed mRNAs ( $P < 0.05$ ).

## Discussion and Conclusions

The host response to infection with *C. trachomatis* includes the induction of pro-inflammatory cytokines and chemokines which leads to innate and adaptive immune cell recruitment and activation [187]. Although the immune response is critical to the clearance of infection, the cellular immune response in particular can cause tissue damage that promotes fibrosis and can lead to infertility [75]. Considering that infection with *C. trachomatis* is often asymptomatic, the objective of these two experiments was to identify inflammatory mediators induced during the later phases of low-dose *C. trachomatis* genital infection in order to advance our understanding of disease progression and the immune response involved in potentially asymptomatic chronic inflammation.

It is well known that susceptibility to *C. trachomatis* infection is genetically controlled in mice. Both Tuffrey et al., [188-190] and Peterson et al., [184-186] have shown that human serovars of *C. trachomatis* can infect the genital tract of mice, specifically C3H/HeJ mice. Progesterone pretreatment is necessary, but this strain of mice remains culture positive for more than 4 weeks following infection [185]. In the current study, infected mice continued to have positive vaginal *C. trachomatis* cultures for the duration of the experiments with IFUs lower when the mice were killed compared to the first two weeks of infection.

In experiment 1, mice were killed 28 days post-infection. In vaginal tissue, mRNA encoding several cytokines and chemokines was affected by infection with *C. trachomatis*. Among differentially-regulated genes in vaginal samples, the

expression of mRNA encoding chemokine (c-c motif) ligand 4 (*Ccl4*), also known as macrophage inflammatory protein-1 $\beta$  (*MIP-1 $\beta$* ), a potent lymphocyte chemoattractant, was induced at 28 days of infection, with greater than a 6-fold increase compared to controls. C-C motif chemokines are a subgroup of chemokines with two adjacent cysteine residues near the amino terminus [191]. Yilma et al., 2013, reported an increase in *Ccl4* production in mouse macrophages during the early response to *C. trachomatis* infection; therefore, our results suggest that this cytokine is actively involved in both the early response and late phases of infection. [192]. Interestingly, *Ccl4* is highly related to macrophage inflammatory protein-1 $\alpha$  (*Ccl3*) and it is thought that these C-C motif chemokines are co-secreted to recruit specific T cell subsets during the immune response [193, 194]. In our study, expression of mRNA encoding *Ccl3* in the vagina was also increased at 28 days post-infection. Of all the differentially affected mRNAs in vaginal tissue, the largest fold-change in 28 day infected samples was seen in the induction of mRNA encoding CD40 ligand (*Cd40lg*). *Cd40lg* is mostly found on the surface of CD4<sup>+</sup> T cells and its interaction with Cd40 is required in the activation of humoral and cellular immune responses [195].

Within the uterus, treatment affected the expression of mRNA for five C-X-C motif chemokines. C-X-C motif chemokines are a subgroup of chemokines that have amino terminus cysteine residues separated by one amino acid [191]. Most notable is the induction of mRNA encoding chemokine (c-x-c motif) ligand 9 (*Cxcl9*). Previous studies have reported that *Cxcl9* peaks during the early phases of infection in the upper genital tract and may be involved in Th1 responses [73], our results

suggest that within the uterus, Cxcl9-mediated inflammation remains ongoing even after the initial phase of infection. The expression of mRNA encoding several interleukins was also induced in the infected mouse uterus at 28 days post-infection, including *Il1b*, *Il12a*, *Il12b*, *Il16*, *Il18*, and *Il27*. Notably, *Il12* is also reported to be involved in Th1 responses [196]. In our results, mRNA for *Il12* subunit alpha (*Il12a*) and subunit beta (*Il12b*) was induced at 28 days after infection. Several tumor necrosis factor family members and interferons were also induced, supporting the hypothesis that inflammation remains active and ongoing within the uterus during the late, resolution phase of infection.

When compared to the response observed in vaginal and uterine tissues at 28 days, the oviduct had fewer mRNA differentially expressed after infection of mice with *C. trachomatis*. The expression of mRNA encoding two genes was increased and one gene decreased. *C. trachomatis*-induced cell death within the oviduct is of concern due to long term sequelae, especially when considering that upon initial intracellular invasion of epithelial cells, *C. trachomatis* has the ability to prevent apoptosis of infected cells, therefore promoting infection [74, 179, 180]. Interestingly, the expression of mRNA encoding fas ligand (TNF superfamily, member 6; *FasL*), a key mediator of apoptosis, was not affected by treatment at 28 days post infection within the oviduct.

In experiment 2, mice were killed 35 days post-infection. The level of mRNA encoding 4 interleukins (*Il10*, *Il11*, *Il1rn*, *Il1a*) was increased and 1 interleukin (*Il18*) decreased in vaginal tissue collected at 35 days post-infection. Of these, *Il18* is reported to interact with *Il12* to stimulate interferon gamma (Ifn- $\gamma$ ) production

from NK cells during the early host response to infection [197]. Although studies have reported that *Ifn- $\gamma$*  is crucial for immune cell responses to *C. trachomatis* [197-199], the expression of mRNA for *Il12* did not differ at 35 days after infection and there was a decrease in levels of mRNA for *Il18*. Furthermore, *Ifn- $\gamma$*  had the greatest fold change of all differentially induced mRNA in the infected vaginal tissues, suggesting that *Ifn- $\gamma$*  production is being stimulated by other immunoregulatory factors at this later stage of infection. The increase in expression of mRNA encoding *Il10* within vaginal samples collected at 35 days after infection was not expected. Interleukin-10 is considered an anti-inflammatory cytokine and a recent study using *C. trachomatis* infected HeLa cells demonstrated that exogenous *Il10* treatment decreased several inflammatory cytokines including *Tnf* [200, 201].

Similar to vaginal tissues, uterine samples collected 35 days post-infection with *C. trachomatis* had increased expression of *Il10* and *Tnf*. Furthermore, an increase in adiponectin (*Adipoq*) was observed. Similar to *Il10*, *Adipoq* has anti-inflammatory properties including regulating cell defense and survival during stress conditions [202, 203]. In addition, a dramatic increase in the expression of mRNA for *Cxcl11* (102-fold change) was observed. *Cxcl11* shares features with *Cxcl9* and *Cxcl10*, including induction by interferons and expression on activated Th1 cells [204, 205]. It is reported that the Th1 response is crucial for controlling *C. trachomatis* infection, our results that mRNA for these transcripts were induced within the infected uterus is therefore consistent with other studies.

Within the oviduct mRNA encoding 13 genes was increased and one gene decreased at 35 days after infection. The expression of mRNA encoding *fasl*

increased at 35 days after infection with a 15-fold-change. In addition, changes in mRNA for other inflammatory mediators involved in tissue damage were detected, including *Il1-a*, which is released from lysed cells and acts by stimulating further cytokine release from neighboring cells [72]. Interestingly, levels of mRNA for Leukemia inhibitory factor (*Lif*) were increased in 35 day infected oviducts. Guney et al., 2008, demonstrated that LIF expression is increased in the oviducts of woman with ectopic pregnancies compared to non-pregnant woman [206]. Furthermore, Ji et al., 2009, proposed that LIF facilitates implantation of the conceptus in the oviduct when the stromal surface is exposed due to epithelial cell shedding caused by chronic inflammation [207]. The results shown here warrant further investigation especially since *C. trachomatis* has the ability to not only disrupt infected epithelial cells, but also non-infected cells in proximity to the infection [74]. In oviductal epithelia, these changes in gene expression and disruption of cellular processes can increase the risk of chronic inflammation-induced pelvic inflammatory disease and infertility.

Overall, this study examined the coordinated and concurrent expression of mRNA encoding multiple cytokines in spatially distinct sections of the reproductive tract. We investigated the later stages of infection using a relatively low infectious dose in order to obtain a better understanding of the genetic mechanisms involved in chronic inflammation and cellular damage. Differences in the magnitude of response to infection in differing regions of the reproductive tract were expected, as were differences in the level of expression of specific mRNAs within a tissue over time [73], illustrating well the dynamic nature of the inflammatory response to

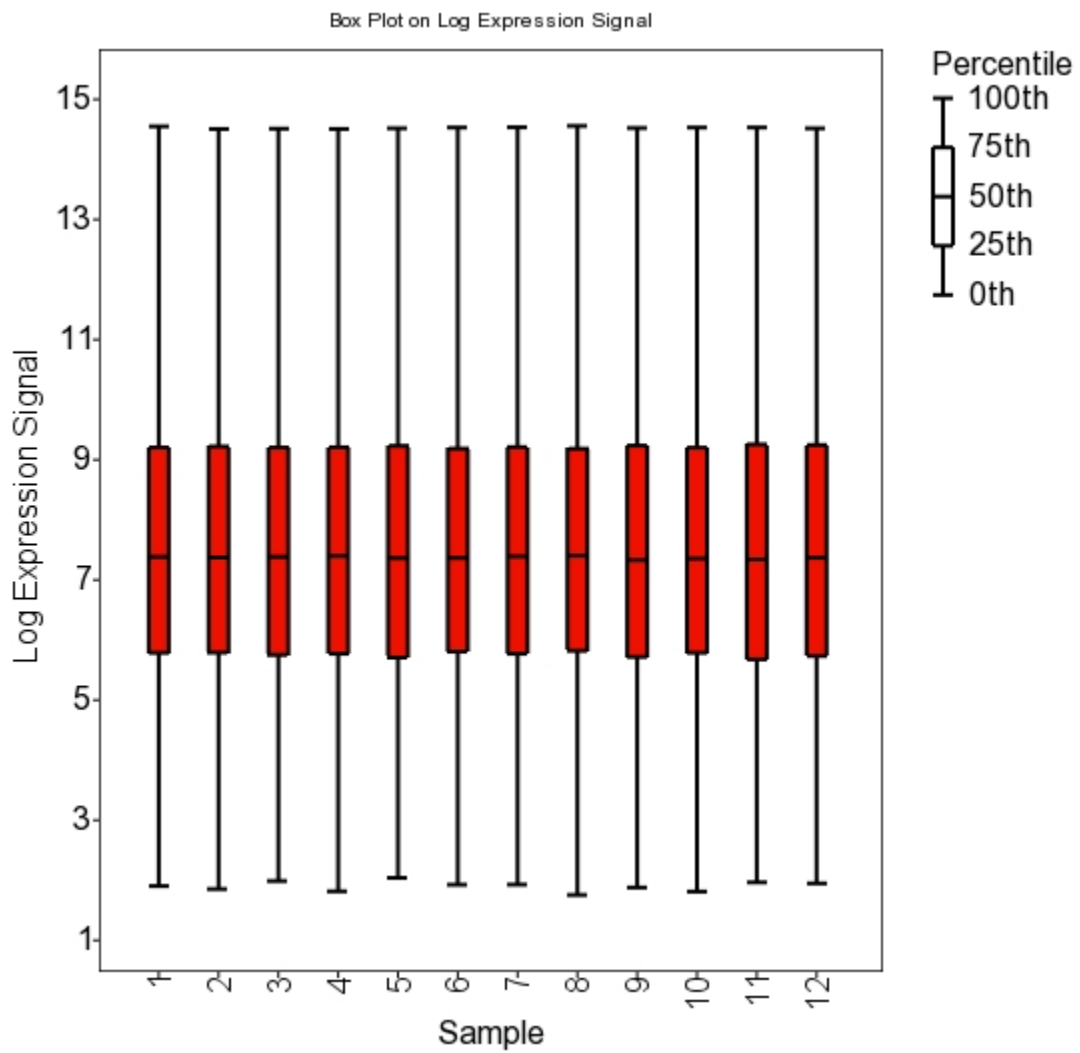
infection and the need for inclusive analyses of inflammatory mediators.

Understanding the mechanisms involved in the inflammatory response at late stages of infection should aid in the development of treatment options that minimize chronic inflammation-induced pelvic inflammatory disease and infertility.

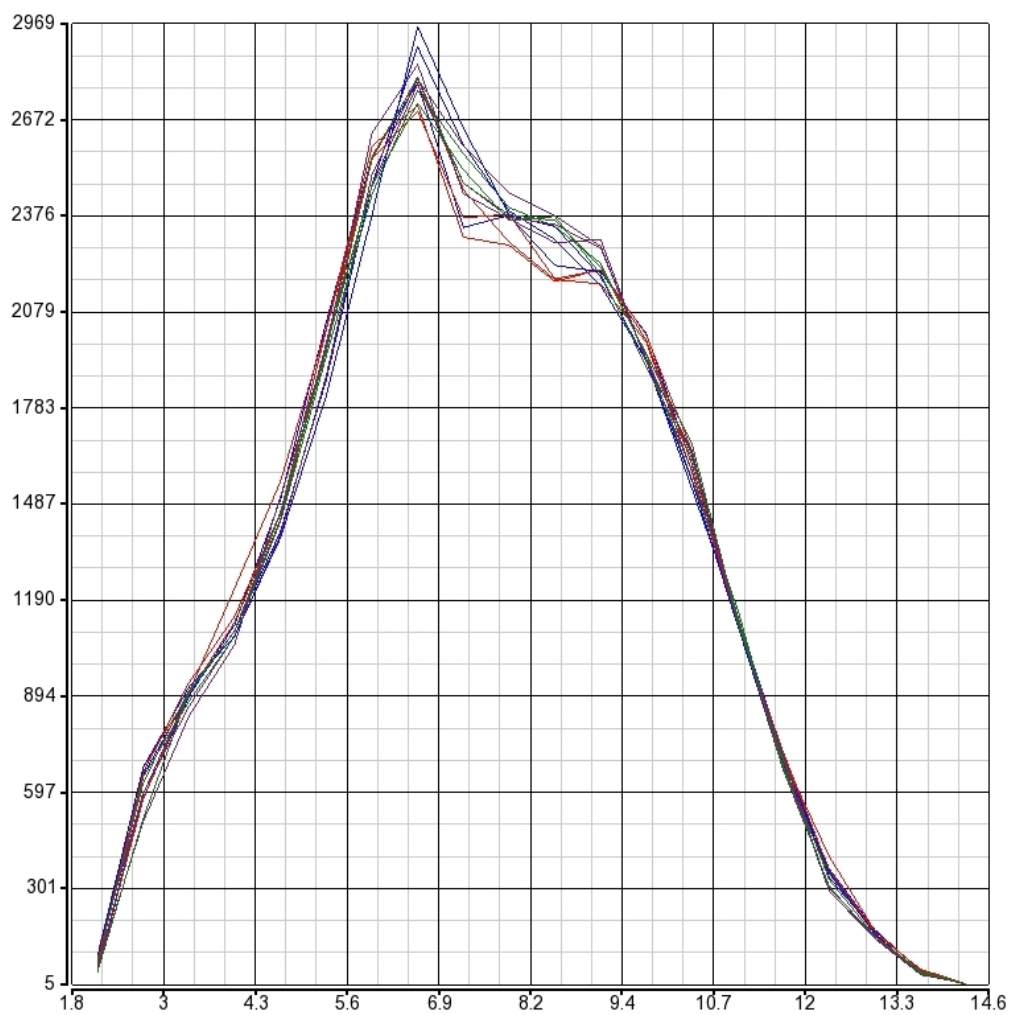
## APPENDIX 2.

### SUPPLEMENTARY TABLES AND FIGURES

**Supplementary Figure 1.** Box plot of the  $\log_2$  expression signal for each sample (microarray chip).

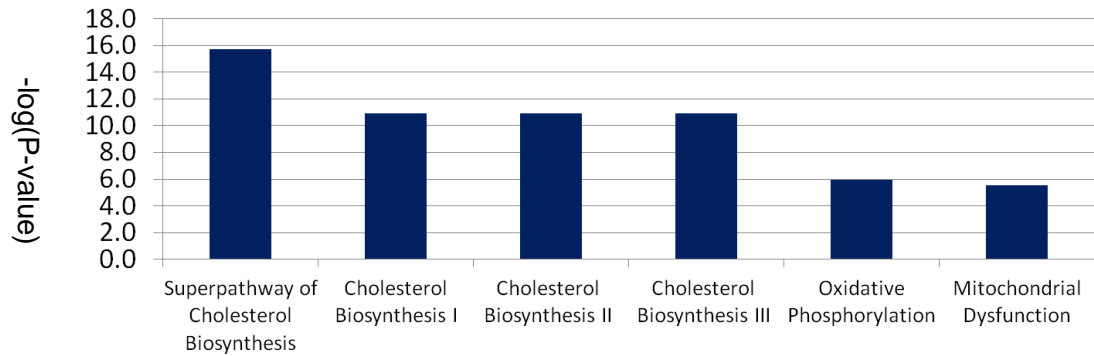


**Supplementary Figure 2.** Overlapping sample signal intensity histogram indicating the frequency of transcripts at specific signal intensity values.

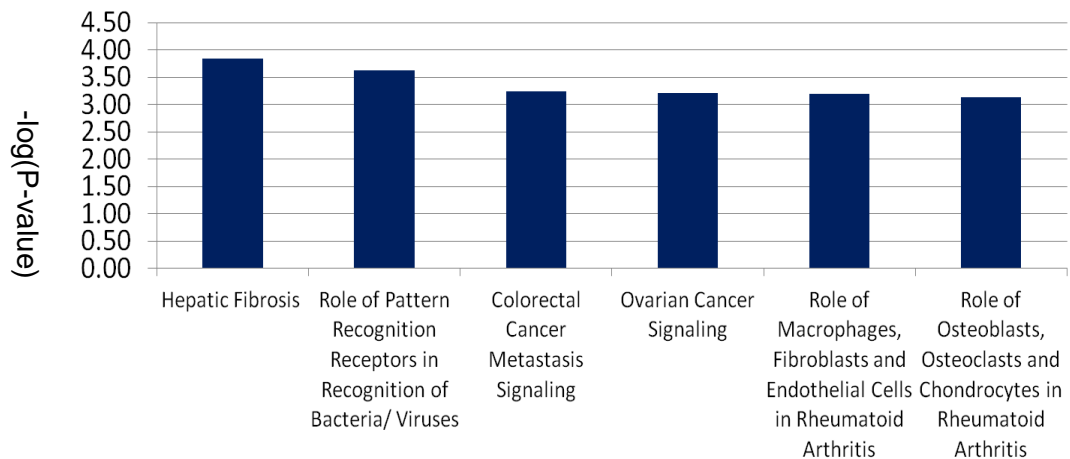


**Supplementary Figure 3.** Top 6 Canonical pathways from up- and down-regulated differentially expressed genes within epithelial cells of the ampulla in the follicular versus luteal phase. Ingenuity Pathway Analysis software was used to determine significant pathways based on the number of significant genes expressed within the pathway using Fischer’s Exact test ( $P < 0.05$ ).

A) Ampulla: Up-regulated pathways in the follicular versus luteal phases

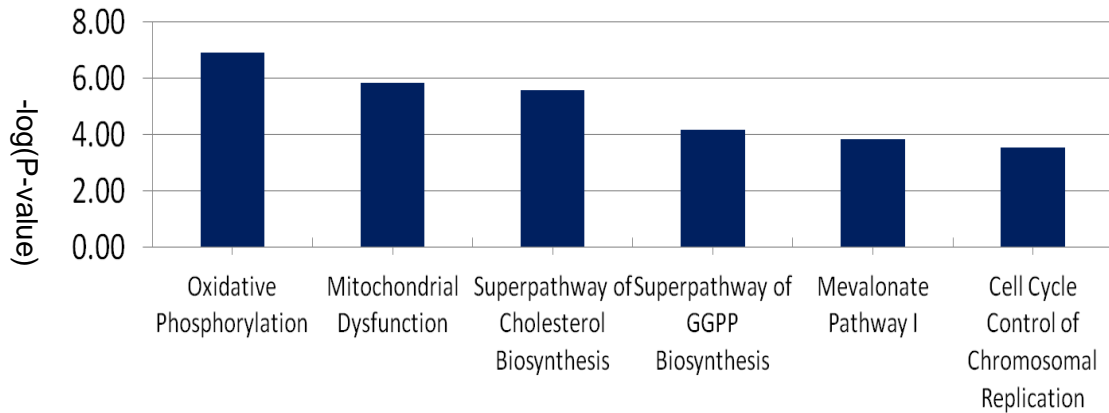


B) Ampulla: Down-regulated pathways in the follicular versus luteal phases

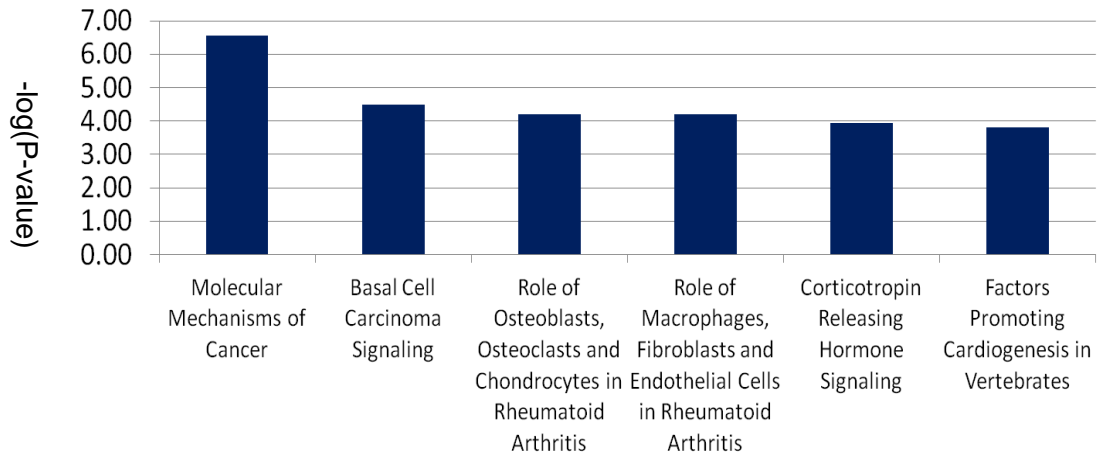


**Supplementary Figure 4.** Top 6 Canonical pathways from up- and down-regulated differentially expressed genes within epithelial cells of the isthmus in the follicular versus luteal phase. Ingenuity Pathway Analysis software was used to determine significant pathways based on the number of significant genes expressed within the pathway using Fischer's Exact test ( $P < 0.05$ ).

A) Isthmus: Up-regulated pathways in the follicular versus luteal phases



B) Isthmus: Down-regulated pathways in the follicular versus luteal phases



**Supplementary Table 1.** Differentially expressed genes from PMSG-treated ESR1KO versus PMSG-treated mouse oviducts. Significance set to  $P < 0.01$ , fold-change  $> 2$ .

Gene Symbol	Gene Description	p-value	Fold-Change
1-Mar	membrane-associated ring finger (C3HC4) 1	0.001	6.96
0610007L01Rik	RIKEN cDNA 0610007L01 gene	< 0.001	-2.71
0610010012Rik	RIKEN cDNA 0610010012 gene	< 0.001	-3.08
1110003E01Rik	RIKEN cDNA 1110003E01 gene	< 0.001	-2.21
1110017F19Rik	RIKEN cDNA 1110017F19 gene	0.003	3.26
1110018J18Rik	RIKEN cDNA 1110018J18 gene	0.001	2.03
1200015M12Rik/ A130040M12Rik	RIKEN cDNA 1200015M12 gene/RIKEN cDNA A130040M12 gene	< 0.001	2.66
1300002E11Rik	RIKEN cDNA 1300002E11 gene	0.001	2.32
1300010F03Rik	RIKEN cDNA 1300010F03 gene	< 0.001	-2.22
1700012D14Rik	RIKEN cDNA 1700012D14 gene	< 0.001	2.00
1700023E05Rik	RIKEN cDNA 1700023E05 gene	0.002	-2.02
2010109K11Rik	RIKEN cDNA 2010109K11 gene	< 0.001	2.22
2010305A19Rik	RIKEN cDNA 2010305A19 gene	0.002	-2.06
2200002K05Rik	RIKEN cDNA 2200002K05 gene	0.003	5.75
2210403K04Rik	RIKEN cDNA 2210403K04 gene	< 0.001	-2.75
2300002M23Rik	RIKEN cDNA 2300002M23 gene	< 0.001	- 524.94
2310014F06Rik	RIKEN cDNA 2310014F06 gene	< 0.001	5.57
2310015A10Rik	RIKEN cDNA 2310015A10 gene	0.001	2.29
2310043J07Rik	RIKEN cDNA 2310043J07 gene	< 0.001	17.00
2310046A06Rik	RIKEN cDNA 2310046A06 gene	0.001	-9.22
2610018G03Rik	RIKEN cDNA 2610018G03 gene	< 0.001	6.14
2610027K06Rik	RIKEN cDNA 2610027K06 gene	0.001	-5.40
2810030E01Rik	RIKEN cDNA 2810030E01 gene	0.001	2.83
2900010M23Rik	RIKEN cDNA 2900010M23 gene	0.001	-2.12
2900056M20Rik	RIKEN cDNA 2900056M20 gene	< 0.001	2.05
3010001F23Rik	RIKEN cDNA 3010001F23 gene	0.001	2.36
LOC100862497	predicted gene 2411/predicted gene 6604	< 0.001	2.08
3110035E14Rik	RIKEN cDNA 3110035E14 gene	< 0.001	-6.77
3632451006Rik	RIKEN cDNA 3632451006 gene	< 0.001	3.77
4833423F13Rik	RIKEN cDNA 4833423F13 gene	0.003	4.52
4930538K18Rik /AU022252	RIKEN cDNA 4930538K18 gene/expressed sequence AU022252	< 0.001	-22.68
4930579D07Rik	RIKEN cDNA 4930579D07 gene	< 0.001	-6.26
4930579G24Rik	RIKEN cDNA 4930579G24 gene	< 0.001	-2.14
5031426D15Rik	RIKEN cDNA 5031426D15 gene	0.001	3.71

**Supplementary Table 1. (Continued)**

5031439G07Rik	RIKEN cDNA 5031439G07 gene	< 0.001	-10.19
5430407P10Rik	RIKEN cDNA 5430407P10 gene	0.005	2.37
5730409E04Rik	RIKEN cDNA 5730409E04Rik gene	< 0.001	2.68
5730469M10Rik	RIKEN cDNA 5730469M10 gene	< 0.001	-3.18
5930412G12Rik	RIKEN cDNA 5930412G12 gene	0.001	6.35
6330403A02Rik	RIKEN cDNA 6330403A02 gene	0.003	4.14
6330403K07Rik	RIKEN cDNA 6330403K07 gene	< 0.001	13.27
6330416G13Rik	RIKEN cDNA 6330416G13 gene	< 0.001	-8.77
6430548M08Rik	RIKEN cDNA 6430548M08 gene	0.001	-8.66
6720401G13Rik	RIKEN cDNA 6720401G13 gene	0.007	2.03
9030224M15Rik	RIKEN cDNA 9030224M15 gene	0.001	-2.97
9130017K11Rik	RIKEN cDNA 9130017K11 gene	0.004	3.06
9230108I15Rik	RIKEN cDNA 9230108I15 gene	< 0.001	2.12
9330159F19Rik	RIKEN cDNA 9330159F19 gene	< 0.001	8.63
9430020K01Rik	RIKEN cDNA 9430020K01 gene	0.002	2.03
9430021M05Rik	RIKEN cDNA 9430021M05 gene	0.005	3.00
9530008L14Rik	RIKEN cDNA 9530008L14 gene	0.001	-3.24
9630033F20Rik	RIKEN cDNA 9630033F20 gene	< 0.001	-2.24
9930013L23Rik	RIKEN cDNA 9930013L23 gene	< 0.001	8.06
9930023K05Rik	RIKEN cDNA 9930023K05 gene	0.001	4.31
A130040M12Rik	RIKEN cDNA A130040M12 gene	< 0.001	2.04
A330049M08Rik	RIKEN cDNA A330049M08 gene	0.002	-4.35
A330068G13Rik	RIKEN cDNA A330068G13 gene	0.002	2.95
A630001G21Rik	RIKEN cDNA A630001G21 gene	0.009	2.75
A830039N20Rik	RIKEN cDNA A830039N20 gene	< 0.001	-3.41
AA986860	expressed sequence AA986860	< 0.001	12.49
Aass	aminoadipate-semialdehyde synthase	< 0.001	-2.15
AB099516/Higd1c/Mettl7a1/Mettl7a2/Mettl7a3	cDNA sequence AB099516/ HIG1 domain family, member 1C/methyltransferase like 7A1	< 0.001	-4.95
Abca5	ATP-binding cassette, sub-family A (ABC1), member 5	0.001	3.37
Abca8a	ATP-binding cassette, sub-family A (ABC1), member 8a	< 0.001	2.48
Abcb11	ATP-binding cassette, sub-family B (MDR/TAP), member 11	0.003	-5.96
Abcc4	ATP-binding cassette, sub-family C (CFTR/MRP), member 4	< 0.001	3.41
Abhd12	abhydrolase domain containing 12	0.002	-4.59
Abhd14b	abhydrolase domain containing 14b	0.002	2.30
Abhd5	abhydrolase domain containing 5	0.004	-2.01

**Supplementary Table 1. (Continued)**

Abhd6	abhydrolase domain containing 6	< 0.001	-2.79
Ablim3	actin binding LIM protein family, member 3	< 0.001	-8.38
Abp1	amiloride binding protein 1 (amine oxidase, copper-containing)	< 0.001	-3.46
Acpp	acid phosphatase, prostate	0.001	6.38
Acsf2	acyl-CoA synthetase family member 2	< 0.001	-2.24
Actn3	actinin alpha 3	< 0.001	9.36
Acy1	aminoacylase 1	0.001	-2.26
Ada	adenosine deaminase	< 0.001	-11.46
Adamts15	a disintegrin-like and metallopeptidase (reprolysin type) with thrombospondin type 1 mo	< 0.001	6.24
Adamts16	a disintegrin-like and metallopeptidase (reprolysin type) with thrombospondin type 1 mo	< 0.001	19.82
Adamts3	a disintegrin-like and metallopeptidase (reprolysin type) with thrombospondin type 1 mo	< 0.001	3.40
Adamts4	a disintegrin-like and metallopeptidase (reprolysin type) with thrombospondin type 1 mo	0.001	-4.50
Adamts8	a disintegrin-like and metallopeptidase (reprolysin type) with thrombospondin type 1 mo	< 0.001	3.93
Adcy8	adenylate cyclase 8	0.006	3.75
Adh7	alcohol dehydrogenase 7 (class IV), mu or sigma polypeptide	< 0.001	-42.46
Adhfe1	alcohol dehydrogenase, iron containing, 1	0.001	-2.01
Adig	adipogenin	< 0.001	-20.62
Adm	adrenomedullin	0.001	-3.55
Adora1	adenosine A1 receptor	< 0.001	3.86
Adssl1	adenylosuccinate synthetase like 1	0.001	4.14
Aen	apoptosis enhancing nuclease	0.003	-2.09
Ager	advanced glycosylation end product-specific receptor	< 0.001	22.77
Agr2	anterior gradient 2 ( <i>Xenopus laevis</i> )	0.004	-3.42
Agrn	agrin	0.001	2.65
Ahsp	alpha hemoglobin stabilizing protein	< 0.001	-17.11
AI256396	EST AI256396	< 0.001	2.88
AI314831	expressed sequence AI314831	0.009	2.19
AI428936	expressed sequence AI428936	< 0.001	3.87
AI504432	expressed sequence AI504432	< 0.001	2.18

**Supplementary Table 1. (Continued)**

AI839979	expressed sequence AI839979	0.001	3.65
Aifm2	apoptosis-inducing factor, mitochondrion-associated 2	< 0.001	2.25
Aipl1	aryl hydrocarbon receptor-interacting protein-like 1	0.002	-7.98
Akap12	A kinase (PRKA) anchor protein (gravin) 12	< 0.001	2.16
Akr1c14	aldo-keto reductase family 1, member C14	< 0.001	-45.65
Akr1c19	aldo-keto reductase family 1, member C19	< 0.001	13.46
Alas2	aminolevulinic acid synthase 2, erythroid	< 0.001	-5.39
Aldh1a3	aldehyde dehydrogenase family 1, subfamily A3	< 0.001	34.76
Aldh1a7	aldehyde dehydrogenase family 1, subfamily A7	0.003	2.32
Aldh1l1	aldehyde dehydrogenase 1 family, member L1	0.009	-2.91
Aldh3b1	aldehyde dehydrogenase 3 family, member B1	< 0.001	-2.05
Alg3	asparagine-linked glycosylation 3 (alpha-1,3-mannosyltransferase)	0.002	-2.68
Alpl	alkaline phosphatase, liver/bone/kidney	< 0.001	-16.48
Als2cl	ALS2 C-terminal like	0.005	2.08
Alx3	aristaless-like homeobox 3	< 0.001	-2.02
Amot	angiomin	< 0.001	3.39
Ampd3	adenosine monophosphate deaminase 3	0.001	-4.04
Angpt4	angiopoietin 4	0.003	4.32
Angptl1	angiopoietin-like 1	< 0.001	3.93
Ankrd33b	ankyrin repeat domain 33B	< 0.001	2.30
Ankrd46	ankyrin repeat domain 46	< 0.001	-3.03
Ano4	anoctamin 4	0.003	-12.39
Ano9	anoctamin 9	0.006	3.70
Anxa9	annexin A9	< 0.001	14.87
Aox1	aldehyde oxidase 1	< 0.001	2.61
Ap1s2	adaptor-related protein complex 1, sigma 2 subunit	< 0.001	3.84
Ap1s3	adaptor-related protein complex AP-1, sigma 3	0.003	2.97
Ap3b2	adaptor-related protein complex 3, beta 2 subunit	< 0.001	6.38
Aplnr	apelin receptor	0.009	-2.64
Apoc1	apolipoprotein C-I	0.001	7.52
Apod	apolipoprotein D	< 0.001	98.02
Apoe	apolipoprotein E	< 0.001	2.98

**Supplementary Table 1. (Continued)**

Apol7a	apolipoprotein L 7a	0.001	-8.07
Apol9a/Apol9b	apolipoprotein L 9a/apolipoprotein L 9b	0.004	-4.51
Aqp5	aquaporin 5	< 0.001	-22.71
Aqp8	aquaporin 8	< 0.001	-32.48
Arg1	arginase, liver	< 0.001	-6.38
Arg2	arginase type II	0.002	-2.47
Arhgap15	Rho GTPase activating protein 15	0.002	2.49
Arhgap20	Rho GTPase activating protein 20	< 0.001	3.31
Arhgap4	Rho GTPase activating protein 4	< 0.001	3.25
Arhgap9	Rho GTPase activating protein 9	< 0.001	4.35
Arhgef16	Rho guanine nucleotide exchange factor (GEF) 16	0.006	2.02
Arhgef17	Rho guanine nucleotide exchange factor (GEF) 17	0.001	2.06
Arl6ip5	ADP-ribosylation factor-like 6 interacting protein 5	< 0.001	-2.60
Arnt2	aryl hydrocarbon receptor nuclear translocator 2	< 0.001	4.26
Arsi	arylsulfatase i	< 0.001	-4.20
Arsj	arylsulfatase J	0.001	-7.15
Arsk	arylsulfatase K	0.001	2.25
Artn	artemin	0.001	8.50
Asb4	ankyrin repeat and SOCS box-containing 4	< 0.001	-16.71
Aspa	aspartoacylase	< 0.001	5.92
Aspn	asporin	< 0.001	-7.72
Asrgl1	asparaginase like 1	< 0.001	-2.31
Atp10b	ATPase, class V, type 10B	0.001	4.55
Atp1a2	ATPase, Na <sup>+</sup> /K <sup>+</sup> transporting, alpha 2 polypeptide	< 0.001	3.70
Atp6v1b1	ATPase, H <sup>+</sup> transporting, lysosomal V1 subunit B1	< 0.001	17.80
Atp6v1c2	ATPase, H <sup>+</sup> transporting, lysosomal V1 subunit C2	0.002	-15.54
Atp8a1	ATPase, aminophospholipid transporter (APLT), class I, type 8A, member 1	0.001	2.15
AU021092	expressed sequence AU021092	< 0.001	3.43
AU022252	expressed sequence AU022252	< 0.001	-2.43
AU040972	expressed sequence AU040972	0.003	-2.35
Auts2	autism susceptibility candidate 2	0.001	3.07
Avpr1a	arginine vasopressin receptor 1A	< 0.001	35.78
AW551984	expressed sequence AW551984	0.001	-8.31

**Supplementary Table 1. (Continued)**

Axin2	axin2	< 0.001	2.85
B230216N24Rik	RIKEN cDNA B230216N24 gene	0.004	2.71
B3galt5	UDP-Gal:betaGlcNAc beta 1,3-galactosyltransferase, polypeptide 5	0.001	-8.42
B3gnt5	UDP-GlcNAc:betaGal beta-1,3-N-acetylglucosaminyltransferase 5	< 0.001	2.42
B3gnt7	UDP-GlcNAc:betaGal beta-1,3-N-acetylglucosaminyltransferase 7	< 0.001	-4.58
B3gnt8	UDP-GlcNAc:betaGal beta-1,3-N-acetylglucosaminyltransferase 8	< 0.001	-16.37
B4galnt2	beta-1,4-N-acetyl-galactosaminyl transferase 2	< 0.001	10.08
B4galt5	UDP-Gal:betaGlcNAc beta 1,4-galactosyltransferase, polypeptide 5	< 0.001	-2.56
B4galt6	UDP-Gal:betaGlcNAc beta 1,4-galactosyltransferase, polypeptide 6	0.001	2.63
Bace2	beta-site APP-cleaving enzyme 2	0.001	-10.49
Bach2	BTB and CNC homology 2	0.001	3.75
Bank1	B cell scaffold protein with ankyrin repeats 1	0.004	2.12
BC021891	cDNA sequence BC021891	0.005	2.18
BC048546	cDNA sequence BC048546	< 0.001	-4.75
BC048679	cDNA sequence BC048679	< 0.001	222.15
Bcas3	breast carcinoma amplified sequence 3	< 0.001	-2.56
Bcat1	branched chain aminotransferase 1, cytosolic	< 0.001	-33.37
Bche	butyrylcholinesterase	0.002	2.47
Bcl11b	B cell leukemia/lymphoma 11B	< 0.001	6.18
Bcl2a1a/Bcl2a1b/Bcl2a1d	B cell leukemia/lymphoma 2 related protein A1a /// B cell leukemia/lymphoma 2 related p	< 0.001	2.56
Bcl2l15	BCL2-like 15	< 0.001	-5.77
Bcl3	B cell leukemia/lymphoma 3	0.002	2.39
Bdh1	3-hydroxybutyrate dehydrogenase, type 1	0.001	-5.53
Beta-s/Hbb-b1/Hbb-b2	hemoglobin subunit beta-1-like /// hemoglobin, beta adult major chain /// hemoglobin, b	< 0.001	-3.72
Bmf	BCL2 modifying factor	0.001	2.28
Bmp5	bone morphogenetic protein 5	< 0.001	2.16
Bmper	BMP-binding endothelial regulator	0.001	2.91

**Supplementary Table 1. (Continued)**

Boc	biregional cell adhesion molecule-related/down-regulated by oncogenes (Cdon) binding pr	< 0.001	2.74
Bpifc	BPI fold containing family C	< 0.001	-8.61
Bst2	bone marrow stromal cell antigen 2	< 0.001	-19.98
Btbd3	BTB (POZ) domain containing 3	0.006	-3.52
Btc	betacellulin, epidermal growth factor family member	0.006	3.25
Bysl	bystin-like	0.003	-2.63
C1ra	complement component 1, r subcomponent A	< 0.001	3.60
C1s	complement component 1, s subcomponent	< 0.001	2.92
C2	complement component 2 (within H-2S)	< 0.001	2.67
C2/Cfb	complement component 2 (within H-2S) / complement factor B	0.004	2.84
C2cd4b	C2 calcium-dependent domain containing 4B	0.002	3.13
C3/LOC100048759	complement component 3/complement C3-like	< 0.001	2.17
C4b/LOC675521	complement component 4B (Chido blood group)/complement C4-B-like	< 0.001	5.36
Cacna1g	calcium channel, voltage-dependent, T type, alpha 1G subunit	< 0.001	9.75
Cacna2d3	calcium channel, voltage-dependent, alpha2/delta subunit 3	0.001	-4.27
Cacnb4	calcium channel, voltage-dependent, beta 4 subunit	< 0.001	3.66
Cadm4	cell adhesion molecule 4	0.004	2.27
Calca	calcitonin/calcitonin-related polypeptide, alpha	< 0.001	8.28
Calcb	calcitonin-related polypeptide, beta	0.002	2.96
Calml3	calmodulin-like 3	0.001	-8.73
Camk2n2	calcium/calmodulin-dependent protein kinase II inhibitor 2	< 0.001	-2.27
Camta1	calmodulin binding transcription activator 1	0.001	-7.40
Capn6	calpain 6	< 0.001	5.87
Car11	carbonic anhydrase 11	< 0.001	2.89
Car12	carbonic anhydrase 12	< 0.001	-9.43
Car13	carbonic anhydrase 13	< 0.001	-5.04
Car9	carbonic anhydrase 9	< 0.001	-7.42
Casp12	caspase 12	< 0.001	2.34

**Supplementary Table 1. (Continued)**

Casp4	caspase 4, apoptosis-related cysteine peptidase	0.001	4.09
Cav1	caveolin 1, caveolae protein	< 0.001	-2.05
Cbs	cystathionine beta-synthase	< 0.001	-13.39
Ccdc109b	coiled-coil domain containing 109B	0.001	3.69
Ccdc141	coiled-coil domain containing 141	0.008	-2.39
Ccdc3	coiled-coil domain containing 3	< 0.001	-15.24
Ccdc67	coiled-coil domain containing 67	0.002	2.39
Ccna1	cyclin A1	0.003	2.51
Ccnd3	cyclin D3	0.005	2.08
Cd163	CD163 antigen	< 0.001	4.54
Cd163l1	CD163 molecule-like 1	0.001	10.07
Cd1d1	CD1d1 antigen	0.001	2.36
Cd44	CD44 antigen	< 0.001	2.21
Cd74	CD74 antigen (invariant polypeptide of major histocompatibility complex, class II antig	0.001	5.17
Cd79b	CD79B antigen	0.002	3.41
Cd84	CD84 antigen	0.001	2.06
Cda	cytidine deaminase	0.004	-4.35
Cdc42ep3	CDC42 effector protein (Rho GTPase binding) 3	< 0.001	2.68
Cdc42se2/LOC100045021	CDC42 small effector 2/CDC42 small effector protein 2-like	< 0.001	-3.13
Cdh11	cadherin 11	< 0.001	2.79
Cdh16	cadherin 16	< 0.001	50.13
Cdk5r1	cyclin-dependent kinase 5, regulatory subunit 1 (p35)	0.001	-3.18
Cdk6	cyclin-dependent kinase 6	0.007	2.01
Cdkn3	cyclin-dependent kinase inhibitor 3	0.003	-2.02
Cdo1	cysteine dioxygenase 1, cytosolic	0.006	7.22
Cdon	cell adhesion molecule-related/down-regulated by oncogenes	< 0.001	2.68
Cdv3	carnitine deficiency-associated gene expressed in ventricle 3	0.006	-2.02
Cebpd	CCAAT/enhancer binding protein (C/EBP), delta	< 0.001	3.84
Celf2	CUGBP, Elav-like family member 2	< 0.001	3.94
Ces2c/Ces2d-ps	carboxylesterase 2C/carboxylesterase 2D, pseudogene	0.007	2.88

**Supplementary Table 1. (Continued)**

Cflar	CASP8 and FADD-like apoptosis regulator	< 0.001	-2.35
Chac1	ChaC, cation transport regulator 1	0.002	-3.74
Chchd7	Coiled-coil-helix-coiled-coil-helix domain containing 7	0.003	2.01
Chdh	choline dehydrogenase	0.004	2.14
Chid1	chitinase domain containing 1	0.003	-2.04
Chl1	cell adhesion molecule with homology to L1CAM	< 0.001	6.73
Chn1	chimerin (chimaerin) 1	< 0.001	-2.76
Chodl	chondrolectin	< 0.001	48.14
Chrdl1	chordin-like 1	< 0.001	2.26
Chrn1	cholinergic receptor, nicotinic, beta polypeptide 1 (muscle)	< 0.001	3.77
Chst11	carbohydrate sulfotransferase 11	< 0.001	-2.11
Chst15	carbohydrate (N-acetylgalactosamine 4-sulfate 6-O) sulfotransferase 15	< 0.001	5.43
Cidea	cell death-inducing DNA fragmentation factor, alpha subunit-like effector A	< 0.001	-8.41
Cish	cytokine inducible SH2-containing protein	0.006	2.94
Clcf1	cardiotrophin-like cytokine factor 1	0.001	3.12
Clcn5	chloride channel 5	0.002	2.72
Cldn11	claudin 11	< 0.001	9.17
Cldn22	claudin 22	< 0.001	-4.69
Cldn23	claudin 23	< 0.001	-8.06
Cldn3	claudin 3	0.002	2.64
Cldn4	claudin 4	0.001	14.66
Cldn9	claudin 9	< 0.001	10.69
Clec7a	C-type lectin domain family 7, member a	0.001	6.54
Cnksr3	Cnksr family member 3	< 0.001	2.67
Cnp	2',3'-cyclic nucleotide 3' phosphodiesterase	0.001	2.15
Cnr1	cannabinoid receptor 1 (brain)	0.004	4.97
Cntf/U05342/Zfp91	ciliary neurotrophic factor/sequence U05342/zinc finger protein 91	< 0.001	4.98
Cntnap2	contactin associated protein-like 2	0.002	-10.42
Coch	coagulation factor C homolog (Limulus polyphemus)	< 0.001	5.78
Col12a1	collagen, type XII, alpha 1	0.001	3.66
Col13a1	collagen, type XIII, alpha 1	< 0.001	9.69
Col14a1	collagen, type XIV, alpha 1	< 0.001	5.55
Col18a1	collagen, type XVIII, alpha 1	0.001	3.28
Col23a1	collagen, type XXIII, alpha 1	0.001	2.78

**Supplementary Table 1. (Continued)**

Col25a1	collagen, type XXV, alpha 1	< 0.001	-9.70
Col4a5	collagen, type IV, alpha 5	< 0.001	2.25
Col4a6	collagen, type IV, alpha 6	< 0.001	3.43
Col6a4	collagen, type VI, alpha 4	< 0.001	-43.10
Col9a2	collagen, type IX, alpha 2	0.007	4.55
Copg2as2	coatomer protein complex, subunit gamma 2, antisense 2	0.001	4.33
Coq3	coenzyme Q3 homolog, methyltransferase (yeast)	< 0.001	-2.07
Cox7a1	cytochrome c oxidase, subunit VIIa 1	< 0.001	-3.11
Cp	ceruloplasmin	< 0.001	6.19
Cpm	carboxypeptidase M	< 0.001	10.72
Cpne8	copine VIII	0.001	-3.67
Cpxm2	carboxypeptidase X 2 (M14 family)	< 0.001	4.63
Crabp2	cellular retinoic acid binding protein II	< 0.001	-22.09
Cradd	CASP2 and RIPK1 domain containing adaptor with death domain	0.001	-2.24
Creb3l4	cAMP responsive element binding protein 3-like 4	0.001	-4.08
Crlf1	cytokine receptor-like factor 1	< 0.001	-39.94
Csf1r	colony stimulating factor 1 receptor	0.001	2.54
Csf3	colony stimulating factor 3 (granulocyte)	< 0.001	-24.43
Csrnp3	cysteine-serine-rich nuclear protein 3	< 0.001	-9.66
Ctf1	cardiotrophin 1	< 0.001	2.86
Ctnnd2	catenin (cadherin associated protein), delta 2	< 0.001	4.93
Ctr9	Ctr9, Paf1/RNA polymerase II complex component, homolog ( <i>S. cerevisiae</i> )	< 0.001	-2.07
Ctsb	cathepsin B	0.002	-3.14
Ctsd	cathepsin D	< 0.001	4.04
Ctso	cathepsin O	< 0.001	2.69
Cx3cl1	chemokine (C-X3-C motif) ligand 1	0.004	2.25
Cxcl12	chemokine (C-X-C motif) ligand 12	< 0.001	4.21
Cxcl14	chemokine (C-X-C motif) ligand 14	0.001	-3.31
Cxcl17	chemokine (C-X-C motif) ligand 17	0.003	3.68
Cxcr7	chemokine (C-X-C motif) receptor 7	< 0.001	-3.32
Cyba	cytochrome b-245, alpha polypeptide	0.001	2.20
Cycs	cytochrome c, somatic	< 0.001	-3.57
Cyp26a1	cytochrome P450, family 26, subfamily a, polypeptide 1	< 0.001	- 131.13

**Supplementary Table 1. (Continued)**

Cyp27a1	cytochrome P450, family 27, subfamily a, polypeptide 1	< 0.001	3.16
Cyp2a4/Cyp2a5	cytochrome P450, family 2, subfamily a, polypeptide 4/cytochrome P450, family 2, subfamily a, polypeptide 5	0.003	9.40
Cyp2d22	cytochrome P450, family 2, subfamily d, polypeptide 22	< 0.001	2.04
Cyp2f2	cytochrome P450, family 2, subfamily f, polypeptide 2	0.002	4.36
Cyp2j11	cytochrome P450, family 2, subfamily j, polypeptide 11	0.002	5.15
Cyp2j9	cytochrome P450, family 2, subfamily j, polypeptide 9	0.004	2.83
Cyp4b1	cytochrome P450, family 4, subfamily b, polypeptide 1	< 0.001	4.90
Cyp4v3	cytochrome P450, family 4, subfamily v, polypeptide 3	< 0.001	2.27
Cyth4	cytohesin 4	0.002	-3.19
D130062J21Rik	RIKEN cDNA D130062J21 gene	< 0.001	7.59
D230004N17Rik	RIKEN cDNA D230004N17 gene	0.001	5.02
D3Bwg0562e	DNA segment, Chr 3, Brigham & Women's Genetics 0562 expressed	< 0.001	2.22
D430041D05Rik	RIKEN cDNA D430041D05 gene	< 0.001	5.36
D630045J12Rik	RIKEN cDNA D630045J12 gene	< 0.001	2.18
Daam1	dishevelled associated activator of morphogenesis 1	0.003	-4.81
Dapk2	death-associated protein kinase 2	0.003	3.96
Dapk3	death-associated protein kinase 3	0.001	-2.13
Dbc1	deleted in bladder cancer 1 (human)	0.001	2.47
Dcc	deleted in colorectal carcinoma	< 0.001	-6.57
Dclk3	doublecortin-like kinase 3	< 0.001	9.33
Dcpp1/Dcpp2/ Dcpp3	demilune cell and parotid protein 1/2/3demilun	< 0.001	- 106.94
Dcpp3	demilune cell and parotid protein 3	< 0.001	- 770.92
Dgka	diacylglycerol kinase, alpha	0.008	2.06
Dgkh	diacylglycerol kinase, eta	0.001	-4.54
Dhcr24	24-dehydrocholesterol reductase	< 0.001	-12.60
Dhrs3	dehydrogenase/reductase (SDR family) member 3	< 0.001	2.43
Dhx58	DEXH (Asp-Glu-X-His) box polypeptide 58	0.003	-4.08

**Supplementary Table 1. (Continued)**

Diap3	diaphanous homolog 3 ( <i>Drosophila</i> )	0.004	-2.43
Dio2	deiodinase, iodothyronine, type II	0.001	-8.32
Dio3os	deiodinase, iodothyronine type III, opposite strand	0.001	5.52
Dkk3	dickkopf homolog 3 ( <i>Xenopus laevis</i> )	0.003	-2.88
Dleu7	deleted in lymphocytic leukemia, 7	< 0.001	-9.50
Dlk1	delta-like 1 homolog ( <i>Drosophila</i> )	0.001	4.52
Dmrta1	doublesex and mab-3 related transcription factor like family A1	< 0.001	-14.21
Dnajc19/Gm15118	DnaJ (Hsp40) homolog, subfamily C, member 19/predicted gene 15118	< 0.001	2.14
Dnase1l2	deoxyribonuclease 1-like 2	0.004	2.55
Dner	delta/notch-like EGF-related receptor	0.003	6.56
Dock8	dedicator of cytokinesis 8	0.006	-2.54
Dpp4	dipeptidylpeptidase 4	0.001	3.66
Dpt	dermatopontin	< 0.001	3.09
Dpyd	dihydropyrimidine dehydrogenase	0.001	3.37
Dram1	DNA-damage regulated autophagy modulator 1	0.002	2.30
Dst	dystonin	0.002	-2.66
Dtd1	D-tyrosyl-tRNA deacylase 1 homolog ( <i>S. cerevisiae</i> )	< 0.001	2.00
Dtna	dystrobrevin alpha	< 0.001	2.42
E230013L22Rik	RIKEN cDNA E230013L22 gene	0.001	-4.43
E330020D12Rik	Riken cDNA E330020D12 gene	0.001	2.19
E430024I08Rik	RIKEN cDNA E430024I08 gene	0.001	2.05
Ear1/Ear12/Ear2/Ear3	eosinophil-associated, ribonuclease A family, member 1/eosinophil-associated, ribon	0.007	3.92
Ear12/Ear2/Ear3	eosinophil-associated, ribonuclease A family, member 12/eosinophil-associated, ribo	< 0.001	5.96
Echdc2	enoyl Coenzyme A hydratase domain containing 2	0.003	2.25
Eda2r	ectodysplasin A2 receptor	< 0.001	2.68
Edem1	ER degradation enhancer, mannosidase alpha-like 1	< 0.001	-2.49
Edil3	EGF-like repeats and discoidin I-like domains 3	< 0.001	4.27
Ednrb	endothelin receptor type B	0.002	-2.30

**Supplementary Table 1.** (Continued)

Efemp1	epidermal growth factor-containing fibulin-like extracellular matrix protein 1	0.002	4.11
Efnb1	ephrin B1	0.001	2.18
Efnb2	ephrin B2	0.002	2.35
Egfl6	EGF-like-domain, multiple 6	0.001	8.00
Egflam	EGF-like, fibronectin type III and laminin G domains	< 0.001	2.31
Ehd3	EH-domain containing 3	0.005	-2.95
Elk3	ELK3, member of ETS oncogene family	0.001	-2.06
Emb	embigin	< 0.001	-9.71
Emilin2	elastin microfibril interfacier 2	< 0.001	-11.84
Enah	enabled homolog (Drosophila)	< 0.001	-3.90
Enc1	ectodermal-neural cortex 1	< 0.001	-2.74
Enpp2	ectonucleotide pyrophosphatase/phosphodiesterase 2	< 0.001	3.17
Enpp3	ectonucleotide pyrophosphatase/phosphodiesterase 3	0.001	3.69
Entpd5	ectonucleoside triphosphate diphosphohydrolase 5	< 0.001	2.51
Epas1	endothelial PAS domain protein 1	0.005	-3.48
Epb4.1l3	erythrocyte protein band 4.1-like 3	< 0.001	2.61
Epha1	Eph receptor A1	0.001	2.78
Epha4	Eph receptor A4	< 0.001	3.23
Ephb2	Eph receptor B2	< 0.001	3.94
Ephb6	Eph receptor B6	0.004	4.07
Eppk1	epiplakin 1	< 0.001	-3.60
Ermp1	endoplasmic reticulum metalloproteinase 1	0.001	2.12
Ern1	endoplasmic reticulum (ER) to nucleus signalling 1	< 0.001	-2.83
Esr1	estrogen receptor 1 (alpha)	0.006	-7.50
Esyt3	extended synaptotagmin-like protein 3	0.004	3.82
Etfb	electron transferring flavoprotein, beta polypeptide	< 0.001	-2.09
Etl4	enhancer trap locus 4	< 0.001	2.39
Ets2	E26 avian leukemia oncogene 2, 3' domain	< 0.001	-4.50
Etv1	ets variant gene 1	0.002	2.94
Exph5	exophilin 5	0.002	3.60
Expi	extracellular proteinase inhibitor	< 0.001	-6.76
F13a1	coagulation factor XIII, A1 subunit	< 0.001	3.01
F2r	coagulation factor II (thrombin) receptor	< 0.001	2.47

**Supplementary Table 1. (Continued)**

Fabp5	fatty acid binding protein 5, epidermal	< 0.001	-6.58
Fabp5/Gm3601	fatty acid binding protein 5, epidermal/predicted gene 3601	< 0.001	-4.47
Fam105a	family with sequence similarity 105, member A	0.003	2.10
Fam110c	family with sequence similarity 110, member C	0.001	-3.82
Fam176a	family with sequence similarity 176, member A	0.009	-2.28
Fam181b	family with sequence similarity 181, member B	0.001	3.46
Fam184b	family with sequence similarity 184, member B	0.001	2.19
Fam189a1	family with sequence similarity 189, member A1	0.002	-5.13
Fam194a	family with sequence similarity 194, member A	0.001	-3.99
Fam198b	family with sequence similarity 198, member B	0.001	2.73
Fam47e	family with sequence similarity 47, member E	0.003	-2.35
Fam54b	family with sequence similarity 54, member B	< 0.001	-2.21
Fam57a	family with sequence similarity 57, member A	< 0.001	-7.28
Fam65b	family with sequence similarity 65, member B	< 0.001	-13.56
Fasn	fatty acid synthase	< 0.001	-2.27
Fbln1	fibulin 1	< 0.001	5.22
Fbln2	fibulin 2	< 0.001	-5.96
Fbxo7	F-box protein 7	< 0.001	-2.27
Fbxw17	F-box and WD-40 domain protein 17	< 0.001	-2.56
Fcgbp	Fc fragment of IgG binding protein	0.002	2.30
Fcna	ficolin A	0.001	3.14
Fdft1	farnesyl diphosphate farnesyl transferase 1	< 0.001	-2.08
Fdps	farnesyl diphosphate synthetase	< 0.001	-4.01
Fez1	fasciculation and elongation protein zeta 1 (zygin I)	< 0.001	2.76
Fgf1	fibroblast growth factor 1	0.003	2.92
Fgf11	fibroblast growth factor 11	< 0.001	4.04
Fgf18	fibroblast growth factor 18	< 0.001	38.17
Fgfbp1	fibroblast growth factor binding protein 1	0.002	4.07

**Supplementary Table 1. (Continued)**

Fgfr1	fibroblast growth factor receptor-like 1	0.001	-2.17
Fgf	c-fos induced growth factor	< 0.001	-3.21
Fkbp11	FK506 binding protein 11	< 0.001	-6.24
Flnb	filamin, beta	< 0.001	-2.55
Flrt3	fibronectin leucine rich transmembrane protein 3	< 0.001	2.80
Fmo1	flavin containing monooxygenase 1	< 0.001	10.51
Fmo2	flavin containing monooxygenase 2	0.003	6.57
Fmod	fibromodulin	< 0.001	3.59
Fn1	fibronectin 1	0.002	-9.25
Fndc1	fibronectin type III domain containing 1	0.005	2.84
Fosl2	fos-like antigen 2	< 0.001	-2.31
Foxq1	forkhead box Q1	0.003	5.61
Foxred2	FAD-dependent oxidoreductase domain containing 2	0.003	2.53
Frem1	Fras1 related extracellular matrix protein 1	0.003	3.22
Frzb	frizzled-related protein	0.006	-2.01
Fxc1	fractured callus expressed transcript 1	< 0.001	-2.17
Fyn	Fyn proto-oncogene	< 0.001	-2.65
Fzd1	frizzled homolog 1 (Drosophila)	< 0.001	2.56
Fzd10	frizzled homolog 10 (Drosophila)	0.001	3.91
Fzd3	frizzled homolog 3 (Drosophila)	< 0.001	3.27
Fzd5	frizzled homolog 5 (Drosophila)	< 0.001	-3.20
Fzd7	frizzled homolog 7 (Drosophila)	< 0.001	2.66
G0s2	G0/G1 switch gene 2	0.002	3.29
G6pc2	glucose-6-phosphatase, catalytic, 2	< 0.001	42.88
G6pc3	glucose 6 phosphatase, catalytic, 3	0.002	-3.02
G6pd2/G6pdx	glucose-6-phosphate dehydrogenase 2/glucose-6-phosphate dehydrogenase X-linked	< 0.001	-7.36
G6pdx	glucose-6-phosphate dehydrogenase X-linked	< 0.001	-4.98
Gabra1	gamma-aminobutyric acid (GABA) A receptor, subunit alpha 1	0.007	2.38
Gabra3	gamma-aminobutyric acid (GABA) A receptor, subunit alpha 3	< 0.001	3.39
Gabrp	gamma-aminobutyric acid (GABA) A receptor, pi	< 0.001	6.37
Gadd45a	growth arrest and DNA-damage-inducible 45 alpha	< 0.001	-9.44
Gale	galactose-4-epimerase, UDP	< 0.001	-4.90

**Supplementary Table 1. (Continued)**

Ganc	glucosidase, alpha; neutral C	< 0.001	6.80
Garnl3	GTPase activating RANGAP domain-like 3	< 0.001	2.01
Gas2l3	growth arrest-specific 2 like 3	< 0.001	4.87
Gas6	growth arrest specific 6	0.003	-2.04
Gatsl2	GATS protein-like 2	< 0.001	-2.15
Gbp8	guanylate-binding protein 8	< 0.001	-14.28
Gclc	glutamate-cysteine ligase, catalytic subunit	< 0.001	-3.53
Gcnt2	glucosaminyl (N-acetyl) transferase 2, I-branching enzyme	0.003	2.55
Gda	guanine deaminase	< 0.001	-2.61
Gdap10	ganglioside-induced differentiation-associated-protein 10	0.003	2.93
Gdf10	growth differentiation factor 10	0.001	3.72
Gfra2	glial cell line derived neurotrophic factor family receptor alpha 2	0.001	3.43
Ghrh	growth hormone releasing hormone	< 0.001	-20.55
Gja1	gap junction protein, alpha 1	0.002	-32.21
Gja4	gap junction protein, alpha 4	0.002	-3.21
Gjb2	gap junction protein, beta 2	0.004	4.12
Gla	galactosidase, alpha	< 0.001	-2.21
Glb1l2	galactosidase, beta 1-like 2	0.001	2.67
Glb1l3	galactosidase, beta 1 like 3	< 0.001	11.48
Glce	glucuronyl C5-epimerase	< 0.001	2.35
Gldc	glycine decarboxylase	< 0.001	17.16
Glis2	GLIS family zinc finger 2	0.002	2.65
Glt25d2	glycosyltransferase 25 domain containing 2	0.003	-8.55
Gm11545	predicted gene 11545	< 0.001	2.61
Gm11787/Lyn	predicted gene 11787/Yamaguchi sarcoma viral (v-yes-1) oncogene homolog	0.006	-2.11
Gm13502/Idi1	predicted gene 13502/isopentenyl-diphosphate delta isomerase	0.002	-2.14
Gm14005	predicted gene 14005	< 0.001	-3.27
Gm17249	predicted gene, 17249	0.001	2.22
Gm19439	predicted gene, 19439	< 0.001	-5.61
Gm20033	predicted gene, 20033	< 0.001	2.89
Gm20245	predicted gene, 20245	0.001	2.09
Gm266	predicted gene 266	0.003	3.05
Gm3776/Gsta1/Gsta2	predicted gene 3776/glutathione S-transferase, alpha 1 (Ya)/glutathione S-trans	< 0.001	3.66

**Supplementary Table 1. (Continued)**

Gm8615/Gnpda1	glucosamine-6-phosphate deaminase 1 pseudogene/glucosamine-6-phosphate deaminase 1	< 0.001	-2.27
Gmgs	GDP-mannose 4, 6-dehydratase	0.001	-3.32
Gmppb	GDP-mannose pyrophosphorylase B	< 0.001	-2.87
Gna14	guanine nucleotide binding protein, alpha 14	0.004	-2.13
Gnai1	guanine nucleotide binding protein (G protein), alpha inhibiting 1	< 0.001	2.34
Gng12	guanine nucleotide binding protein (G protein), gamma 12	< 0.001	-3.73
Gng2	guanine nucleotide binding protein (G protein), gamma 2	< 0.001	-9.95
Gng4	guanine nucleotide binding protein (G protein), gamma 4	< 0.001	4.91
Gnpda1	glucosamine-6-phosphate deaminase 1	< 0.001	-2.40
Got2	glutamate oxaloacetate transaminase 2, mitochondrial	< 0.001	-3.00
Gp1bb	glycoprotein 1b, beta polypeptide	< 0.001	-20.90
Gp1bb/ Sept5	glycoprotein 1b, beta polypeptide/septin 5	0.004	-2.40
Gpam	glycerol-3-phosphate acyltransferase, mitochondrial	< 0.001	-2.29
Gpc1	glypican 1	< 0.001	4.53
Gpc6	glypican 6	< 0.001	2.38
Gpr160	G protein-coupled receptor 160	< 0.001	3.92
Gpr182	G protein-coupled receptor 182	< 0.001	3.56
Gpr30	G protein-coupled receptor 30	0.007	2.98
Gpr88	G-protein coupled receptor 88	0.002	3.42
Gprasp2	G protein-coupled receptor associated sorting protein 2	0.001	2.80
Gpt	glutamic pyruvic transaminase, soluble	< 0.001	2.46
Gpx1	glutathione peroxidase 1	0.001	-2.11
Gramd3	GRAM domain containing 3	< 0.001	3.57
Gramd4	GRAM domain containing 4	< 0.001	2.27
Greb1	gene regulated by estrogen in breast cancer protein	< 0.001	-64.60
Grhpr	glyoxylate reductase/hydroxypyruvate reductase	< 0.001	-3.05
Gria1	glutamate receptor, ionotropic, AMPA1 (alpha 1)	< 0.001	-46.45
Grip1	glutamate receptor interacting protein 1	< 0.001	4.22

**Supplementary Table 1. (Continued)**

Grm4	glutamate receptor, metabotropic 4	< 0.001	2.60
Grm7	glutamate receptor, metabotropic 7	0.003	2.68
Gsta2	glutathione S-transferase, alpha 2 (Yc2)	0.002	3.01
Gsta3	glutathione S-transferase, alpha 3	< 0.001	6.74
Gstm6	glutathione S-transferase, mu 6	0.002	-4.04
Gstm7	glutathione S-transferase, mu 7	< 0.001	5.36
Gstt1	glutathione S-transferase, theta 1	< 0.001	2.31
Gtf2f2	general transcription factor IIF, polypeptide 2	0.004	-2.22
Gucy1a2	guanylate cyclase 1, soluble, alpha 2	0.001	2.79
Gulo	gulonolactone (L-) oxidase	< 0.001	-12.69
Gyk	glycerol kinase	0.001	2.07
H19	H19 fetal liver mRNA	< 0.001	10.78
H2-DMb1/DMb2	histocompatibility 2, class II, locus Mb1/ locus Mb2	0.001	3.10
Hba-a1/-a2	hemoglobin alpha, adult chain 1/adult chain 2	0.001	-4.75
Heph1	hephaestin-like 1	< 0.001	-8.97
Hey1	hairy/enhancer-of-split related with YRPW motif 1	0.001	-3.75
Hfe	hemochromatosis	0.001	2.41
Higd1a	HIG1 domain family, member 1A	< 0.001	-2.02
Hilpda	hypoxia inducible lipid droplet associated	0.004	2.18
Hip1r	huntingtin interacting protein 1 related	0.001	-3.75
Hist1h3b/1h3c/1h3d/1h3e/1h3f2/h3b/2h3c1/2h3c2	histone cluster 1/2	0.008	-2.41
Hivep3	human immunodeficiency virus type I enhancer binding protein 3	< 0.001	3.99
Hlf	hepatic leukemia factor	0.001	3.57
Hmga2	high mobility group AT-hook 2	< 0.001	3.04
Homer2	homer homolog 2 (Drosophila)	< 0.001	3.36
Hook1	hook homolog 1 (Drosophila)	< 0.001	2.74
Hopx	HOP homeobox	0.003	-2.64
Hoxc5	homeobox C5	0.001	2.04
Hp	haptoglobin	< 0.001	-14.47
Hpca	hippocalcin	0.002	6.36
Hpgds	hematopoietic prostaglandin D synthase	< 0.001	-73.37
Hpse	heparanase	0.005	2.29

**Supplementary Table 1. (Continued)**

Hs3st3a1	heparan sulfate (glucosamine) 3-O-sulfotransferase 3A1	0.009	3.46
Hs6st1	heparan sulfate 6-O-sulfotransferase 1	0.008	2.20
Hsd11b2	hydroxysteroid 11-beta dehydrogenase 2	< 0.001	-9.28
Hsd17b11	hydroxysteroid (17-beta) dehydrogenase 11	0.008	-2.02
Hspb2	heat shock protein 2	< 0.001	-3.70
Hspb7	heat shock protein family, member 7 (cardiovascular)	< 0.001	-9.39
Hyal1/Nat6	hyaluronoglucosaminidase 1/N-acetyltransferase 6	0.003	-2.75
Icam1	intercellular adhesion molecule 1	< 0.001	3.74
Id2	inhibitor of DNA binding 2	0.004	2.01
Idua	Iduronidase, alpha-L-	< 0.001	-3.04
Ier3	immediate early response 3	< 0.001	-2.85
Ifi2711	interferon, alpha-inducible protein 27 like 1	0.006	-2.49
Ifi2712a	interferon, alpha-inducible protein 27 like 2A	< 0.001	-3.98
Igf2	insulin-like growth factor 2	< 0.001	6.31
Igfbp3	insulin-like growth factor binding protein 3	0.001	2.72
Ikzf1	IKAROS family zinc finger 1	0.001	3.03
Ikzf4	IKAROS family zinc finger 4	0.001	2.60
Il13ra2	interleukin 13 receptor, alpha 2	0.003	4.48
Il15	interleukin 15	< 0.001	2.70
Il15ra	interleukin 15 receptor, alpha chain	< 0.001	4.59
Il17ra	interleukin 17 receptor A	0.005	-3.56
Il17rb	interleukin 17 receptor B	< 0.001	14.38
Il17re	interleukin 17 receptor E	0.002	3.00
Il18bp	interleukin 18 binding protein	< 0.001	-20.01
Il18r1	interleukin 18 receptor 1	< 0.001	19.45
Il1r1	interleukin 1 receptor, type I	0.001	2.14
Il33	interleukin 33	< 0.001	11.69
Il7	interleukin 7	0.001	3.94
Irs1	insulin receptor substrate 1	< 0.001	-2.49
Irs4	insulin receptor substrate 4	< 0.001	11.64
Islr	immunoglobulin superfamily containing leucine-rich repeat	< 0.001	3.85
Ism1	isthmin 1 homolog (zebrafish)	0.001	2.80
Itga8	integrin alpha 8	0.001	-2.82
Itgae	integrin alpha E, epithelial-associated	0.001	2.33
Itgb3	integrin beta 3	0.001	-5.64

**Supplementary Table 1. (Continued)**

Itgbl1	integrin, beta-like 1	< 0.001	3.61
Jakmip1	janus kinase and microtubule interacting protein 1	0.003	2.86
Jam2	junction adhesion molecule 2	< 0.001	2.81
Jph4	junctophilin 4	0.001	-6.63
Jub	ajuba	0.002	-2.45
Kank4	KN motif and ankyrin repeat domains 4	0.002	4.92
Kcna1	potassium voltage-gated channel, shaker-related subfamily, member 1	0.001	5.76
Kcna5	potassium voltage-gated channel, shaker-related subfamily, member 5	< 0.001	6.29
Kcnc2	potassium voltage gated channel, Shaw-related subfamily, member 2	0.002	5.00
Kcnd2	potassium voltage-gated channel, Shal-related family, member 2	< 0.001	3.73
Kcnf1	potassium voltage-gated channel, subfamily F, member 1	< 0.001	-14.19
Kcng4	potassium voltage-gated channel, subfamily G, member 4	0.001	6.39
Kcnip1	Kv channel-interacting protein 1	< 0.001	9.85
Kcnj8	potassium inwardly-rectifying channel, subfamily J, member 8	0.001	-3.34
Kcnk13	potassium channel, subfamily K, member 13	< 0.001	-4.63
Kcnk2	potassium channel, subfamily K, member 2	< 0.001	-6.50
Kcnk5	potassium channel, subfamily K, member 5	0.006	-2.71
Kcnma1	potassium large conductance calcium-activated channel, subfamily M, alpha member 1	0.002	-3.53
Kcnmb1	potassium large conductance calcium-activated channel, subfamily M, beta member 1	0.009	-2.73
Kcnmb4	potassium large conductance calcium-activated channel, subfamily M, beta member 4	< 0.001	-3.18
Kctd5	potassium channel tetramerisation domain containing 5	0.005	-2.21
Kif5c	kinesin family member 5C	< 0.001	-4.08
Kirrel	kin of IRRE like ( <i>Drosophila</i> )	< 0.001	2.43
Kit	kit oncogene	0.001	-4.78
Klf12	Kruppel-like factor 12	0.001	2.75
Klhdc10	kelch domain containing 10	0.004	-2.51

**Supplementary Table 1. (Continued)**

Klh14	kelch-like 14 (Drosophila)	0.002	2.01
Klh129	kelch-like 29 (Drosophila)	0.005	-3.09
Klk1	kallikrein 1	< 0.001	-9.56
Klk1b1	kallikrein 1-related peptidase b1	< 0.001	-62.94
Klk1b21	kallikrein 1-related peptidase b21	< 0.001	-53.58
Klk1b22/Klk1b9	kallikrein 1-related peptidase b22/ b9	< 0.001	-20.97
Klk1b24	kallikrein 1-related peptidase b24	< 0.001	-73.19
Klk8	kallikrein related-peptidase 8	< 0.001	16.42
Krt13	keratin 13	0.001	10.11
Krt15	keratin 15	0.002	5.23
Krt36	keratin 36	0.008	2.28
Krt85	keratin 85	< 0.001	-5.61
Ky	kyphoscoliosis peptidase	0.001	2.10
L1cam	L1 cell adhesion molecule	< 0.001	6.72
Lamb2	laminin, beta 2	0.001	2.15
Larp1b	La ribonucleoprotein domain family, member 1B	< 0.001	-2.08
Lass3	LAG1 homolog, ceramide synthase 3	< 0.001	5.46
Lass4	LAG1 homolog, ceramide synthase 4	< 0.001	2.36
Lcn2	lipocalin 2	0.001	2.59
Ldb3	LIM domain binding 3	0.003	-2.38
Ldha	lactate dehydrogenase A	< 0.001	-2.10
Lemd1	LEM domain containing 1	< 0.001	12.18
Lgals3	lectin, galactose binding, soluble 3	0.006	2.13
Lgals3bp	lectin, galactoside-binding, soluble, 3 binding protein	0.002	-2.45
Lgi1	leucine-rich repeat LGI family, member 1	< 0.001	14.42
Lgi2	leucine-rich repeat LGI family, member 2	< 0.001	2.93
Lgi3	leucine-rich repeat LGI family, member 3	0.001	6.93
Lgr5	leucine rich repeat containing G protein coupled receptor 5	< 0.001	11.36
Lgr6	leucine-rich repeat-containing G protein-coupled receptor 6	0.001	-2.72
Lhx1	LIM homeobox protein 1	< 0.001	3.97
Lima1	LIM domain and actin binding 1	< 0.001	2.00
Ren1/Ren2	renin-1-like/renin 1 structural/renin 2 tandem duplication of Ren1	< 0.001	-13.71
Loxl2	lysyl oxidase homolog 2-like/lysyl oxidase-like 2	0.001	-4.56
LOC621549	uncharacterized LOC621549	< 0.001	3.86

**Supplementary Table 1. (Continued)**

Tcrb-J/Trbv1	T-cell receptor beta-2 chain C region-like/T cell receptor beta, joining region	0.001	2.75
Loxl1	lysyl oxidase-like 1	0.001	2.20
Lpar3	lysophosphatidic acid receptor 3	0.002	-2.40
Lpcat2	lysophosphatidylcholine acyltransferase 2	0.008	2.10
Lrat	lecithin-retinol acyltransferase (phosphatidylcholine-retinol-O-acyltransferase)	< 0.001	-53.53
Lrig1	leucine-rich repeats and immunoglobulin-like domains 1	< 0.001	2.77
Lrp4	low density lipoprotein receptor-related protein 4	< 0.001	4.81
Lrpap1	low density lipoprotein receptor-related protein associated protein 1	0.001	2.09
Lrrc17	leucine rich repeat containing 17	0.001	2.42
Lrrc31	leucine rich repeat containing 31	0.003	4.04
Lrrc41	leucine rich repeat containing 41	< 0.001	-2.41
Lrrc4c	leucine rich repeat containing 4C	0.001	2.25
Lrrc59	leucine rich repeat containing 59	0.001	-2.90
Lrrc8a/Phyhd1	leucine rich repeat containing 8A/phytanoyl-CoA dioxygenase domain containing 1	< 0.001	2.59
Lrrcc1	leucine rich repeat and coiled-coil domain containing 1	< 0.001	3.28
Lrrn1	leucine rich repeat protein 1, neuronal	0.001	2.63
Lrrn4	leucine rich repeat neuronal 4	0.001	2.63
Lrrtm1	leucine rich repeat transmembrane neuronal 1	< 0.001	29.44
Lsamp	limbic system-associated membrane protein	0.009	2.15
Lsp1	lymphocyte specific 1	0.001	2.41
Ltbp2	latent transforming growth factor beta binding protein 2	< 0.001	3.85
Ltbp3	latent transforming growth factor beta binding protein 3	< 0.001	2.31
Ltf	lactotransferrin	< 0.001	3.15
Lum	lumican	0.002	-4.30
Ly6e	lymphocyte antigen 6 complex, locus E	0.001	2.17
Ly6f	lymphocyte antigen 6 complex, locus F	0.001	-6.51
Ly6h	lymphocyte antigen 6 complex, locus H	0.001	3.09
Lynx1	Ly6/neurotoxin 1	0.002	2.74
Lypd6	LY6/PLAUR domain containing 6	0.010	2.70

**Supplementary Table 1. (Continued)**

Lyz1	lysozyme 1	0.001	2.52
Lyz2	lysozyme 2	0.001	2.84
Mab21l3	mab-21-like 3 ( <i>C. elegans</i> )	0.001	13.96
Mad2l2	MAD2 mitotic arrest deficient-like 2	< 0.001	-2.13
Maf	avian musculoaponeurotic fibrosarcoma (v-maf) AS42 oncogene homolog	< 0.001	3.00
Mal	myelin and lymphocyte protein, T cell differentiation protein	0.003	2.52
Man2a1	mannosidase 2, alpha 1	< 0.001	2.60
Maob	monoamine oxidase B	0.001	3.32
Map2k1	mitogen-activated protein kinase kinase 1	0.001	-2.10
Map2k4	mitogen-activated protein kinase kinase 4	< 0.001	-3.25
Mapk10	mitogen-activated protein kinase 10	< 0.001	-4.08
Mapk8ip1	mitogen-activated protein kinase 8 interacting protein 1	< 0.001	2.34
Mapt	microtubule-associated protein tau	0.008	2.77
Matn2	matrilin 2	< 0.001	4.82
Mboat2	membrane bound O-acyltransferase domain containing 2	< 0.001	-3.32
Mbp	myelin basic protein	0.002	5.82
Mcoln2	mucolipin 2	0.003	-3.69
Med12l	mediator of RNA polymerase II transcription, subunit 12 homolog (yeast)-like	< 0.001	2.50
Meg3	maternally expressed 3	0.005	2.50
Megf10	multiple EGF-like-domains 10	0.001	-4.19
Megf6	multiple EGF-like-domains 6	< 0.001	2.08
Met	met proto-oncogene	0.001	2.74
Mettl7a1	methyltransferase like 7A1	< 0.001	-3.11
Mfsd2a	major facilitator superfamily domain containing 2A	< 0.001	-5.78
Mfsd4	major facilitator superfamily domain containing 4	< 0.001	-3.59
Mgat3	mannoside acetylglucosaminyltransferase 3	< 0.001	2.71
Mgat4a	mannoside acetylglucosaminyltransferase 4, isoenzyme A	0.001	2.43
Mgl2	macrophage galactose N-acetyl-galactosamine specific lectin 2	0.001	3.86
Mgst3	microsomal glutathione S-transferase 3	0.001	-3.26
Mia1	melanoma inhibitory activity 1	0.001	7.48

**Supplementary Table 1. (Continued)**

Mlc1	megalencephalic leukoencephalopathy with subcortical cysts 1 homolog (human)	0.001	-21.79
Mmd	monocyte to macrophage differentiation-associated	0.001	-2.13
Mmd2	monocyte to macrophage differentiation-associated 2	0.001	-21.55
Mmp10	matrix metalloproteinase 10	0.001	7.28
Mmp16	matrix metalloproteinase 16	< 0.001	2.22
Mmp23	matrix metalloproteinase 23	< 0.001	2.69
Mmp9	matrix metalloproteinase 9	< 0.001	2.81
Mogat2	monoacylglycerol O-acyltransferase 2	0.001	-6.05
Moxd1	monooxygenase, DBH-like 1	< 0.001	4.24
Mpp6	membrane protein, palmitoylated 6 (MAGUK p55 subfamily member 6)	0.008	2.82
Mpped2	metallophosphoesterase domain containing 2	0.003	-4.04
Mpzl2	myelin protein zero-like 2	0.001	3.58
Mrc1	mannose receptor, C type 1	0.001	2.00
MsrB2	methionine sulfoxide reductase B2	0.001	-2.91
Mt3	metallothionein 3	< 0.001	-5.88
Mtap6	microtubule-associated protein 6	< 0.001	-3.47
Muc1	mucin 1, transmembrane	< 0.001	5.44
Muc4	mucin 4	0.001	8.01
Mustn1	musculoskeletal, embryonic nuclear protein 1	0.002	-3.79
Mvd	mevalonate (diphospho) decarboxylase	0.001	-2.36
Mybpc2	myosin binding protein C, fast-type	< 0.001	5.99
Myd88	myeloid differentiation primary response gene 88	0.002	2.07
Myh14	myosin, heavy polypeptide 14	< 0.001	-2.57
Myh7	myosin, heavy polypeptide 7, cardiac muscle, beta	0.001	-6.27
Myl4	myosin, light polypeptide 4	0.004	-2.46
MyliP	myosin regulatory light chain interacting protein	< 0.001	2.54
Myo10	myosin X	< 0.001	-3.10
Myo1f	myosin IF	0.001	2.19
Myo3b	myosin IIIB	0.007	4.15
Naaa	N-acylethanolamine acid amidase	< 0.001	-2.21
Nab1	Ngfi-A binding protein 1	0.001	2.99
NalcN	sodium leak channel, non-selective	< 0.001	4.46

**Supplementary Table 1. (Continued)**

Nampt	nicotinamide phosphoribosyltransferase	0.001	2.40
Napepld	N-acyl phosphatidylethanolamine phospholipase D	0.003	2.19
Nars2	asparaginyl-tRNA synthetase 2 (mitochondrial)(putative)	< 0.001	-2.26
Nav1	neuron navigator 1	0.001	2.37
Ncald	neurocalcin delta	0.002	-2.70
Ncbp1	nuclear cap binding protein subunit 1	< 0.001	-2.72
Ndrg1	N-myc downstream regulated gene 1	0.001	5.53
Nefl	neurofilament, light polypeptide	0.004	4.53
Nell1	NEL-like 1 (chicken)	0.002	3.24
Net1	neuroepithelial cell transforming gene 1	< 0.001	-2.65
Neu2	neuraminidase 2	0.002	2.92
Nfat5	nuclear factor of activated T cells 5	< 0.001	2.01
Nfatc2ip	nuclear factor of activated T cells, cytoplasmic, calcineurin dependent 2 interacting p	0.002	-2.38
Nfatc4	nuclear factor of activated T cells, cytoplasmic, calcineurin dependent 4	0.001	2.00
Nfe2l3	nuclear factor, erythroid derived 2, like 3	0.001	7.40
Nfkbia	nuclear factor of kappa light polypeptide gene enhancer in B cells inhibitor, alpha	< 0.001	-2.40
Nfkbie	nuclear factor of kappa light polypeptide gene enhancer in B cells inhibitor, epsilon	0.001	3.00
Ng23	Ng23 protein	< 0.001	2.58
Nhlrc1	NHL repeat containing 1	0.006	-2.55
Nid1	nidogen 1	< 0.001	2.07
Nid2	nidogen 2	< 0.001	3.30
Nipsnap1	4-nitrophenylphosphatase domain and non-neuronal SNAP25-like protein homolog 1	< 0.001	2.96
Nkd1	naked cuticle 1 homolog (Drosophila)	0.002	2.21
Nkd2	naked cuticle 2 homolog (Drosophila)	< 0.001	3.44
Nlrp6	NLR family, pyrin domain containing 6	< 0.001	-3.40
Nmnat2	nicotinamide nucleotide adenyltransferase 2	0.004	-4.52
Nostrin	nitric oxide synthase trafficker	< 0.001	-4.08
Notum	notum pectinacetyltransferase homolog (Drosophila)	< 0.001	8.56
Nov	nephroblastoma overexpressed gene	0.001	4.61
Npas3	neuronal PAS domain protein 3	0.001	2.95
Npl	N-acetylneuraminate pyruvate lyase	0.001	5.70

**Supplementary Table 1. (Continued)**

Npnt	nephronectin	0.003	2.40
Npr2	natriuretic peptide receptor 2	< 0.001	-3.36
Nptx1	neuronal pentraxin 1	< 0.001	-9.91
Npy2r	neuropeptide Y receptor Y2	< 0.001	3.35
Nr2f2	nuclear receptor subfamily 2, group F, member 2	< 0.001	2.22
Nrg4	neuregulin 4	0.005	-3.02
Nrip1	nuclear receptor interacting protein 1	< 0.001	-3.81
Nrp2	neuropilin 2	0.001	-2.67
Nsg2	neuron specific gene family member 2	< 0.001	9.18
Nt5c	5',3'-nucleotidase, cytosolic	< 0.001	-2.20
Nt5e	5' nucleotidase, ecto	< 0.001	8.94
Ntn1	netrin 1	0.001	2.72
Ntrk2	neurotrophic tyrosine kinase, receptor, type 2	< 0.001	2.77
Ntrk3	neurotrophic tyrosine kinase, receptor, type 3	< 0.001	3.63
Nup50	nucleoporin 50	< 0.001	-2.22
Nupr1	nuclear protein 1	< 0.001	4.05
Nus1	nuclear undecaprenyl pyrophosphate synthase 1 homolog ( <i>S. cerevisiae</i> )	0.004	-2.85
Oas1a	2'-5' oligoadenylate synthetase 1A	0.003	-2.87
Obscn	obscurin, cytoskeletal calmodulin and titin-interacting RhoGEF	< 0.001	5.78
Ocln	occludin	0.002	2.46
Ogfr11	opioid growth factor receptor-like 1	< 0.001	2.57
Ogn	osteoglycin	< 0.001	-3.12
Olfm2	olfactomedin 2	0.001	-10.65
Olfm4	olfactomedin 4	< 0.001	13.69
Olfml1	olfactomedin-like 1	< 0.001	3.99
Olfml3	olfactomedin-like 3	0.001	2.15
Olig3	oligodendrocyte transcription factor 3	0.003	-3.57
Omd	osteomodulin	< 0.001	-7.63
Osbpl1a	oxysterol binding protein-like 1A	< 0.001	-7.50
Osmr	oncostatin M receptor	< 0.001	4.34
Osr1	odd-skipped related 1 ( <i>Drosophila</i> )	0.002	3.81
Otub2	OTU domain, ubiquitin aldehyde binding 2	0.002	-3.19
Oxtr	oxytocin receptor	< 0.001	-35.01
P2ry12	purinergic receptor P2Y, G-protein coupled 12	< 0.001	2.37

**Supplementary Table 1. (Continued)**

Pacsin1	protein kinase C and casein kinase substrate in neurons 1	< 0.001	-15.22
Pacsin3	protein kinase C and casein kinase substrate in neurons 3	0.004	2.09
Padi1	peptidyl arginine deiminase, type I	< 0.001	-11.65
Padi2	peptidyl arginine deiminase, type II	< 0.001	-24.17
Pak3	p21 protein (Cdc42/Rac)-activated kinase 3	< 0.001	-16.89
Palld	palladin, cytoskeletal associated protein	< 0.001	9.80
Panx1	pannexin 1	0.002	-2.82
Pappa2	pappalysin 2	< 0.001	7.12
Paqr5	progesterin and adipoQ receptor family member V	0.003	3.08
Paqr8	progesterin and adipoQ receptor family member VIII	0.002	-2.92
Pcdh17	protocadherin 17	< 0.001	-25.08
Pcdh19	protocadherin 19	< 0.001	2.50
Pcdh8	protocadherin 8	0.002	9.87
Pcdh9	protocadherin 9	0.001	2.73
Pcdha1/10/11/12/2/3/4/5/6/7/8/9/Pcdhac1/2	protocadherin alpha 1//10/11/12/2/3/4/5/6/7/8/9/	0.002	-2.39
Pcsk5	proprotein convertase subtilisin/kexin type 5	0.002	2.33
Pde4d	phosphodiesterase 4D, cAMP specific	< 0.001	3.26
Pde7a	phosphodiesterase 7A	0.001	2.00
Pde8b	phosphodiesterase 8B	0.001	-2.25
Pde9a	phosphodiesterase 9A	< 0.001	-4.81
Pdgfc	platelet-derived growth factor, C polypeptide	< 0.001	2.44
Pdgfd	platelet-derived growth factor, D polypeptide	< 0.001	2.12
Pdgfra	platelet derived growth factor receptor, alpha polypeptide	< 0.001	2.81
Pdgfrl	platelet-derived growth factor receptor-like	< 0.001	3.42
Pdia5	protein disulfide isomerase associated 5	< 0.001	-2.03
Pdlim4	PDZ and LIM domain 4	< 0.001	3.24
Pdzrn4	PDZ domain containing RING finger 4	0.002	-4.84
Peg3	paternally expressed 3	0.008	2.06
Pemt	phosphatidylethanolamine N-methyltransferase	< 0.001	-3.32
Pet112l	PET112-like (yeast)	0.001	-2.28
Pfkip	phosphofructokinase, platelet	< 0.001	-2.63

**Supplementary Table 1. (Continued)**

Pgk1	phosphoglycerate kinase 1	< 0.001	-2.12
Pgm2l1	phosphoglucomutase 2-like 1	0.004	-4.08
Pgp	phosphoglycolate phosphatase	< 0.001	-2.67
Pgr	progesterone receptor	0.001	-6.76
Phtf2	putative homeodomain transcription factor 2	0.004	-4.05
Pik3ap1	phosphoinositide-3-kinase adaptor protein 1	0.003	2.62
Pik3r1	phosphatidylinositol 3-kinase, regulatory subunit, polypeptide 1 (p85 alpha)	< 0.001	2.38
Pik3r3	phosphatidylinositol 3 kinase, regulatory subunit, polypeptide 3 (p55)	< 0.001	-2.78
Pion	pigeon homolog (Drosophila)	0.006	2.18
Pip5k1b	phosphatidylinositol-4-phosphate 5-kinase, type 1 beta	< 0.001	-34.98
Pitpnm3	PITPNM family member 3	< 0.001	-10.74
Pla2g10	phospholipase A2, group X	< 0.001	40.80
Pla2g15	phospholipase A2, group XV	< 0.001	2.16
Pla2g5	phospholipase A2, group V	< 0.001	14.32
Plat	plasminogen activator, tissue	< 0.001	3.27
Plcd3	phospholipase C, delta 3	0.001	2.78
Plcl2	phospholipase C-like 2	< 0.001	-2.67
Plcx3	phosphatidylinositol-specific phospholipase C, X domain containing 3	< 0.001	4.70
Plekh1	pleckstrin homology domain containing, family H (with MyTH4 domain) member 1	0.003	-2.14
Pln	phospholamban	0.002	-5.38
Plod2	procollagen lysine, 2-oxoglutarate 5-dioxygenase 2	0.001	-5.50
Pls1	plastin 1 (I-isoform)	< 0.001	-4.26
Pmm2	phosphomannomutase 2	< 0.001	-2.29
Pnck	pregnancy upregulated non-ubiquitously expressed CaM kinase	0.002	2.59
Podn	podocan	0.001	9.28
Podxl	podocalyxin-like	< 0.001	3.75
Polg2	polymerase (DNA directed), gamma 2, accessory subunit	0.004	2.02
Poln	DNA polymerase N	0.006	4.73
Ppap2b	phosphatidic acid phosphatase type 2B	< 0.001	2.09
Pparg	peroxisome proliferator activated receptor gamma	0.002	-12.69

**Supplementary Table 1. (Continued)**

Ppargc1a	peroxisome proliferative activated receptor, gamma, coactivator 1 alpha	0.002	3.37
Ppargc1b	peroxisome proliferative activated receptor, gamma, coactivator 1 beta	0.001	-2.49
Ppl	periplakin	< 0.001	5.62
Ppm1e	protein phosphatase 1E (PP2C domain containing)	0.001	-2.29
Ppp2r2c	protein phosphatase 2 (formerly 2A), regulatory subunit B (PR 52), gamma isoform	< 0.001	-8.28
Prdm1	PR domain containing 1, with ZNF domain	< 0.001	4.10
Preld2	PRELI domain containing 2	0.001	2.36
Prelp	proline arginine-rich end leucine-rich repeat	< 0.001	3.19
Prkcb	protein kinase C, beta	0.001	2.89
Prkce	protein kinase C, epsilon	< 0.001	-2.96
Prkd1	protein kinase D1	0.005	3.00
Prkg2	protein kinase, cGMP-dependent, type II	0.004	3.73
Prlr	prolactin receptor	0.001	-3.32
Prodh	proline dehydrogenase	0.001	2.70
Prosapip1	ProSAPiP1 protein	< 0.001	4.00
Prr18	proline rich region 18	0.001	-2.26
Prrg3	proline rich Gla (G-carboxyglutamic acid) 3 (transmembrane)	< 0.001	2.99
Prtg	protogenin homolog (Gallus gallus)	< 0.001	2.80
Psm3	proteasome (prosome, macropain) 26S subunit, non-ATPase, 3	0.001	-2.47
Ptgds	prostaglandin D2 synthase (brain)	0.001	3.05
Ptger4	prostaglandin E receptor 4 (subtype EP4)	< 0.001	-2.36
Ptgs1	prostaglandin-endoperoxide synthase 1	0.002	2.58
Pthlh	parathyroid hormone-like peptide	< 0.001	4.58
Ptn	pleiotrophin	0.002	3.94
Ptpdc1	protein tyrosine phosphatase domain containing 1	< 0.001	2.72
Ptprr	protein tyrosine phosphatase, receptor type, R	0.005	3.13
Ptpru	protein tyrosine phosphatase, receptor type, U	0.004	2.50
Pycr2	pyrroline-5-carboxylate reductase family, member 2	< 0.001	-2.93
Qsox1	quiescin Q6 sulfhydryl oxidase 1	0.004	-2.40

**Supplementary Table 1. (Continued)**

Rab15	RAB15, member RAS oncogene family	0.001	3.12
Rab17	RAB17, member RAS oncogene family	0.001	7.62
Rab20	RAB20, member RAS oncogene family	0.006	-2.42
Rab37	RAB37, member of RAS oncogene family	< 0.001	-30.23
Rad18	RAD18 homolog ( <i>S. cerevisiae</i> )	< 0.001	-3.66
Raly	hnRNP-associated with lethal yellow	< 0.001	-2.94
Ramp3	receptor (calcitonin) activity modifying protein 3	< 0.001	-41.52
Rap1gap2	RAP1 GTPase activating protein 2	0.001	-4.17
Rapgef3	Rap guanine nucleotide exchange factor (GEF) 3	< 0.001	3.21
Rapgef4	Rap guanine nucleotide exchange factor (GEF) 4	< 0.001	-4.21
Rarb	retinoic acid receptor, beta	< 0.001	9.69
Rarres2	retinoic acid receptor responder (tazarotene induced) 2	< 0.001	2.04
Rasd1	RAS, dexamethasone-induced 1	< 0.001	-42.74
Rasgrf1	RAS protein-specific guanine nucleotide-releasing factor 1	0.003	4.64
Rasl11a	RAS-like, family 11, member A	< 0.001	2.25
Rassf2	Ras association (RalGDS/AF-6) domain family member 2	0.002	2.37
Rassf4	Ras association (RalGDS/AF-6) domain family member 4	< 0.001	3.60
Rassf5	Ras association (RalGDS/AF-6) domain family member 5	< 0.001	-14.02
Rbbp9	retinoblastoma binding protein 9	0.003	2.96
Rbfox3	RNA binding protein, fox-1 homolog ( <i>C. elegans</i> ) 3	0.004	5.71
Rbm20	RNA binding motif protein 20	< 0.001	-7.29
Rbp1	retinol binding protein 1, cellular	< 0.001	3.16
Rbp4	retinol binding protein 4, plasma	< 0.001	-2.01
Rbpms	RNA binding protein gene with multiple splicing	0.003	-2.18
Reck	reversion-inducing-cysteine-rich protein with kazal motifs	0.001	3.01
Reep1	receptor accessory protein 1	< 0.001	2.46
Reep2	receptor accessory protein 2	< 0.001	-2.32
Reps2	RALBP1 associated Eps domain containing protein 2	< 0.001	2.16
Rerg	RAS-like, estrogen-regulated, growth-inhibitor	0.001	-7.37

**Supplementary Table 1. (Continued)**

Retnla	resistin like alpha	< 0.001	12.77
Rftn1	raftlin lipid raft linker 1	< 0.001	-2.75
Rgs13	regulator of G-protein signaling 13	0.007	-7.21
Rgs18	regulator of G-protein signaling 18	0.002	2.13
Rhbdl2	rhomboid, veinlet-like 2 (Drosophila)	0.001	2.81
Rhbdl3	rhomboid, veinlet-like 3 (Drosophila)	< 0.001	5.72
Rhoj	ras homolog gene family, member J	< 0.001	2.29
Rhou	ras homolog gene family, member U	0.002	2.13
Rims1	regulating synaptic membrane exocytosis 1	0.001	-3.56
Rims2	regulating synaptic membrane exocytosis 2	0.009	2.60
Rmnd5b	required for meiotic nuclear division 5 homolog B ( <i>S. cerevisiae</i> )	0.001	-2.01
Rnf125	ring finger protein 125	< 0.001	4.09
Rnf157	ring finger protein 157	0.004	2.99
Rnf43	ring finger protein 43	0.001	2.97
Ror1	receptor tyrosine kinase-like orphan receptor 1	< 0.001	2.89
Rora	RAR-related orphan receptor alpha	0.001	2.23
Rprm	reprimin, TP53 dependent G2 arrest mediator candidate	< 0.001	-3.20
Rrbp1	ribosome binding protein 1	0.004	-2.46
Rsad1	radical S-adenosyl methionine domain containing 1	< 0.001	-5.91
Rspo1	R-spondin homolog ( <i>Xenopus laevis</i> )	< 0.001	4.54
Rtn1	reticulon 1	< 0.001	-28.78
Rtn4	reticulon 4	0.002	-2.45
Rtp4	receptor transporter protein 4	0.005	-2.09
Runx2	runt related transcription factor 2	0.001	2.41
S100a8	S100 calcium binding protein A8 (calgranulin A)	0.001	20.77
S100a9	S100 calcium binding protein A9 (calgranulin B)	0.001	17.86
Sacs	sacsin	0.007	-2.38
Samsn1	SAM domain, SH3 domain and nuclear localization signals, 1	< 0.001	2.09
Sc4mol	sterol-C4-methyl oxidase-like	< 0.001	-2.32
Scara3	scavenger receptor class A, member 3	< 0.001	4.61
Scara5	scavenger receptor class A, member 5 (putative)	< 0.001	12.09
Scarb2	scavenger receptor class B, member 2	< 0.001	-2.85
Schip1	Schwannomin interacting protein 1	< 0.001	2.95
Scube2	signal peptide, CUB domain, EGF-like 2	0.004	3.37

**Supplementary Table 1. (Continued)**

Scx	scleraxis	0.009	2.11
Sectm1a	secreted and transmembrane 1A	0.001	-4.94
Sema4d	sema domain, immunoglobulin domain (Ig), transmembrane domain (TM) and short cytoplasmic	0.004	2.23
Sema5b	sema domain, seven thrombospondin repeats (type 1 and type 1-like), transmembrane domain	< 0.001	2.18
Sema6d	sema domain, transmembrane domain (TM), and cytoplasmic domain, (semaphorin) 6D	0.005	-2.16
Serpina1b	serine (or cysteine) peptidase inhibitor, clade A, member 1B	< 0.001	27.57
Serpina9	serine (or cysteine) peptidase inhibitor, clade A (alpha-1 antitrypsin, antitrypsin)	< 0.001	-9.58
Serpina11	serine (or cysteine) peptidase inhibitor, clade B (ovalbumin), member 11	< 0.001	-34.12
Serpina1	serine (or cysteine) peptidase inhibitor, clade F, member 1	0.001	2.20
Serpina1	serine (or cysteine) peptidase inhibitor, clade G, member 1	< 0.001	2.73
Setd4	SET domain containing 4	< 0.001	-4.28
Sfmbt2	Scm-like with four mbt domains 2	< 0.001	2.50
Sfrp1	secreted frizzled-related protein 1	0.002	3.66
Sfrp2	secreted frizzled-related protein 2	0.001	2.90
Sftpd	surfactant associated protein D	< 0.001	-8.90
Sgk1	serum/glucocorticoid regulated kinase 1	0.002	-2.87
Sgsm1	small G protein signaling modulator 1	0.005	-6.52
Sh2d4a	SH2 domain containing 4A	0.006	2.42
Sh3bgr	SH3-binding domain glutamic acid-rich protein	< 0.001	2.91
Sh3gl2	SH3-domain GRB2-like 2	< 0.001	2.60
Shisa2	shisa homolog 2 ( <i>Xenopus laevis</i> )	< 0.001	-2.81
Shisa3	shisa homolog 3 ( <i>Xenopus laevis</i> )	0.002	5.84
Shisa9	shisa homolog 9 ( <i>Xenopus laevis</i> )	< 0.001	2.01
Skap1	src family associated phosphoprotein 1	< 0.001	3.49
Slc10a3	solute carrier family 10 (sodium/bile acid cotransporter family), member 3	0.001	-2.01
Slc12a2	solute carrier family 12, member 2	0.002	-4.05
Slc15a2	solute carrier family 15 (H <sup>+</sup> /peptide transporter), member 2	< 0.001	2.68

**Supplementary Table 1. (Continued)**

Slc16a4	Solute carrier family 16 (monocarboxylic acid transporters), member 4	< 0.001	2.15
Slc1a1	solute carrier family 1 (neuronal/epithelial high affinity glutamate transporter, syste	0.008	2.44
Slc1a4	solute carrier family 1 (glutamate/neutral amino acid transporter), member 4	0.009	-3.87
Slc22a21	solute carrier family 22 (organic cation transporter), member 21	< 0.001	2.58
Slc22a23	solute carrier family 22, member 23	0.002	2.36
Slc24a3	solute carrier family 24 (sodium/potassium/calcium exchanger), member 3	< 0.001	3.38
Slc25a18	solute carrier family 25 (mitochondrial carrier), member 18	0.004	-3.75
Slc25a35	solute carrier family 25, member 35	0.002	-3.87
Slc25a5	solute carrier family 25 (mitochondrial carrier, adenine nucleotide translocator)	< 0.001	-2.63
Slc27a2	solute carrier family 27 (fatty acid transporter), member 2	0.001	4.16
Slc28a3	solute carrier family 28 (sodium-coupled nucleoside transporter), member 3	< 0.001	-5.08
Slc30a2	solute carrier family 30 (zinc transporter), member 2	0.003	6.45
Slc35b1	solute carrier family 35, member B1	< 0.001	-2.48
Slc38a1	solute carrier family 38, member 1	< 0.001	-4.37
Slc39a4	solute carrier family 39 (zinc transporter), member 4	0.003	2.73
Slc43a1	solute carrier family 43, member 1	0.001	4.94
Slc47a1	solute carrier family 47, member 1	< 0.001	10.81
Slc52a3	solute carrier protein family 52, member 3	< 0.001	4.39
Slc6a14	solute carrier family 6 (neurotransmitter transporter), member 14	< 0.001	5.76
Slc6a2	solute carrier family 6 (neurotransmitter transporter, noradrenalin), member 2	< 0.001	-77.20
Slc6a4	solute carrier family 6 (neurotransmitter transporter, serotonin), member 4	< 0.001	-16.45
Slc7a11	solute carrier family 7 (cationic amino acid transporter, y+ system), member 11	< 0.001	-4.05
Slc7a2	solute carrier family 7 (cationic amino acid transporter, y+ system), member 2	< 0.001	2.42

**Supplementary Table 1.** (Continued)

Slco2a1	solute carrier organic anion transporter family, member 2a1	0.002	-3.68
Slco2b1	solute carrier organic anion transporter family, member 2b1	0.002	2.01
Slco3a1	solute carrier organic anion transporter family, member 3a1	< 0.001	-7.21
Slco4c1	solute carrier organic anion transporter family, member 4C1	0.001	4.09
Slit2	slit homolog 2 (Drosophila)	< 0.001	3.31
Slit3	slit homolog 3 (Drosophila)	< 0.001	2.55
Slpi	secretory leukocyte peptidase inhibitor	< 0.001	4.64
Smagp	small cell adhesion glycoprotein	0.001	2.35
Smarcd3	SWI/SNF related, matrix associated, actin dependent regulator of chromatin, subfamily d	0.006	2.68
Smoc1	SPARC related modular calcium binding 1	0.005	3.87
Snai2	snail homolog 2 (Drosophila)	0.003	-2.63
Snca	synuclein, alpha	< 0.001	-6.03
Snaip	synuclein, alpha interacting protein (synphilin)	0.005	-2.52
Snhg11	small nucleolar RNA host gene 11	< 0.001	6.12
Snhg4	small nucleolar RNA host gene 4 (non-protein coding)	0.001	-2.09
Sntg2	syntrophin, gamma 2	< 0.001	-6.77
Snx29	sorting nexin 29	0.003	2.25
Snx30	sorting nexin family member 30	0.001	2.00
Socs2	suppressor of cytokine signaling 2	0.001	-6.06
Sorbs1	sorbin and SH3 domain containing 1	< 0.001	2.11
Sorl1	sortilin-related receptor, LDLR class A repeats-containing	0.001	2.31
Sowahb	sosondowah ankyrin repeat domain family member B	0.004	3.19
Sox18	SRY-box containing gene 18	< 0.001	-12.80
Sox2ot	SOX2 overlapping transcript (non-protein coding)	0.003	-5.59
Sox3	SRY-box containing gene 3	< 0.001	-3.92
Sox9	SRY-box containing gene 9	0.001	-3.39
Spdef	SAM pointed domain containing ets transcription factor	< 0.001	-39.53
Spdya	speedy homolog A (Xenopus laevis)	0.002	3.19

**Supplementary Table 1. (Continued)**

Speer4a	spermatogenesis associated glutamate (E)-rich protein 4a	< 0.001	-4.27
Speer4b	spermatogenesis associated glutamate (E)-rich protein 4b	0.001	-4.65
Sphk1	sphingosine kinase 1	0.002	3.10
Spink4	serine peptidase inhibitor, Kazal type 4	0.002	-2.80
Spink8	serine peptidase inhibitor, Kazal type 8	0.001	5.39
Spnb3	spectrin beta 3	0.008	2.22
Spon1	spondin 1, (f-spondin) extracellular matrix protein	0.001	-3.68
Sprr2f	small proline-rich protein 2F	0.001	-16.47
Spsb4	splA/ryanodine receptor domain and SOCS box containing 4	< 0.001	-4.37
Srprb /// Trf	signal recognition particle receptor, B subunit /// transferrin	< 0.001	5.30
Srpx	sushi-repeat-containing protein	< 0.001	5.34
Srr	serine racemase	0.001	2.49
Ssbp2	single-stranded DNA binding protein 2	< 0.001	2.15
St6gal1	beta galactoside alpha 2,6 sialyltransferase 1	< 0.001	4.22
St6gal2	beta galactoside alpha 2,6 sialyltransferase 2	0.001	3.54
St8sia2	ST8 alpha-N-acetyl-neuraminide alpha-2,8-sialyltransferase 2	0.001	3.26
St8sia6	ST8 alpha-N-acetyl-neuraminide alpha-2,8-sialyltransferase 6	0.002	2.33
Stat5a	signal transducer and activator of transcription 5A	< 0.001	-44.22
Stbd1	starch binding domain 1	0.001	-2.18
Stc2	stanniocalcin 2	< 0.001	-6.51
Steap2	six transmembrane epithelial antigen of prostate 2	0.001	2.02
Stk39	serine/threonine kinase 39	0.001	-4.00
Stoml3	stomatin (Epb7.2)-like 3	< 0.001	-4.41
Stx1b	syntaxin 1B	0.001	6.26
Stxbp6	syntaxin binding protein 6 (amisyn)	0.001	2.23
Sulf1	sulfatase 1	< 0.001	3.26
Sult1d1	sulfotransferase family 1D, member 1	0.003	4.62
Sult1e1	sulfotransferase family 1E, member 1	< 0.001	46.32
Sv2b	synaptic vesicle glycoprotein 2 b	0.005	-5.12
Sval2	seminal vesicle antigen-like 2	0.001	-12.93

**Supplementary Table 1. (Continued)**

Svep1	sushi, von Willebrand factor type A, EGF and pentraxin domain containing 1	< 0.001	5.99
Syn2	synapsin II	< 0.001	-91.45
Synpr	synaptoporin	< 0.001	22.32
Syt9	synaptotagmin IX	< 0.001	4.27
Tac1	tachykinin 1	0.008	-2.07
Tacc1	transforming, acidic coiled-coil containing protein 1	0.010	-3.61
Tbc1d16	TBC1 domain family, member 16	0.001	2.18
Tbc1d4	TBC1 domain family, member 4	< 0.001	-3.26
Tbx2	T-box 2	< 0.001	-3.31
Tenc1	tensin like C1 domain-containing phosphatase	0.001	3.01
Tes	testis derived transcript	0.004	-2.28
Tex2	testis expressed gene 2	< 0.001	-6.44
Tgfb2	transforming growth factor, beta 2	0.001	2.46
Tgfb3	transforming growth factor, beta 3	< 0.001	2.36
Tgfbi	transforming growth factor, beta induced	< 0.001	4.05
Thbs1	thrombospondin 1	0.006	-5.14
Thbs1/X99384	thrombospondin 1/cDNA sequence X99384	0.004	-2.69
Thbs2	thrombospondin 2	0.001	2.25
Thsd7a	thrombospondin, type I, domain containing 7A	0.003	3.35
Tiam2	T cell lymphoma invasion and metastasis 2	0.005	-6.37
Timp2	tissue inhibitor of metalloproteinase 2	< 0.001	2.20
Tln2	talin 2	0.007	2.32
Tlr2	toll-like receptor 2	0.001	2.22
Tm7sf2	transmembrane 7 superfamily member 2	< 0.001	-3.72
Tmc7	transmembrane channel-like gene family 7	< 0.001	-8.53
Tmeff2	transmembrane protein with EGF-like and two follistatin-like domains 2	0.001	-5.45
Tmem100	transmembrane protein 100	< 0.001	-3.65
Tmem132c	transmembrane protein 132C	< 0.001	8.57
Tmem132e	transmembrane protein 132E	0.001	-13.35
Tmem140	transmembrane protein 140	< 0.001	3.70
Tmem159	transmembrane protein 159	0.003	2.13
Tmem191c	transmembrane protein 191C	0.002	2.52
Tmem194b	transmembrane protein 194B	0.001	2.72
Tmem229b	transmembrane protein 229B	0.001	-3.30
Tmem26	transmembrane protein 26	0.001	3.11
Tmem30b	transmembrane protein 30B	0.006	2.39

**Supplementary Table 1. (Continued)**

Tmem50b	transmembrane protein 50B	0.001	-2.17
Tmem86a	transmembrane protein 86A	< 0.001	-7.40
Tmem90b	transmembrane protein 90B	0.001	10.03
Tmie	transmembrane inner ear	< 0.001	3.13
Tmod1	tropomodulin 1	< 0.001	-4.09
Tmod2	tropomodulin 2	0.001	3.93
Tmprss13	transmembrane protease, serine 13	< 0.001	12.07
Tnfrsf1b	tumor necrosis factor receptor superfamily, member 1b	< 0.001	2.48
Tnfrsf21	tumor necrosis factor receptor superfamily, member 21	< 0.001	6.14
Tnik	TRAF2 and NCK interacting kinase	0.002	2.40
Tnnc1	troponin C, cardiac/slow skeletal	0.001	-6.24
Tnnt1	troponin T1, skeletal, slow	< 0.001	8.93
Tns4	tensin 4	0.001	-2.10
Tnxb	tenascin XB	0.002	4.43
Tom1l2	target of myb1-like 2 (chicken)	0.001	-2.08
Trank1	tetratricopeptide repeat and ankyrin repeat containing 1	< 0.001	7.07
Trdn	triadin	< 0.001	-18.32
Trim62	tripartite motif-containing 62	0.002	-2.47
Trp53inp2	transformation related protein 53 inducible nuclear protein 2	< 0.001	-3.64
Trpc4	transient receptor potential cation channel, subfamily C, member 4	< 0.001	-8.59
Trpc6	transient receptor potential cation channel, subfamily C, member 6	0.006	-2.68
Trpm3	transient receptor potential cation channel, subfamily M, member 3	0.001	3.95
Trpm6	transient receptor potential cation channel, subfamily M, member 6	0.001	4.54
Tshr	thyroid stimulating hormone receptor	< 0.001	- 121.71
Tshz2	teashirt zinc finger family member 2	< 0.001	2.34
Tslp	thymic stromal lymphopoietin	< 0.001	7.33
Tspan11	tetraspanin 11	0.001	2.39
Tspan33	tetraspanin 33	0.001	2.52
Tspyl3	TSPY-like 3	< 0.001	2.09
Tstd2	thiosulfate sulfurtransferase (rhodanese)-like domain containing 2	0.001	-2.23
Ttc14	tetratricopeptide repeat domain 14	< 0.001	2.08

**Supplementary Table 1. (Continued)**

Ttc3	tetratricopeptide repeat domain 3	< 0.001	2.17
Ttc39b	tetratricopeptide repeat domain 39B	0.003	-2.44
Ttc39c	tetratricopeptide repeat domain 39C	< 0.001	-5.48
Txndc16	thioredoxin domain containing 16	0.001	2.05
Txndc17	thioredoxin domain containing 17	< 0.001	-2.13
Tyw1	tRNA-yW synthesizing protein 1 homolog ( <i>S. cerevisiae</i> )	0.006	-2.20
Ube2g2	ubiquitin-conjugating enzyme E2G 2	0.001	-2.12
Ube2u	ubiquitin-conjugating enzyme E2U (putative)	0.002	-2.63
Umod	uromodulin	0.001	2.46
Unc5cl	unc-5 homolog C ( <i>C. elegans</i> )-like	< 0.001	-16.94
Upb1	ureidopropionase, beta	0.001	3.20
Upk1a	uroplakin 1A	< 0.001	-77.14
Upk3b	uroplakin 3B	< 0.001	2.81
Uqcrq	ubiquinol-cytochrome c reductase, complex III subunit VII	0.001	-2.31
Uroc1	urocanase domain containing 1	0.001	-4.88
Vldlr	very low density lipoprotein receptor	0.001	-3.55
Vprep3	pre-B lymphocyte gene 3	0.001	-3.37
Vps37d	vacuolar protein sorting 37D (yeast)	0.001	3.53
Vstm2a	V-set and transmembrane domain containing 2A	< 0.001	8.91
Vwa1	von Willebrand factor A domain containing 1	< 0.001	2.83
Vwa2	von Willebrand factor A domain containing 2	0.001	5.02
Vwa3b	von Willebrand factor A domain containing 3B	0.002	-5.39
Wasf1	WAS protein family, member 1	< 0.001	-3.40
Wdr91	WD repeat domain 91	0.001	2.29
Wfdc12	WAP four-disulfide core domain 12	< 0.001	-16.20
Wfdc2	WAP four-disulfide core domain 2	< 0.001	7.33
Wfikkn2	WAP, follistatin/kazal, immunoglobulin, kunitz and netrin domain containing 2	< 0.001	13.88
Wfs1	Wolfram syndrome 1 homolog (human)	< 0.001	-3.99
Wipf3	WAS/WASL interacting protein family, member 3	< 0.001	10.65
Wispl	WNT1 inducible signaling pathway protein 1	< 0.001	2.99
Wnk4	WNK lysine deficient protein kinase 4	0.001	2.86

**Supplementary Table 1. (Continued)**

Wnt11	wingless-related MMTV integration site 11	< 0.001	4.06
Wnt5b	wingless-related MMTV integration site 5B	< 0.001	3.45
Wnt7a	wingless-related MMTV integration site 7A	< 0.001	17.49
Wnt9a	wingless-type MMTV integration site 9A	0.001	2.97
Zc3hc1	zinc finger, C3HC type 1	< 0.001	-2.46
Zcchc24	zinc finger, CCHC domain containing 24	0.002	2.08
Zfhx4	zinc finger homeodomain 4	0.003	2.00
Zfp185	zinc finger protein 185	< 0.001	2.37
Zfp239	zinc finger protein 239	< 0.001	-2.25
Zfp354b	zinc finger protein 354B	< 0.001	2.30
Zfp52	zinc finger protein 52	0.001	-3.02
Zfp612	zinc finger protein 612	< 0.001	2.30
Zfp784	zinc finger protein 784	0.002	2.23
Zfp882	zinc finger protein 882	0.001	3.31
Zg16	zymogen granule protein 16	0.001	-9.50
Zkscan4	zinc finger with KRAB and SCAN domains 4	0.002	2.32
Zmat1	zinc finger, matrin type 1	0.002	2.10
Zmpste24	zinc metallopeptidase, STE24 homolog (S. cerevisiae)	< 0.001	2.44
Zxdc	ZXD family zinc finger C	< 0.001	-2.28

## LITERATURE CITED

1. Sunderam, S., Kissin, D.M., Crawford, S.B., Folger, S.G., Jamieson, D.J., Barfield, W.D., Centers for Disease, C., and Prevention, *Assisted reproductive technology surveillance--United States, 2011*. MMWR Surveill Summ, 2014. **63**(10): p. 1-28.
2. Garcia-Ulloa, A.C. and Arrieta, O., *Tubal occlusion causing infertility due to an excessive inflammatory response in patients with predisposition for keloid formation*. Med Hypotheses, 2005. **65**(5): p. 908-14.
3. Wright, V.C., Chang, J., Jeng, G., Macaluso, M., Centers for Disease, C., and Prevention, *Assisted reproductive technology surveillance--United States, 2005*. MMWR Surveill Summ, 2008. **57**(5): p. 1-23.
4. Kattal, N., Cohen, J., and Barmat, L.I., *Role of coculture in human in vitro fertilization: a meta-analysis*. Fertil Steril, 2008. **90**(4): p. 1069-76.
5. Lucy, M.C., *Reproductive loss in high-producing dairy cattle: where will it end?* J Dairy Sci, 2001. **84**(6): p. 1277-93.
6. Eddy, C.A. and Pauerstein, C.J., *Anatomy and physiology of the fallopian tube*. Clin Obstet Gynecol, 1980. **23**(4): p. 1177-93.
7. Hunter, R.H., *Components of oviduct physiology in eutherian mammals*. Biol Rev Camb Philos Soc, 2012. **87**(1): p. 244-55.
8. Abe, H., *The mammalian oviductal epithelium: regional variations in cytological and functional aspects of the oviductal secretory cells*. Histol Histopathol, 1996. **11**(3): p. 743-68.
9. Suarez, S.S., *Regulation of sperm storage and movement in the mammalian oviduct*. Int J Dev Biol, 2008. **52**(5-6): p. 455-62.
10. Menezo, Y. and Guerin, P., *The mammalian oviduct: biochemistry and physiology*. Eur J Obstet Gynecol Reprod Biol, 1997. **73**(1): p. 99-104.
11. Hunter, R.H., Cook, B., and Poyser, N.L., *Regulation of oviduct function in pigs by local transfer of ovarian steroids and prostaglandins: a mechanism to influence sperm transport*. Eur J Obstet Gynecol Reprod Biol, 1983. **14**(4): p. 225-32.
12. Cicinelli, E., Einer-Jensen, N., Hunter, R.H., Cignarelli, M., Cignarelli, A., Colafoglio, G., Tinelli, R., and Pinto, V., *Peritoneal fluid concentrations of progesterone in women are higher close to the corpus luteum compared with elsewhere in the abdominal cavity*. Fertil Steril, 2009. **92**(1): p. 306-10.
13. Brenner, R.M., *Renewal of oviduct cilia during the menstrual cycle of the rhesus monkey*. Fertil Steril, 1969. **20**(4): p. 599-611.
14. Russe, I. and Liebich, H.G., *Maturation of secretory granules in the endosalpinx one to four days post coitum in sheep*. Cell Tissue Res, 1979. **201**(1): p. 145-58.
15. Abe, H. and Oikawa, T., *Observations by scanning electron microscopy of oviductal epithelial cells from cows at follicular and luteal phases*. Anat Rec, 1993. **235**(3): p. 399-410.
16. Abe, H., *Regional variations in the ultrastructural features of secretory cells in the rat oviductal epithelium*. Anat Rec, 1994. **240**(1): p. 77-85.
17. Yaniz, J.L., Lopez-Gatius, F., Santolaria, P., and Mullins, K.J., *Study of the functional anatomy of bovine oviductal mucosa*. Anat Rec, 2000. **260**(3): p. 268-78.
18. Bauersachs, S., Rehfeld, S., Ulbrich, S.E., Mallok, S., Prella, K., Wenigerkind, H., Einspanier, R., Blum, H., and Wolf, E., *Monitoring gene expression changes in bovine*

- oviduct epithelial cells during the oestrous cycle*. J Mol Endocrinol, 2004. **32**(2): p. 449-66.
19. Ulbrich, S.E., Kettler, A., and Einspanier, R., *Expression and localization of estrogen receptor alpha, estrogen receptor beta and progesterone receptor in the bovine oviduct in vivo and in vitro*. J Steroid Biochem Mol Biol, 2003. **84**(2-3): p. 279-89.
  20. Straub, R.H., *The complex role of estrogens in inflammation*. Endocr Rev, 2007. **28**(5): p. 521-74.
  21. Shao, R., Egecioglu, E., Weijdegard, B., Kopchick, J.J., Fernandez-Rodriguez, J., Andersson, N., and Billig, H., *Dynamic regulation of estrogen receptor-alpha isoform expression in the mouse fallopian tube: mechanistic insight into estrogen-dependent production and secretion of insulin-like growth factors*. Am J Physiol Endocrinol Metab, 2007. **293**(5): p. E1430-42.
  22. Shao, R., Weijdegard, B., Fernandez-Rodriguez, J., Egecioglu, E., Zhu, C., Andersson, N., Thurin-Kjellberg, A., Bergh, C., and Billig, H., *Ciliated epithelial-specific and regional-specific expression and regulation of the estrogen receptor-beta2 in the fallopian tubes of immature rats: a possible mechanism for estrogen-mediated transport process in vivo*. Am J Physiol Endocrinol Metab, 2007. **293**(1): p. E147-58.
  23. Bridges, P.J., Jeoung, M., Shim, S., Park, J.Y., Lee, J.E., Sapsford, L.A., Trudgen, K., Ko, C., Gye, M.C., and Jo, M., *Hematopoietic prostaglandin D synthase: an ESR1-dependent oviductal epithelial cell synthase*. Endocrinology, 2012. **153**(4): p. 1925-35.
  24. Mangelsdorf, D.J., Thummel, C., Beato, M., Herrlich, P., Schutz, G., Umesono, K., Blumberg, B., Kastner, P., Mark, M., Chambon, P., and Evans, R.M., *The nuclear receptor superfamily: the second decade*. Cell, 1995. **83**(6): p. 835-9.
  25. Okada, A., Ohta, Y., Inoue, S., Hiroi, H., Muramatsu, M., and Iguchi, T., *Expression of estrogen, progesterone and androgen receptors in the oviduct of developing, cycling and pre-implantation rats*. J Mol Endocrinol, 2003. **30**(3): p. 301-15.
  26. Wijayagunawardane, M.P., Miyamoto, A., and Sato, K., *Prostaglandin E2, prostaglandin F2 alpha and endothelin-1 production by cow oviductal epithelial cell monolayers: effect of progesterone, estradiol 17 beta, oxytocin and luteinizing hormone*. Theriogenology, 1999. **52**(5): p. 791-801.
  27. Lim, H., Paria, B.C., Das, S.K., Dinchuk, J.E., Langenbach, R., Trzaskos, J.M., and Dey, S.K., *Multiple female reproductive failures in cyclooxygenase 2-deficient mice*. Cell, 1997. **91**(2): p. 197-208.
  28. Oda, S., Gabler, C., Holder, C., and Einspanier, R., *Differential expression of cyclooxygenase 1 and cyclooxygenase 2 in the bovine oviduct*. J Endocrinol, 2006. **191**(1): p. 263-74.
  29. Yamamoto, Y., Kobayashi, Y., and Okuda, K., *Purified culture systems for bovine oviductal stromal cells*. J Reprod Dev, 2014. **60**(1): p. 73-7.
  30. Kobayashi, Y., Wakamiya, K., Kohka, M., Yamamoto, Y., and Okuda, K., *Summer heat stress affects prostaglandin synthesis in the bovine oviduct*. Reproduction, 2013. **146**(2): p. 103-10.
  31. Marey, M.A., Liu, J., Kowsar, R., Haneda, S., Matsui, M., Sasaki, M., Takashi, S., Hayakawa, H., Wijayagunawardane, M.P., Hussein, F.M., and Miyamoto, A., *Bovine oviduct epithelial cells downregulate phagocytosis of sperm by neutrophils: prostaglandin E2 as a major physiological regulator*. Reproduction, 2014. **147**(2): p. 211-9.

32. Kodithuwakku, S.P., Miyamoto, A., and Wijayagunawardane, M.P., *Spermatozoa stimulate prostaglandin synthesis and secretion in bovine oviductal epithelial cells*. *Reproduction*, 2007. **133**(6): p. 1087-94.
33. Wijayagunawardane, M.P., Miyamoto, A., Cerbito, W.A., Acosta, T.J., Takagi, M., and Sato, K., *Local distributions of oviductal estradiol, progesterone, prostaglandins, oxytocin and endothelin-1 in the cyclic cow*. *Theriogenology*, 1998. **49**(3): p. 607-18.
34. Ikawa, M., Tokuhiko, K., Yamaguchi, R., Benham, A.M., Tamura, T., Wada, I., Satouh, Y., Inoue, N., and Okabe, M., *Calsperin is a testis-specific chaperone required for sperm fertility*. *J Biol Chem*, 2011. **286**(7): p. 5639-46.
35. Hagaman, J.R., Moyer, J.S., Bachman, E.S., Sibony, M., Magyar, P.L., Welch, J.E., Smithies, O., Kregel, J.H., and O'Brien, D.A., *Angiotensin-converting enzyme and male fertility*. *Proc Natl Acad Sci U S A*, 1998. **95**(5): p. 2552-7.
36. Yamaguchi, R., Muro, Y., Isotani, A., Tokuhiko, K., Takumi, K., Adham, I., Ikawa, M., and Okabe, M., *Disruption of ADAM3 impairs the migration of sperm into oviduct in mouse*. *Biol Reprod*, 2009. **81**(1): p. 142-6.
37. Hunter, R.H. and Leglise, P.C., *Tubal surgery in the rabbit: fertilization and polyspermy after resection of the isthmus*. *Am J Anat*, 1971. **132**(1): p. 45-52.
38. Hunter, R.H. and Leglise, P.C., *Polyspermic fertilization following tubal surgery in pigs, with particular reference to the role of the isthmus*. *J Reprod Fertil*, 1971. **24**(2): p. 233-46.
39. Hung, P.H. and Suarez, S.S., *Regulation of sperm storage and movement in the ruminant oviduct*. *Soc Reprod Fertil Suppl*, 2010. **67**: p. 257-66.
40. Calvete, J.J., Raida, M., Sanz, L., Wempe, F., Scheit, K.H., Romero, A., and Topfer-Petersen, E., *Localization and structural characterization of an oligosaccharide O-linked to bovine PDC-109. Quantitation of the glycoprotein in seminal plasma and on the surface of ejaculated and capacitated spermatozoa*. *FEBS Lett*, 1994. **350**(2-3): p. 203-6.
41. Leblond, E., Desnoyers, L., and Manjunath, P., *Phosphorylcholine-binding proteins from the seminal fluids of different species share antigenic determinants with the major proteins of bovine seminal plasma*. *Mol Reprod Dev*, 1993. **34**(4): p. 443-9.
42. Elliott, R.M., Lloyd, R.E., Fazeli, A., Sostaric, E., Georgiou, A.S., Satake, N., Watson, P.F., and Holt, W.V., *Effects of HSPA8, an evolutionarily conserved oviductal protein, on boar and bull spermatozoa*. *Reproduction*, 2009. **137**(2): p. 191-203.
43. Breitbart, H., *Intracellular calcium regulation in sperm capacitation and acrosomal reaction*. *Mol Cell Endocrinol*, 2002. **187**(1-2): p. 139-44.
44. Hiradate, Y., Inoue, H., Kobayashi, N., Shirakata, Y., Suzuki, Y., Gotoh, A., Roh, S.G., Uchida, T., Katoh, K., Yoshida, M., Sato, E., and Tanemura, K., *Neurotensin enhances sperm capacitation and acrosome reaction in mice*. *Biol Reprod*, 2014. **91**(2): p. 53.
45. Ignatz, G.G., Lo, M.C., Perez, C.L., Gwathmey, T.M., and Suarez, S.S., *Characterization of a fucose-binding protein from bull sperm and seminal plasma that may be responsible for formation of the oviductal sperm reservoir*. *Biol Reprod*, 2001. **64**(6): p. 1806-11.
46. Hunter, R.H. and Nichol, R., *A preovulatory temperature gradient between the isthmus and ampulla of pig oviducts during the phase of sperm storage*. *J Reprod Fertil*, 1986. **77**(2): p. 599-606.
47. Bahat, A., Eisenbach, M., and Tur-Kaspa, I., *Perioovulatory increase in temperature difference within the rabbit oviduct*. *Hum Reprod*, 2005. **20**(8): p. 2118-21.
48. Bahat, A., Tur-Kaspa, I., Gakamsky, A., Giojalas, L.C., Breitbart, H., and Eisenbach, M., *Thermotaxis of mammalian sperm cells: a potential navigation mechanism in the female genital tract*. *Nat Med*, 2003. **9**(2): p. 149-50.

49. Kaupp, U.B., *100 years of sperm chemotaxis*. J Gen Physiol, 2012. **140**(6): p. 583-6.
50. Kaupp, U.B., Kashikar, N.D., and Weyand, I., *Mechanisms of sperm chemotaxis*. Annu Rev Physiol, 2008. **70**: p. 93-117.
51. Caballero, J.N., Gervasi, M.G., Veiga, M.F., Dalvit, G.C., Perez-Martinez, S., Cetica, P.D., and Vazquez-Levin, M.H., *Epithelial cadherin is present in bovine oviduct epithelial cells and gametes, and is involved in fertilization-related events*. Theriogenology, 2014. **81**(9): p. 1189-206.
52. Carrasco, L.C., Coy, P., Aviles, M., Gadea, J., and Romar, R., *Glycosidase determination in bovine oviducal fluid at the follicular and luteal phases of the oestrous cycle*. Reprod Fertil Dev, 2008. **20**(7): p. 808-17.
53. Buhi, W.C., *Characterization and biological roles of oviduct-specific, oestrogen-dependent glycoprotein*. Reproduction, 2002. **123**(3): p. 355-62.
54. Killian, G., *Physiology and endocrinology symposium: evidence that oviduct secretions influence sperm function: a retrospective view for livestock*. J Anim Sci, 2011. **89**(5): p. 1315-22.
55. Suarez, S., *Gamete and zygote transport*, in *The physiology of Reproduction*, E. Knobil and J. Neill, Editors. 2006, Raven Press: New York. p. 133-148.
56. Buhi, W.C., Alvarez, I.M., and Kouba, A.J., *Secreted proteins of the oviduct*. Cells Tissues Organs, 2000. **166**(2): p. 165-79.
57. Ghersevich, S., Massa, E., and Zumoffen, C., *Oviductal secretion and gamete interaction*. Reproduction, 2015. **149**(1): p. R1-R14.
58. Szostek, A.Z., Siemieniuch, M.J., Deptula, K., Woclawek-Potocka, I., Majewska, M., Okuda, K., and Skarzynski, D.J., *Ovarian steroids modulate tumor necrosis factor-alpha and nitric oxide-regulated prostaglandin secretion by cultured bovine oviductal epithelial cells*. Domest Anim Endocrinol, 2011. **41**(1): p. 14-23.
59. Leese, H.J., *The formation and function of oviduct fluid*. J Reprod Fertil, 1988. **82**(2): p. 843-56.
60. Kavanaugh, J.F., Grippo, A.A., and Killian, G.J., *Cannulation of the bovine ampullary and isthmic oviduct*. J Invest Surg, 1992. **5**(1): p. 11-7.
61. Sturmey, R.G., Reis, A., Leese, H.J., and McEvoy, T.G., *Role of fatty acids in energy provision during oocyte maturation and early embryo development*. Reprod Domest Anim, 2009. **44 Suppl 3**: p. 50-8.
62. Ellington, J.E., Ignatz, G.G., Ball, B.A., Meyers-Wallen, V.N., and Currie, W.B., *De novo protein synthesis by bovine uterine tube (oviduct) epithelial cells changes during co-culture with bull spermatozoa*. Biol Reprod, 1993. **48**(4): p. 851-6.
63. Abe, H., Sendai, Y., Satoh, T., and Hoshi, H., *Bovine oviduct-specific glycoprotein: a potent factor for maintenance of viability and motility of bovine spermatozoa in vitro*. Mol Reprod Dev, 1995. **42**(2): p. 226-32.
64. Hill, J.L., Walker, S.K., Brown, G.H., and Nancarrow, C.D., *The effects of an estrus-associated oviductal glycoprotein on the in vitro fertilization and development of ovine oocytes matured in vitro*. Theriogenology, 1996. **46**(8): p. 1379-1388.
65. Gandolfi, F., Brevini, T.A., Richardson, L., Brown, C.R., and Moor, R.M., *Characterization of proteins secreted by sheep oviduct epithelial cells and their function in embryonic development*. Development, 1989. **106**(2): p. 303-12.
66. Lee, K.F., Yao, Y.Q., Kwok, K.L., Xu, J.S., and Yeung, W.S., *Early developing embryos affect the gene expression patterns in the mouse oviduct*. Biochem Biophys Res Commun, 2002. **292**(2): p. 564-70.

67. Lee, Y.L., Cheong, A.W., Chow, W.N., Lee, K.F., and Yeung, W.S., *Regulation of complement-3 protein expression in human and mouse oviducts*. Mol Reprod Dev, 2009. **76**(3): p. 301-8.
68. Shan, W. and Liu, J., *Inflammation: a hidden path to breaking the spell of ovarian cancer*. Cell Cycle, 2009. **8**(19): p. 3107-11.
69. Crum, C.P., Drapkin, R., Kindelberger, D., Medeiros, F., Miron, A., and Lee, Y., *Lessons from BRCA: the tubal fimbria emerges as an origin for pelvic serous cancer*. Clin Med Res, 2007. **5**(1): p. 35-44.
70. CDC, *Sexually transmitted disease surveillance, 2009*. Available at: <http://www.cdc.gov/std/stats09/default.htm>, 2010.
71. Westrom, L., Joesoef, R., Reynolds, G., Hagdu, A., and Thompson, S.E., *Pelvic inflammatory disease and fertility. A cohort study of 1,844 women with laparoscopically verified disease and 657 control women with normal laparoscopic results*. Sex Transm Dis, 1992. **19**(4): p. 185-92.
72. Rasmussen, S.J., Eckmann, L., Quayle, A.J., Shen, L., Zhang, Y.X., Anderson, D.J., Fierer, J., Stephens, R.S., and Kagnoff, M.F., *Secretion of proinflammatory cytokines by epithelial cells in response to Chlamydia infection suggests a central role for epithelial cells in chlamydial pathogenesis*. Clinical Investigation, 1997. **99**(1): p. 77-87.
73. Maxion, H.K. and Kelly, K.A., *Chemokine expression patterns differ within anatomically distinct regions of the genital tract during Chlamydia trachomatis infection*. Infect Immun, 2002. **70**(3): p. 1538-46.
74. Kessler, M., Zielecki, J., Thieck, O., Mollenkopf, H.J., Fotopoulou, C., and Meyer, T.F., *Chlamydia trachomatis disturbs epithelial tissue homeostasis in fallopian tubes via paracrine Wnt signaling*. American journal of pathology, 2012. **180**(1): p. 186-98.
75. Brunham, R.C. and Rey-Ladino, J., *Immunology of Chlamydia infection: implications for a Chlamydia trachomatis vaccine*. Nat Rev Immunol, 2005. **5**(2): p. 149-61.
76. Kowsar, R., Hambruch, N., Marey, M.A., Liu, J., Shimizu, T., Pfarrer, C., and Miyamoto, A., *Evidence for a novel, local acute-phase response in the bovine oviduct: progesterone and lipopolysaccharide up-regulate alpha 1-acid-glycoprotein expression in epithelial cells in vitro*. Mol Reprod Dev, 2014. **81**(9): p. 861-70.
77. Kowsar, R., Hambruch, N., Liu, J., Shimizu, T., Pfarrer, C., and Miyamoto, A., *Regulation of innate immune function in bovine oviduct epithelial cells in culture: the homeostatic role of epithelial cells in balancing Th1/Th2 response*. J Reprod Dev, 2013. **59**(5): p. 470-8.
78. *Recent advances in medically assisted conception. Report of a WHO Scientific Group*. World Health Organ Tech Rep Ser, 1992. **820**: p. 1-111.
79. Diskin, M.G. and Morris, D.G., *Embryonic and early foetal losses in cattle and other ruminants*. Reprod Domest Anim, 2008. **43 Suppl 2**: p. 260-7.
80. Bylander, A., Nutu, M., Wellander, R., Goksor, M., Billig, H., and Larsson, D.G., *Rapid effects of progesterone on ciliary beat frequency in the mouse fallopian tube*. Reprod Biol Endocrinol, 2010. **8**: p. 48.
81. Wanggren, K., Stavreus-Evers, A., Olsson, C., Andersson, E., and Gemzell-Danielsson, K., *Regulation of muscular contractions in the human Fallopian tube through prostaglandins and progestagens*. Hum Reprod, 2008. **23**(10): p. 2359-68.
82. Parada-Bustamante, A., Orihuela, P.A., Rios, M., Cuevas, C.A., Orostica, M.L., Velasquez, L.A., Villalon, M.J., and Croxatto, H.B., *A non-genomic signaling pathway shut down by mating changes the estradiol-induced gene expression profile in the rat oviduct*. Reproduction, 2010. **139**(3): p. 631-44.

83. Shao, R., Nutu, M., Karlsson-Lindahl, L., Benrick, A., Weijdegard, B., Lager, S., Egecioglu, E., Fernandez-Rodriguez, J., Gemzell-Danielsson, K., Ohlsson, C., Jansson, J.O., and Billig, H., *Downregulation of cilia-localized Il-6R alpha by 17beta-estradiol in mouse and human fallopian tubes*. *Am J Physiol Cell Physiol*, 2009. **297**(1): p. C140-51.
84. Valle, G.R., Cassali, G.D., Nogueira, J.C., Castro, A.C., Reis, A.M., Cardoso, F.M., Figueiredo, C.B., and Nascimento, E.F., *Nuclear estrogen and progesterone receptors in the oviduct of heifers under natural and superovulated estrous cycles*. *Anim Reprod Sci*, 2007. **101**(1-2): p. 28-37.
85. Saint-Dizier, M., Sandra, O., Ployart, S., Chebrout, M., and Constant, F., *Expression of nuclear progesterone receptor and progesterone receptor membrane components 1 and 2 in the oviduct of cyclic and pregnant cows during the post-ovulation period*. *Reprod Biol Endocrinol*, 2012. **10**: p. 76.
86. Shirley, B. and Reeder, R.L., *Cyclic changes in the ampulla of the rat oviduct*. *J Exp Zool*, 1996. **276**(2): p. 164-73.
87. Reeder, R.L. and Shirley, B., *Deciliation in the ampulla of the rat oviduct and effects of estrogen on the process*. *J Exp Zool*, 1999. **283**(1): p. 71-80.
88. Bureau, M., Bailey, J.L., and Sirard, M.A., *Binding regulation of porcine spermatozoa to oviductal vesicles in vitro*. *J Androl*, 2002. **23**(2): p. 188-93.
89. Hunter, R.H., *Sperm release from oviduct epithelial binding is controlled hormonally by peri-ovulatory graafian follicles*. *Mol Reprod Dev*, 2008. **75**(1): p. 167-74.
90. Ded, L., Dostalova, P., Dorosh, A., Dvorakova-Hortova, K., and Peknicova, J., *Effect of estrogens on boar sperm capacitation in vitro*. *Reprod Biol Endocrinol*, 2010. **8**: p. 87.
91. Fujinoki, M., *Suppression of progesterone-enhanced hyperactivation in hamster spermatozoa by estrogen*. *Reproduction*, 2010. **140**(3): p. 453-64.
92. Carlson, D., Black, D.L., and Howe, G.R., *Oviduct secretion in the cow*. *J Reprod Fertil*, 1970. **22**(3): p. 549-52.
93. Hugentobler, S.A., Diskin, M.G., Leese, H.J., Humpherson, P.G., Watson, T., Sreenan, J.M., and Morris, D.G., *Amino acids in oviduct and uterine fluid and blood plasma during the estrous cycle in the bovine*. *Mol Reprod Dev*, 2007. **74**(4): p. 445-54.
94. Jo, M., Gieske, M.C., Payne, C.E., Wheeler-Price, S.E., Gieske, J.B., Ignatius, I.V., Curry, T.E., Jr., and Ko, C., *Development and application of a rat ovarian gene expression database*. *Endocrinology*, 2004. **145**(11): p. 5384-96.
95. Winuthayanon, W., Hewitt, S.C., and Korach, K.S., *Uterine Epithelial Cell Estrogen Receptor Alpha-Dependent and -Independent Genomic Profiles That Underlie Estrogen Responses in Mice*. *Biol Reprod*, 2014.
96. Minten, M.A., Bilby, T.R., Bruno, R.G., Allen, C.C., Madsen, C.A., Wang, Z., Sawyer, J.E., Tibary, A., Neibergs, H.L., Geary, T.W., Bauersachs, S., and Spencer, T.E., *Effects of fertility on gene expression and function of the bovine endometrium*. *PLoS One*, 2013. **8**(8): p. e69444.
97. Partek, D., *Partek documentation: turning data into discovery*. Partek Incorporated, St. Louis, 2009.
98. Bridges, P.J. and Fortune, J.E., *Regulation, action and transport of prostaglandins during the periovulatory period in cattle*. *Mol Cell Endocrinol*, 2007. **263**(1-2): p. 1-9.
99. Bridges, P.J., Komar, C.M., and Fortune, J.E., *Gonadotropin-induced expression of messenger ribonucleic acid for cyclooxygenase-2 and production of prostaglandins E and F2alpha in bovine preovulatory follicles are regulated by the progesterone receptor*. *Endocrinology*, 2006. **147**(10): p. 4713-22.

100. Komar, C.M., Berndtson, A.K., Evans, A.C., and Fortune, J.E., *Decline in circulating estradiol during the periovulatory period is correlated with decreases in estradiol and androgen, and in messenger RNA for p450 aromatase and p450 17alpha-hydroxylase, in bovine preovulatory follicles*. Biol Reprod, 2001. **64**(6): p. 1797-805.
101. Bridges, P.J. and Fortune, J.E., *Characteristics of developing prolonged dominant follicles in cattle*. Domest Anim Endocrinol, 2003. **25**(2): p. 199-214.
102. Pedersen, M.E., Ozdas, O.B., Farstad, W., Tverdal, A., and Olsaker, I., *Effects of bovine oviduct epithelial cells, fetal calf serum and bovine serum albumin on gene expression in single bovine embryos produced in the synthetic oviduct fluid culture system*. Reprod Fertil Dev, 2005. **17**(8): p. 751-7.
103. Rottmayer, R., Ulbrich, S.E., Kolle, S., Prella, K., Neumueller, C., Sinowatz, F., Meyer, H.H., Wolf, E., and Hiendleder, S., *A bovine oviduct epithelial cell suspension culture system suitable for studying embryo-maternal interactions: morphological and functional characterization*. Reproduction, 2006. **132**(4): p. 637-48.
104. Bridges, P.J., Jeoung, M., Kim, H., Kim, J.H., Lee, D.R., Ko, C., and Baker, D.J., *Methodology matters: IVF versus ICSI and embryonic gene expression*. Reprod Biomed Online, 2011. **23**(2): p. 234-44.
105. Irizarry, R.A., Hobbs, B., Collin, F., Beazer-Barclay, Y.D., Antonellis, K.J., Scherf, U., and Speed, T.P., *Exploration, normalization, and summaries of high density oligonucleotide array probe level data*. Biostatistics, 2003. **4**(2): p. 249-64.
106. D, P., *Partek documentation: turning data into discovery.*, 2009, Partek Inc., St. Louis, MO.
107. Eisenhart, C., *The assumptions underlying the analysis of variance*. Biometrics, 1947. **3**(1): p. 1-21.
108. Tamhane, C., A., and Dunlop, D.D., *Statistics and Data Analysis from Elementary to Intermediate*. Prentice Hall, 2000: p. 473-474.
109. Edgar, R., Domrachev, M., and Lash, A.E., *Gene Expression Omnibus: NCBI gene expression and hybridization array data repository*. Nucleic Acids Res, 2002. **30**(1): p. 207-10.
110. Cerny, K.L., Garbacik, S., Skees, C., Burris, W.R., Matthews, J.C., and Bridges, P.J., *Gestational form of Selenium in Free-Choice Mineral Mixes Affects Transcriptome Profiles of the Neonatal Calf Testis, Including those of Steroidogenic and Spermatogenic Pathways*. Biol Trace Elem Res, 2015.
111. Livak, K.J. and Schmittgen, T.D., *Analysis of relative gene expression data using real-time quantitative PCR and the 2(-Delta Delta C(T)) Method*. Methods, 2001. **25**(4): p. 402-8.
112. Cerny, K.L., Garbacik, S., Skees, C., Burris, W.R., Matthews, J.C., and Bridges, P.J., *Form of selenium in free-choice mineral mixes of dams affects transcriptome profiles, including those of steroidogenic and spermatogenic pathways, of the neonatal calf testis*. Biological Trace Element Research, 2015. **Submitted**.
113. Wang, Y., Barbacioru, C., Hyland, F., Xiao, W., Hunkapiller, K.L., Blake, J., Chan, F., Gonzalez, C., Zhang, L., and Samaha, R.R., *Large scale real-time PCR validation on gene expression measurements from two commercial long-oligonucleotide microarrays*. BMC Genomics, 2006. **7**: p. 59.
114. Gabler, C., Killian, G.J., and Einspanier, R., *Differential expression of extracellular matrix components in the bovine oviduct during the oestrous cycle*. Reproduction, 2001. **122**(1): p. 121-30.

115. Reinecke, M., *Neurotensin in the human fallopian tube: immunohistochemical localization and effects of synthetic neurotensin on motor activity in vitro*. *Neurosci Lett*, 1987. **73**(3): p. 220-4.
116. Sayasith, K., Brown, K.A., Lussier, J.G., Dore, M., and Sirois, J., *Characterization of bovine early growth response factor-1 and its gonadotropin-dependent regulation in ovarian follicles prior to ovulation*. *J Mol Endocrinol*, 2006. **37**(2): p. 239-50.
117. Diaz-Fontdevila, M. and Bustos-Obregon, E., *Cholesterol and polyunsaturated acid enriched diet: effect on kinetics of the acrosome reaction in rabbit spermatozoa*. *Mol Reprod Dev*, 1993. **35**(2): p. 176-80.
118. Sheriff, D.S. and Ali, E.F., *Perspective on plasma membrane cholesterol efflux and spermatozoal function*. *J Hum Reprod Sci*, 2010. **3**(2): p. 68-75.
119. Ehrenwald, E., Foote, R.H., and Parks, J.E., *Bovine oviductal fluid components and their potential role in sperm cholesterol efflux*. *Mol Reprod Dev*, 1990. **25**(2): p. 195-204.
120. Henault, M.A. and Killian, G.J., *Composition and morphology of lipid droplets from oviduct epithelial cells*. *Anat Rec*, 1993. **237**(4): p. 466-74.
121. Grippo, A.A., Anderson, S.H., Chapman, D.A., Henault, M.A., and Killian, G.J., *Cholesterol, phospholipid and phospholipase activity of ampullary and isthmic fluid from the bovine oviduct*. *J Reprod Fertil*, 1994. **102**(1): p. 87-93.
122. Reade, C.J., McVey, R.M., Tone, A.A., Finlayson, S.J., McAlpine, J.N., Fung-Kee-Fung, M., and Ferguson, S.E., *The fallopian tube as the origin of high grade serous ovarian cancer: review of a paradigm shift*. *J Obstet Gynaecol Can*, 2014. **36**(2): p. 133-40.
123. Sherman-Baust, C.A., Kuhn, E., Valle, B.L., Shih Ie, M., Kurman, R.J., Wang, T.L., Amano, T., Ko, M.S., Miyoshi, I., Araki, Y., Lehrmann, E., Zhang, Y., Becker, K.G., and Morin, P.J., *A genetically engineered ovarian cancer mouse model based on fallopian tube transformation mimics human high-grade serous carcinoma development*. *J Pathol*, 2014. **233**(3): p. 228-37.
124. van der Horst, P.H., van der Zee, M., Heijmans-Antonissen, C., Jia, Y., DeMayo, F.J., Lydon, J.P., van Deurzen, C.H., Ewing, P.C., Burger, C.W., and Blok, L.J., *A mouse model for endometrioid ovarian cancer arising from the distal oviduct*. *Int J Cancer*, 2014. **135**(5): p. 1028-37.
125. Schmaltz-Panneau, B., Cordova, A., Dhorne-Pollet, S., Hennequet-Antier, C., Uzbekova, S., Martinot, E., Doret, S., Martin, P., Mermillod, P., and Locatelli, Y., *Early bovine embryos regulate oviduct epithelial cell gene expression during in vitro co-culture*. *Anim Reprod Sci*, 2014. **149**(3-4): p. 103-16.
126. Wijayagunawardane, M.P. and Miyamoto, A., *Tumor necrosis factor alpha system in the bovine oviduct: a possible mechanism for embryo transport*. *J Reprod Dev*, 2004. **50**(1): p. 57-62.
127. Wijayagunawardane, M.P., Miyamoto, A., Taquahashi, Y., Gabler, C., Acosta, T.J., Nishimura, M., Killian, G., and Sato, K., *In vitro regulation of local secretion and contraction of the bovine oviduct: stimulation by luteinizing hormone, endothelin-1 and prostaglandins, and inhibition by oxytocin*. *J Endocrinol*, 2001. **168**(1): p. 117-30.
128. Talo, A., *Myoelectrical activity and transport of unfertilized ova in the oviduct of the mouse in vitro*. *J Reprod Fertil*, 1980. **60**(1): p. 53-8.
129. Gauvreau, D., Moisan, V., Roy, M., Fortier, M.A., and Bilodeau, J.F., *Expression of prostaglandin E synthases in the bovine oviduct*. *Theriogenology*, 2010. **73**(1): p. 103-11.
130. Perez Martinez, S., Hermoso, M., Farina, M., Ribeiro, M.L., Rapanelli, M., Espinosa, M., Villalon, M., and Franchi, A., *17-beta-Estradiol upregulates COX-2 in the rat oviduct*. *Prostaglandins Other Lipid Mediat*, 2006. **80**(3-4): p. 155-64.

131. Balsinde, J., Winstead, M.V., and Dennis, E.A., *Phospholipase A(2) regulation of arachidonic acid mobilization*. FEBS Lett, 2002. **531**(1): p. 2-6.
132. Dennis, E.A., *Diversity of group types, regulation, and function of phospholipase A2*. J Biol Chem, 1994. **269**(18): p. 13057-60.
133. Morishita, T., Nozaki, M., Sano, M., Yokoyama, M., Nakamura, G., and Nakano, H., *Changes in phospholipase A2 activity of the rabbit ampullary epithelium by ovarian steroids*. Prostaglandins Leukot Essent Fatty Acids, 1993. **48**(4): p. 315-8.
134. Manjunath, P., Sairam, M.R., and Uma, J., *Purification of four gelatin-binding proteins from bovine seminal plasma by affinity chromatography*. Biosci Rep, 1987. **7**(3): p. 231-8.
135. Harrington, W.R., Sheng, S., Barnett, D.H., Petz, L.N., Katzenellenbogen, J.A., and Katzenellenbogen, B.S., *Activities of estrogen receptor alpha- and beta-selective ligands at diverse estrogen responsive gene sites mediating transactivation or transrepression*. Mol Cell Endocrinol, 2003. **206**(1-2): p. 13-22.
136. Katzenellenbogen, B.S., Montano, M.M., Ediger, T.R., Sun, J., Ekena, K., Lazennec, G., Martini, P.G., McInerney, E.M., Delage-Mourroux, R., Weis, K., and Katzenellenbogen, J.A., *Estrogen receptors: selective ligands, partners, and distinctive pharmacology*. Recent Prog Horm Res, 2000. **55**: p. 163-93; discussion 194-5.
137. Tremblay, G.B., Tremblay, A., Copeland, N.G., Gilbert, D.J., Jenkins, N.A., Labrie, F., and Giguere, V., *Cloning, chromosomal localization, and functional analysis of the murine estrogen receptor beta*. Mol Endocrinol, 1997. **11**(3): p. 353-65.
138. Walter, P., Green, S., Greene, G., Krust, A., Bornert, J.M., Jeltsch, J.M., Staub, A., Jensen, E., Scrace, G., Waterfield, M., and et al., *Cloning of the human estrogen receptor cDNA*. Proc Natl Acad Sci U S A, 1985. **82**(23): p. 7889-93.
139. Dixon, D., Couse, J.F., and Korach, K.S., *Disruption of the estrogen receptor gene in mice*. Toxicol Pathol, 1997. **25**(5): p. 518-20.
140. Hamilton, K.J., Arao, Y., and Korach, K.S., *Estrogen hormone physiology: reproductive findings from estrogen receptor mutant mice*. Reprod Biol, 2014. **14**(1): p. 3-8.
141. Gieske, M.C., Kim, H.J., Legan, S.J., Koo, Y., Krust, A., Chambon, P., and Ko, C., *Pituitary gonadotroph estrogen receptor-alpha is necessary for fertility in females*. Endocrinology, 2008. **149**(1): p. 20-7.
142. Jeoung, M. and Bridges, P.J., *Cyclic regulation of apoptotic gene expression in the mouse oviduct*. Reprod Fertil Dev, 2011. **23**(5): p. 638-44.
143. Sweet, R.L., *Treatment of acute pelvic inflammatory disease*. Infect Dis Obstet Gynecol, 2011. **2011**: p. 561909.
144. Passey, R.J., Xu, K., Hume, D.A., and Geczy, C.L., *S100A8: emerging functions and regulation*. J Leukoc Biol, 1999. **66**(4): p. 549-56.
145. Kerkhoff, C., Klempt, M., and Sorg, C., *Novel insights into structure and function of MRP8 (S100A8) and MRP14 (S100A9)*. Biochim Biophys Acta, 1998. **1448**(2): p. 200-11.
146. Okamura, H., Tsutsi, H., Komatsu, T., Yutsudo, M., Hakura, A., Tanimoto, T., Torigoe, K., Okura, T., Nukada, Y., Hattori, K., and et al., *Cloning of a new cytokine that induces IFN-gamma production by T cells*. Nature, 1995. **378**(6552): p. 88-91.
147. Kusumoto, K., Murakami, Y., Otsuki, M., Kanayama, M., Takeuchi, S., and Takahashi, S., *Interleukin-18 (IL-18) mRNA expression and localization of IL-18 mRNA-expressing cells in the mouse uterus*. Zoolog Sci, 2005. **22**(9): p. 1003-10.
148. Tsuji, Y., Tamaoki, T.H., Hasegawa, A., Kashiwamura, S., Iemoto, A., Ueda, H., Muranaka, J., Adachi, S., Furuyama, J., Okamura, H., and Koyama, K., *Expression of interleukin-18 and its receptor in mouse ovary*. Am J Reprod Immunol, 2001. **46**(5): p. 349-57.

149. Murakami, Y., Otsuki, M., Kusumoto, K., Takeuchi, S., and Takahashi, S., *Estrogen inhibits interleukin-18 mRNA expression in the mouse uterus*. J Reprod Dev, 2005. **51**(5): p. 639-47.
150. Otsuki, M., Kusumoto, K., Murakami, Y., Kanayama, M., Takeuchi, S., and Takahashi, S., *Expression of interleukin-18 receptor mRNA in the mouse endometrium*. J Reprod Dev, 2007. **53**(1): p. 59-68.
151. Lee, K.F., Xu, J.S., Lee, Y.L., and Yeung, W.S., *Demilune cell and parotid protein from murine oviductal epithelium stimulates preimplantation embryo development*. Endocrinology, 2006. **147**(1): p. 79-87.
152. Lindzey, J. and Korach, K.S., *Developmental and physiological effects of estrogen receptor gene disruption in mice*. Trends Endocrinol Metab, 1997. **8**(4): p. 137-45.
153. Perfettini, J.L., Darville, T., Gachelin, G., Souque, P., Huerre, M., Dautry-Varsat, A., and Ojcius, D.M., *Effect of Chlamydia trachomatis infection and subsequent tumor necrosis factor alpha secretion on apoptosis in the murine genital tract*. Infect Immun, 2000. **68**(4): p. 2237-44.
154. Davies, D., Meade, K.G., Herath, S., Eckersall, P.D., Gonzalez, D., White, J.O., Conlan, R.S., O'Farrelly, C., and Sheldon, I.M., *Toll-like receptor and antimicrobial peptide expression in the bovine endometrium*. Reprod Biol Endocrinol, 2008. **6**: p. 53.
155. Cronin, J.G., Turner, M.L., Goetze, L., Bryant, C.E., and Sheldon, I.M., *Toll-like receptor 4 and MYD88-dependent signaling mechanisms of the innate immune system are essential for the response to lipopolysaccharide by epithelial and stromal cells of the bovine endometrium*. Biol Reprod, 2012. **86**(2): p. 51.
156. Itoh, H., Nasu, K., Nishida, M., Matsumoto, H., Yuge, A., and Narahara, H., *Human oviductal stromal fibroblasts, but not oviductal epithelial cells, express Toll-like receptor 4: the site-specific mucosal immunity of the human fallopian tube against bacterial infection*. Am J Reprod Immunol, 2006. **56**(2): p. 91-101.
157. Deb, K., Chaturvedi, M.M., and Jaiswal, Y.K., *A 'minimum dose' of lipopolysaccharide required for implantation failure: assessment of its effect on the maternal reproductive organs and interleukin-1alpha expression in the mouse*. Reproduction, 2004. **128**(1): p. 87-97.
158. Mayorga, M., Iborra, A., Estany, S., and Martinez, P., *Protective effect of vitamin E in an animal model of LPS-induced inflammation*. Am J Reprod Immunol, 2004. **52**(6): p. 356-61.
159. Diamond, A.K., Sweet, L.M., Oppenheimer, K.H., Bradley, D.F., and Phillippe, M., *Modulation of monocyte chemotactic protein-1 expression during lipopolysaccharide-induced preterm delivery in the pregnant mouse*. Reprod Sci, 2007. **14**(6): p. 548-59.
160. Phillippe, M., Diamond, A.K., Sweet, L.M., Oppenheimer, K.H., and Bradley, D.F., *Expression of coagulation-related protein genes during LPS-induced preterm delivery in the pregnant mouse*. Reprod Sci, 2011. **18**(11): p. 1071-9.
161. Brecchia, G., Menchetti, L., Cardinali, R., Castellini, C., Polisca, A., Zerani, M., Maranesi, M., and Boiti, C., *Effects of a bacterial lipopolysaccharide on the reproductive functions of rabbit does*. Anim Reprod Sci, 2014. **147**(3-4): p. 128-34.
162. Caligioni, C.S., *Assessing reproductive status/stages in mice*. Curr Protoc Neurosci, 2009. **Appendix 4**: p. Appendix 4I.
163. Geiss, G.K., Bumgarner, R.E., Birditt, B., Dahl, T., Dowidar, N., Dunaway, D.L., Fell, H.P., Ferree, S., George, R.D., Grogan, T., James, J.J., Maysuria, M., Mitton, J.D., Oliveri, P., Osborn, J.L., Peng, T., Ratcliffe, A.L., Webster, P.J., Davidson, E.H., Hood, L., and

- Dimitrov, K., *Direct multiplexed measurement of gene expression with color-coded probe pairs*. Nat Biotechnol, 2008. **26**(3): p. 317-25.
164. Koti, M., Siu, A., Clement, I., Bidarimath, M., Turashvili, G., Edwards, A., Rahimi, K., Masson, A.M., and Squire, J.A., *A distinct pre-existing inflammatory tumour microenvironment is associated with chemotherapy resistance in high-grade serous epithelial ovarian cancer*. Br J Cancer, 2015. **112 Suppl**: p. 1215-22.
165. Bromfield, J.J. and Sheldon, I.M., *Lipopolysaccharide reduces the primordial follicle pool in the bovine ovarian cortex ex vivo and in the murine ovary in vivo*. Biol Reprod, 2013. **88**(4): p. 98.
166. Ibrahim, S., Salilew-Wondim, D., Rings, F., Hoelker, M., Neuhoﬀ, C., Tholen, E., Looft, C., Schellander, K., and Tesfaye, D., *Expression pattern of inflammatory response genes and their regulatory micrnas in bovine oviductal cells in response to lipopolysaccharide: implication for early embryonic development*. PLoS One, 2015. **10**(3): p. e0119388.
167. Shibahara, H., Hirano, Y., Ayustawati, Kikuchi, K., Taneichi, A., Fujiwara, H., Takamizawa, S., and Sato, I., *Chemokine bioactivity of RANTES is elevated in the sera of infertile women with past Chlamydia trachomatis infection*. Am J Reprod Immunol, 2003. **49**(3): p. 169-73.
168. Jin, L., Batra, S., Douda, D.N., Palaniyar, N., and Jeyaseelan, S., *CXCL1 contributes to host defense in polymicrobial sepsis via modulating T cell and neutrophil functions*. J Immunol, 2014. **193**(7): p. 3549-58.
169. Balasubramaniam, E.S., Van Noorden, S., and El-Bahrawy, M., *The expression of interleukin (IL)-6, IL-8, and their receptors in fallopian tubes with ectopic tubal gestation*. Fertil Steril, 2012. **98**(4): p. 898-904.
170. CDC, *Sexually transmitted disease surveillance, 2009*: Atlanta, GA: US Department of Health and Human Services, CDC; 2010. Available at <http://www.cdc.gov/std/stats09/default.htm>. Accessed Sept. 23, 2013.
171. Gomes, J.P., Borrego, M.J., Atik, B., Santo, I., Azevedo, J., Brito de Sa, A., Nogueira, P., and Dean, D., *Correlating Chlamydia trachomatis infectious load with urogenital ecological success and disease pathogenesis*. Microbes Infect, 2006. **8**(1): p. 16-26.
172. Agrawal, T., Vats, V., Salhan, S., and Mittal, A., *Determination of chlamydial load and immune parameters in asymptomatic, symptomatic and infertile women*. FEMS Immunol Med Microbiol, 2009. **55**(2): p. 250-7.
173. Paavonen, J. and Lehtinen, M., *Chlamydial pelvic inflammatory disease*. Hum Reprod Update, 1996. **2**(6): p. 519-29.
174. Soper, D.E., *Pelvic inflammatory disease*. Obstetrics and gynecology, 2010. **116**(2 Pt 1): p. 419-28.
175. Miyairi, I., Ramsey, K.H., and Patton, D.L., *Duration of untreated chlamydial genital infection and factors associated with clearance: review of animal studies*. Infectious Diseases, 2010. **201 Suppl 2**: p. S96-103.
176. Moulder, J.W., *Interaction of chlamydiae and host cells in vitro*. Microbiol Rev, 1991. **55**(1): p. 143-90.
177. Zhong, G., Fan, P., Ji, H., Dong, F., and Huang, Y., *Identification of a chlamydial protease-like activity factor responsible for the degradation of host transcription factors*. J Exp Med, 2001. **193**(8): p. 935-42.
178. Zhong, G., Fan, T., and Liu, L., *Chlamydia inhibits interferon gamma-inducible major histocompatibility complex class II expression by degradation of upstream stimulatory factor 1*. J Exp Med, 1999. **189**(12): p. 1931-8.

179. Igietseme, J.U., Omosun, Y., Partin, J., Goldstein, J., He, Q., Joseph, K., Ellerson, D., Ansari, U., Eko, F.O., Bandea, C., Zhong, G., and Black, C.M., *Prevention of Chlamydia-induced infertility by inhibition of local caspase activity*. J Infect Dis, 2013. **207**(7): p. 1095-104.
180. Zhong, G., *Chlamydia trachomatis secretion of proteases for manipulating host signaling pathways*. Front Microbiol, 2011. **2**: p. 14.
181. Belay, T., Eko, F.O., Ananaba, G.A., Bowers, S., Moore, T., Lyn, D., and Igietseme, J.U., *Chemokine and chemokine receptor dynamics during genital chlamydial infection*. Infect Immun, 2002. **70**(2): p. 844-50.
182. Darville, T., O'Neill, J.M., Andrews, C.W., Jr., Nagarajan, U.M., Stahl, L., and Ojcius, D.M., *Toll-like receptor-2, but not Toll-like receptor-4, is essential for development of oviduct pathology in chlamydial genital tract infection*. J Immunol, 2003. **171**(11): p. 6187-97.
183. Byrne, G.I., *Chlamydia trachomatis strains and virulence: rethinking links to infection prevalence and disease severity*. J Infect Dis, 2010. **201 Suppl 2**: p. S126-33.
184. Peterson, E.M., You, J.Z., Motin, V., and de la Maza, L.M., *Intranasal immunization with Chlamydia trachomatis, serovar E, protects from a subsequent vaginal challenge with the homologous serovar*. Vaccine, 1999. **17**(22): p. 2901-7.
185. Slepenskin, A., Chu, H., Elofsson, M., Keyser, P., and Peterson, E.M., *Protection of mice from a Chlamydia trachomatis vaginal infection using a Salicylidene acylhydrazide, a potential microbicide*. Infectious Diseases, 2011. **204**(9): p. 1313-20.
186. Peterson, E.M., Cheng, X., Motin, V.L., and de la Maza, L.M., *Effect of immunoglobulin G isotype on the infectivity of Chlamydia trachomatis in a mouse model of intravaginal infection*. Infect Immun, 1997. **65**(7): p. 2693-9.
187. Darville, T. and Hiltke, T.J., *Pathogenesis of genital tract disease due to Chlamydia trachomatis*. Infectious Diseases, 2010. **201 Suppl 2**: p. S114-25.
188. Tuffrey, M., Alexander, F., Woods, C., and Taylor-Robinson, D., *Genetic susceptibility to chlamydial salpingitis and subsequent infertility in mice*. J Reprod Fertil, 1992. **95**(1): p. 31-8.
189. Tuffrey, M., Alexander, F., Conlan, W., Woods, C., and Ward, M., *Heterotypic protection of mice against chlamydial salpingitis and colonization of the lower genital tract with a human serovar F isolate of Chlamydia trachomatis by prior immunization with recombinant serovar L1 major outer-membrane protein*. J Gen Microbiol, 1992. **138 Pt 8**: p. 1707-15.
190. Tuffrey, M., Alexander, F., and Taylor-Robinson, D., *Severity of salpingitis in mice after primary and repeated inoculation with a human strain of Chlamydia trachomatis*. J Exp Pathol (Oxford), 1990. **71**(3): p. 403-10.
191. Laing, K.J. and Secombes, C.J., *Chemokines*. Dev Comp Immunol, 2004. **28**(5): p. 443-60.
192. Yilma, A.N., Singh, S.R., Morici, L., and Dennis, V.A., *Flavonoid Naringenin: A Potential Immunomodulator for Chlamydia trachomatis Inflammation*. Mediators Inflamm, 2013. **2013**: p. 102457.
193. Taub, D.D., Conlon, K., Lloyd, A.R., Oppenheim, J.J., and Kelvin, D.J., *Preferential migration of activated CD4+ and CD8+ T cells in response to MIP-1 alpha and MIP-1 beta*. Science, 1993. **260**(5106): p. 355-8.
194. Schall, T.J., Bacon, K., Camp, R.D., Kaspari, J.W., and Goeddel, D.V., *Human macrophage inflammatory protein alpha (MIP-1 alpha) and MIP-1 beta chemokines attract distinct populations of lymphocytes*. J Exp Med, 1993. **177**(6): p. 1821-6.
195. Teruel, M., Simeon, C.P., Broen, J., Vonk, M.C., Carreira, P., Camps, M.T., Garcia-Portales, R., Delgado-Frias, E., Gallego, M., Espinosa, G., Beretta, L., Airo, P., Lunardi, C.,

- Riemekasten, G., Witte, T., Krieg, T., Kreuter, A., Distler, J.H., Hunzelmann, N., Koeleman, B.P., Voskuyl, A.E., Schuerwegh, A.J., Gonzalez-Gay, M.A., Radstake, T.R., and Martin, J., *Analysis of the association between CD40 and CD40 ligand polymorphisms and systemic sclerosis*. *Arthritis Res Ther*, 2012. **14**(3): p. R154.
196. Perry, L.L., Feilzer, K., and Caldwell, H.D., *Immunity to Chlamydia trachomatis is mediated by T helper 1 cells through IFN-gamma-dependent and -independent pathways*. *J Immunol*, 1997. **158**(7): p. 3344-52.
197. Hook, C.E., Matyszak, M.K., and Gaston, J.S., *Infection of epithelial and dendritic cells by Chlamydia trachomatis results in IL-18 and IL-12 production, leading to interferon-gamma production by human natural killer cells*. *FEMS immunology and medical microbiology*, 2005. **45**(2): p. 113-20.
198. Ito, J.I. and Lyons, J.M., *Role of gamma interferon in controlling murine chlamydial genital tract infection*. *Infect Immun*, 1999. **67**(10): p. 5518-21.
199. Al-Zeer, M.A., Al-Younes, H.M., Lauster, D., Abu Lubad, M., and Meyer, T.F., *Autophagy restricts Chlamydia trachomatis growth in human macrophages via IFNG-inducible guanylate binding proteins*. *Autophagy*, 2013. **9**(1): p. 50-62.
200. Yilma, A.N., Singh, S.R., Fairley, S.J., Taha, M.A., and Dennis, V.A., *The anti-inflammatory cytokine, interleukin-10, inhibits inflammatory mediators in human epithelial cells and mouse macrophages exposed to live and UV-inactivated Chlamydia trachomatis*. *Mediators of inflammation*, 2012. **2012**: p. 520174.
201. Sabat, R., Grutz, G., Warszawska, K., Kirsch, S., Witte, E., Wolk, K., and Geginat, J., *Biology of interleukin-10*. *Cytokine Growth Factor Rev*, 2010. **21**(5): p. 331-44.
202. Wu, L., Xu, B., Fan, W., Zhu, X., Wang, G., and Zhang, A., *Adiponectin protects Leydig cells against proinflammatory cytokines by suppressing the nuclear factor-kappaB signaling pathway*. *The FEBS journal*, 2013. **280**(16): p. 3920-7.
203. Kobayashi, H., Ouchi, N., Kihara, S., Walsh, K., Kumada, M., Abe, Y., Funahashi, T., and Matsuzawa, Y., *Selective suppression of endothelial cell apoptosis by the high molecular weight form of adiponectin*. *Circ Res*, 2004. **94**(4): p. e27-31.
204. Loetscher, M., Gerber, B., Loetscher, P., Jones, S.A., Piali, L., Clark-Lewis, I., Baggiolini, M., and Moser, B., *Chemokine receptor specific for IP10 and mig: structure, function, and expression in activated T-lymphocytes*. *Experimental Medicine*, 1996. **184**(3): p. 963-9.
205. Yang, C.H., Wei, L., Pfeffer, S.R., Du, Z., Murti, A., Valentine, W.J., Zheng, Y., and Pfeffer, L.M., *Identification of CXCL11 as a STAT3-dependent gene induced by IFN*. *Immunology*, 2007. **178**(2): p. 986-92.
206. Guney, M., Erdemoglu, E., Oral, B., Karahan, N., and Mungan, T., *Leukemia inhibitory factor (LIF) is immunohistochemically localized in tubal ectopic pregnancy*. *Acta Histochemica*, 2008. **110**(4): p. 319-23.
207. Ji, Y.F., Chen, L.Y., Xu, K.H., Yao, J.F., and Shi, Y.F., *Locally elevated leukemia inhibitory factor in the inflamed fallopian tube resembles that found in tubal pregnancy*. *Fertility and Sterility*, 2009. **91**(6): p. 2308-14.

## VITA

**Katheryn L. Cerny**

---

### **Education**

**Ph.D. Animal and Food Sciences** University of Kentucky 2012-present (defense date: June 10<sup>th</sup>, 2015)

Dissertation Advisor: PJ Bridges, Ph.D.

*Dissertation Title:* Steroid-dependent regulation of the oviduct: cross-species transcriptomal analyses.

**M.S. Veterinary Science**, University of Kentucky 2010-2012

Thesis Advisor: EL Squires, M.S., Ph.D., DACT(hon)

*Thesis Title:* Presence of bacteria in the reproductive tract of healthy stallions and its relation to the fertility of mares.

**B.S. Animal Science**, California Polytechnic State University, San Luis Obispo 2000-2005

### **Summary of Ph.D. Projects**

- Steroidal regulation of oviductal function in cattle and mice
  - Use global expression profiling to determine differences in steroidal regulation in the oviducts of heifers.
    - Objectives: Using microarray based transcriptional profiling; identify spatial and steroid-dependent changes in mRNA and miRNA expression in epithelial cells isolated from the ampulla and isthmus of heifers.
  - Determine estrogen receptor alpha (ESR1) dependent changes in gene expression in the oviducts using an ESR1 knockout mouse model.
    - Objectives: Using an ESR1 knockout mouse model, microarray based analysis performed in order to identify genes induced by estradiol production and regulated by ESR1.
- Regulation of inflammation in the oviducts
  - Determine the effect of lipopolysaccharide (LPS) on inflammation in the oviducts of mice.
    - Objectives: With LPS as a systemic inflammatory insult, determine expression changes of inflammatory mRNAs in the oviducts of mice

following IP injection with LPS from *E. Coli* using a targeting Nanostring assay.

- Effects of trace mineral supplementation on gonadal function in cattle
  - Describe the neonatal testis transcriptome profiles among calves born to cows supplemented with different forms of dietary selenium throughout gestation.
    - Objectives: A deficiency of selenium reduces fertility in bulls and form of selenium supplemented to cows is known to affect tissue-specific gene expression; therefore, we hypothesized that the form of selenium supplemented to cows during gestation affects the transcriptome of the neonatal bull calf testis, specifically, fertility-associated mRNAs. With selenium supplied as either inorganic, organic, or a 50/50 mix for 4 months prior to breeding and throughout gestation, determine the gene expression profiles of the neonatal calf testis.
  - Determine ovarian dynamics in grazing cows fed differing forms of selenium (Se) in free-choice mineral mixes.
    - Objectives: With selenium supplied as either inorganic, organic, or a 50/50 mix, investigate preovulatory follicular dynamics and whole blood selenium concentrations in grazing cows.

### **Applicable Skills**

**Animal Handling:** Experience handling and caring for multiple species including, cattle, horses, and mice.

**Molecular Biology:** RNA extraction, purification, and quality control; reverse transcription; qPCR; nanostring, microarray.

**Bioinformatics and Statistical Evaluation:** Transcriptional profiling using Partek Genomics Suite, Ingenuity Pathway Analysis (IPA), DAVID bioinformatics resources, Kyoto Encyclopedia of Genes and Genomes (KEGG), Statistical Analysis Software (SAS), and Excel.

**Undergraduate Research Training:** Trained 5 undergraduate students in molecular techniques (RNA extraction, reverse transcription, real-time RT-PCR) needed for targeted gene expression analysis and directed large scale real-time RT-

PCR experiment, requiring collation of multiple datasets produced from these undergraduates using their learned techniques.

**Teaching Opportunities:** Guest lectures for the Spring 2015 semester in the Department of Animal and Food Sciences (University of Kentucky) instructing ASC 364: Reproductive Physiology of Farm Animals.

### **Professional Memberships**

American Society of Animal Science (2013-present)

Society for the Study of Reproduction (2013-present)

American Embryo Transfer Association (2013-present)

Animal and Food Sciences Graduate Association (2012-present)

Kentucky Thoroughbred Farm Managers Club (2005-2014, 2009 board member)

### **Professional Positions Held**

- Graduate Research Assistant, Animal and Food Sciences Department, University of Kentucky, March 2012-Present.
- Graduate Research Assistant, Veterinary Science Department, University of Kentucky, January 2010-March 2012.
- Thoroughbred Farm Manager, Margaux Farm, LLC, March 2005- December 2009.
- Student Intern, Kentucky Equine Management Internship, Spring 2004.

### **Peer Reviewed Publications**

**KL Cerny**, E Garrett, L Anderson and PJ Bridges. Steroid-dependent regulation of bovine oviductal epithelial cells: a transcriptomal analysis. 2015. In Press. *Biology and Endocrinology*.

**KL Cerny**, S Garbacik, C Skees, WR Burris, JC Matthews and PJ Bridges. 2015. Form of selenium in free-choice mineral mixes of dams affects transcriptome profiles, including those of steroidogenic and spermatogenic pathways, of the neonatal calf testis. In Press, *Biological Trace Element Research*.

**KL Cerny**, TV Little, CF Scoggin, RJ Coleman, BA Ball, MHT Troedsson, EL Squires. 2014. Variations of potentially pathogenic bacteria found on the external genitalia of stallions during the breeding season. *Equine Vet Science*, 35(2): Pages 170-173.

S Hughes, **KL Cerny**, JR Campos, MHT Troedsson, B Ball, EL Squires. 2014. The use of equine follicle stimulating hormone to increase chorionic gonadotropin in the pregnant mare. *Equine Vet Science*, 34(8): Pages 1021-1024.

**KL Cerny**, TV Little, CF Scoggin, RJ Coleman, MHT Troedsson, EL Squires. 2014. Presence of bacteria on the external genitalia of healthy stallions and its transmission to the mare at the time of breeding by live cover. *Equine Vet Science*, 34(3): Pages 369-374.

**KL Cerny**, S Hughes, JR Campos, RJ Coleman, MHT Troedsson, EL Squires. 2013. Fertility of mares inseminated with frozen-thawed semen processed by single layer centrifugation through a colloid. *J Equine Vet Science*, 32(5): Pages 289-291.

### **Manuscripts in Preparation**

**KL Cerny**, PJ Bridges. Intraperitoneal administration of lipopolysaccharide induces differential expression of mRNA encoding inflammatory mediators in the oviducts of mice. Manuscript in Preparation.

**KL Cerny**, C. Ko and PJ Bridges. Estrogen receptor alpha (ESR1) dependent regulation of gene expression in the mouse oviduct. Manuscript in Preparation.

**KL Cerny**, L Anderson, WR Burris, M Rhoads, JC Matthews and PJ Bridges. Effects of form of selenium in free-choice mineral mixes of grazing cows on ovarian dynamics. Manuscript in Preparation.

### **Gene Expression Omnibus (publicly available datasets)**

GSE62382: Affymetrix Bovine Gene 1.0 ST array (13 microarrays). Effect of form of gestational Selenium on gene expression in the neonatal calf testis. **KL Cerny**, JC Matthews and PJ Bridges. Record release date 10/16/2014.

GSE62461: Qiagen Mouse Cytokines and Chemokines RT2 profiler PCR array - PAMM-150A (36 arrays). Differential expression of mRNA encoding cytokines and chemokines in the reproductive tract after infection of mice with *Chlamydia trachomatis*. **KL Cerny**, M Van Fleet, A Slepkin, EM Peterson, PJ Bridges. Record release date 10/18/2014.

GSE62570: Affymetrix WT Btau 4.0 array (16 microarrays). Pituitary gene expression profiles of growing beef steers grazing high versus low endophyte-infected tall fescue grass. JC Matthews, R Hegge, **KL Cerny**, PJ Bridges. Record release date 10/23/2014.

GSE63969: Affymetrix Bovine Gene 1.0 ST array (12 microarrays). Steroid-dependent regulation of bovine oviductal epithelial cells: a transcriptomal analysis. **KL Cerny**, E Garrett, L Anderson and PJ Bridges. Record release date 3/16/2015.

### **Seminar Presentations**

- Mar 5, 2012: Comparison of protocols used to synchronize the Bovine estrous cycle. Department Seminar Series-Animal and Food Science, University of Kentucky.
- Feb 22, 2012: Presence of bacteria in the reproductive tract of healthy stallions and its relation to the fertility of mares. Master's Defense Seminar-Veterinary Science Department, University of Kentucky.
- May 17, 2011: Fertility of frozen/thawed stallion semen centrifuged through a single layer density gradient. Department Seminar Series-Veterinary Science Department, University of Kentucky.

### **Invited Presentations**

- April 20, 2015: A transcriptomal analysis of bovine oviductal epithelial cells during differing phases of the estrous cycle. Department Seminar Series-Animal and Food Science, University of Kentucky.
- May 31, 2013: Equine Reproduction: What to know prior to breeding. Thoroughbred Owner and Breeders Association annual breeding clinic. Lexington, KY.

### **Abstracts**

#### **Oral Presentations**

**KL Cerny**, E Garrett, L Anderson and PJ Bridges. Steroid-dependent regulation of bovine oviductal epithelial cells: a transcriptomal analysis. American Society of Animal Science, 2015 Southern Section meeting. Abstract #44

**KL Cerny**, TV Little, CF Scoggin, RJ Coleman, MHT Troedsson, EL Squires. 2012. Presence of bacteria in the reproductive tract of healthy stallions and its relation to the fertility of mares. Proc of the 2012 annual conference and symposium of the Society for Theriogenology. P. 427.

**KL Cerny**, S Hughes, JR Campos, MHT Troedsson, EL Squires. 2011. Fertility of mares inseminated with frozen-thawed semen centrifuged through a single layer density gradient. Proc. of the 2011 Equine Science Society Symposium. P. 316-317.

#### **Poster Presentations**

PJ Bridges, **KL Cerny**, M Rhoads, L Anderson, WR Burris, JC Matthews. Form of selenium in free-choice mineral mixes affects ovarian production of progesterone

but not estradiol in cycling beef cows. American Society of Animal Science, 2015 annual meeting.

**KL Cerny**, PJ Bridges. Intraperitoneal administration of lipopolysaccharide induces differential expression of mRNA encoding inflammatory mediators in the oviducts of mice. American Society of Animal Science, 2015 annual meeting.

**KL Cerny**, M Van Fleet, A Slepkin, EM Peterson, PJ Bridges. Differential expression of mRNA encoding cytokines and chemokines in the reproductive tract after infection of mice with *Chlamydia trachomatis*. Biol. Reprod. Special Issue, Proc. of the 46<sup>th</sup> annual meeting of the Soc. for the Study of Reproduction. Abstract #745.

SR Garbacik, JC Matthews, **KL Cerny**, PJ Bridges. Gestational form of supplemental selenium (Se) affects gene expression in the newborn calf testis. I. Steroidogenesis. American Society of Animal Science, 2013 annual meeting. Abstract W370.

S Hughes, **KL Cerny**, JR Campos, MHT Troedsson, EL Squires. 2012. The use of equine follicle stimulating hormone to increase chorionic gonadotropin in the pregnant mare. Proc. of the 17<sup>th</sup> International Congress on Animal Reproduction. P. 613.

### **Awards**

- February 2015: Second place, Graduate student oral presentation competition, American Society of Animal Science Southern Section meeting.
- July 2013: University of Kentucky Graduate School student travel funding
- June 2002: American Society of Animal Science Undergraduate scholarship
- August 2002: Intercollegiate Equestrian Foundation Undergraduate scholarship